Refinement of two methods for estimation of groundwater recharge rates. [DNR-150] 2000

Bradbury, K. R. et al.
[Madison, Wisconsin?]: [publisher not identified], 2000

Final Project Report

REFINEMENT OF TWO METHODS FOR ESTIMATION OF GROUNDWATER RECHARGE RATES

Kenneth R. Bradbury, Principal Investigator
Wisconsin Geological and Natural History Survey
University of Wisconsin-Extension

Weston Dripps, Research Assistant
Dept. of Geology and Geophysics
University of Wisconsin – Madison

Chip Hankley, GIS Specialist
Wisconsin Geological and Natural History Survey
University of Wisconsin-Extension

Mary P. Anderson, co-PI
Dept of Geology and Geophysics
University of Wisconsin-Madison

Kenneth W. Potter, co-PI
Civil and Environmental Engineering
University of Wisconsin-Madison

September 2000

TABLE OF CONTENTS

ABSTRACT

Understanding the spatial distribution of groundwater recharge is a basic prerequisite for effective groundwater resource management and modeling. Recharge, defined as entry of water into the saturated zone, depends on a wide variety of spatially variable parameters including the vegetation, soils, topography, and climate. Its dependence on these variable parameters makes it one of the most difficult and uncertain hydrologic components to quantify in the evaluation of groundwater resources. Although many researchers have proposed techniques for estimating groundwater recharge, only a few studies have considered its spatial variability, and still no standard accepted method exists to quantify recharge for regional groundwater studies.

We have developed a simple soil-water balance model to estimate the annual spatial distribution of groundwater recharge for watersheds in humid areas. The model is based on a modified Thornthwaite – Mather approach (1957) and uses typically available soil, land cover, topographic, and climatic data. The model does not require extensive parameterization, can be practically applied in a relatively short time frame, and is easy to use. The model code is written in Visual Basic and requires Microsoft Excel 2000 to run. ArcView and ARCINFO are used to generate the model input grids.

The model was applied to the Pheasant Branch Creek watershed of south central Wisconsin where the United States Geological Survey (U.S.G.S.) recently completed a groundwater flow model and a calibrated water balance model (PRMS, Leavesley et al., 1983; Steuer, 1999; Hunt and Steuer, 2000). Our model compares reasonably well with the USGS models, and, in most instances, provides similar spatial recharge arrays for the watershed and comparable estimates of groundwater recharge. Our new model presents modelers, planners, and policy makers with a practical tool for providing recharge estimates for modeling and water resource planning purposes.

LIST OF FIGURES AND TABLES

INTRODUCTION

Background

There is currently no standard, accepted method for estimating groundwater recharge rates, yet such information is essential for reliable groundwater models and for rational real-world groundwater protection. In order to address this problem, the Principal Investigators developed a proposal (*Refinement of Two Methods for Estimation of Groundwater Recharge Rates*) for a 1-year project to test and improve recharge estimation, and received funding from the Wisconsin Department of Natural Resources through the Joint Solicitation Program in 1999-2000. This report summarizes the findings of that project.

In the original proposal, we expected to test and refine two methods of estimating groundwater recharge, specifically (1) a coupled water-balance/parameter estimation model and (2) a modified Thornthwaite-Mather soil-water balance model. As the project proceeded, it became clear that a successful result would require that we focus efforts on only one of these two techniques. Accordingly, this project focuses on the Thornthwaite-Mather soil-water balance approach.

Goals and Objectives of Study

There were a number of motivations for this study:

1. Despite all the previous recharge research that has been done, there still is not a simple accepted technique that can be readily and practically applied to estimate recharge distributions at the watershed scale in humid regions.
2. Despite recharge's inherent spatial and temporal variability, there have been few attempts to quantify or incorporate this variability into water resource planning and groundwater modeling efforts. Groundwater modelers often ignore recharge heterogeneity and assume a uniform recharge distribution for their model area. They simply treat recharge as a calibration parameter, adding or subtracting recharge to match recorded streamflows.

The ability to account for recharge heterogeneity is important to groundwater modelers, planners, and policy makers to ensure an accurate water budget, critical for planning and modeling purposes. Consequently, we set out to develop a practical, physically-based model that uses readily available data to estimate the spatial distribution of groundwater recharge at the watershed scale for humid areas like Wisconsin.

The specific goals of this study were to develop and refine a Thornthwaite – Mather soil-water balance model for the estimation of recharge rates and to test this model against results from USGS models for the Pheasant Branch Creek watershed in Dane County, Wisconsin.

Previous Work

There has been extensive recharge research done at a variety of different scales, yet most of the proposed techniques for estimating recharge require complex instrumentation and/or field work and usually do not account for spatial recharge variability. Those studies that have considered

recharge variability (e.g. Faustini, 1985; Sophocleous and McAllister, 1987; Adar et al., 1988; Cook et al., 1989; Stoertz, 1989; Stoertz and Bradbury, 1989; Edmunds and Gaye, 1994; Graham and Tankersley, 1994; Levine and Salvucci, 1999) have typically been data intensive and/or watershed-specific studies. Very few widely-applicable approaches have been developed that can be readily applied at a watershed scale without substantial effort and data collection.

In addition, much of the previous recharge research has focused on arid regions like the U.S. Southwest where water is scarce. Substantially less recharge work has been completed in more humid areas typical of the northcentral, northwestern, and eastern portions of the United States.

A variety of physical and chemical methods exists for estimating groundwater recharge (see Lerner et al., 1990 for a good summary). A brief review of the literature and a synopsis of the common methods follow:

(1) Direct measurement: Many researchers have installed lysimeters to measure groundwater recharge rates (Kitching and Bridge, 1974; Kitching et al., 1977, 1980; Kitching and Day, 1979; Kitching and Shearer, 1982; Wu et al., 1996). Lysimeters provide direct point measurements of recharge, but can be cumbersome to install and alone are inadequate for mapping regional recharge distributions.

(2) Water Balance Techniques: Water balance techniques treat recharge as the residual of all other fluxes within the water balance equation (recharge = precipitation – runoff – evapotranspiration - changes in storage) (Howard and Lloyd, 1979; Rushton and Ward, 1979; Houston, 1982; Rehm et al., 1982; Steenhuis, 1985; Steenhuis and Van Der Molen, 1986; Gleick, 1987; Rushton, 1988; Johansson, 1988; Senarath, 1988; Chiew and McMahon, 1990; Sophocleous, 1991, 1992; Liu and Zhang, 1993; Kennett-Smith et al., 1994; Gee et al., 1994; Kim et al., 1996; Taylor and Howard, 1996; Ragab et al., 1997; Wu et al., 1997). Our model uses a water balance technique to estimate recharge on a grid cell - by - grid cell basis. Most other water balance studies at the watershed scale generate a single water budget for an entire watershed. These studies ignore potential recharge heterogeneity and produce a single recharge estimate for a watershed.

Other water balance studies use stream baseflow estimates as a surrogate for recharge (Meyboom, 1961; Houston, 1988; Nathan and McMahon, 1990; Hoos, 1990; Rutledge and Daniel, 1994; Mau and Winter, 1997; Perez, 1997; Cherkauer, 1999). This method is unable to account for recharge heterogeneity, and provides only a single recharge estimate for an entire watershed.

(3) Water Level Measurements: The magnitude of water level fluctuations in water table wells can be multiplied by the aquifer's specific yield to provide estimates of recharge (Freeze, 1969; Rennolls et al., 1980; Sophocleous, 1991, 1992; Rehm et al., 1982; Houston, 1982; Gillham, 1984; Viswanathan, 1984; Winter, 1986; Johansson, 1987, 1988; Gupta and Paudyal, 1988; Rai and Singh, 1992; Salama et al., 1993; Barnes et al., 1994; Leduc et al., 1997). Water-level fluctuations are easy to monitor, but are site-specific and appropriate estimates of the specific yield have proven more difficult to obtain.

(4) Darcian Approaches: Darcian approaches rely on numerical models of groundwater flow equations to estimate recharge (Freeze and Banner, 1970; Rehm et al., 1982; Sophocleous, 1985; Steenhuis, 1985; Stephens and Knowlton, 1986). Many unsaturated flow models have been developed to estimate recharge although most require a large number of spatially distributed soil parameters (i.e. unsaturated hydraulic conductivity, soil moisture content) which

are typically not available without a detailed, site-specific field study (Krishnamurthi et al., 1977; Kafri and Asher, 1978; Watson, 1980; Jansson and Halldin, 1979, 1980; Davidson, 1985; Morel-Seytoux and Billeca, 1985; Ross, 1990).

(5) Empirical Methods: Empirical techniques correlate recharge to other measurable variables like precipitation or temperature. Numerous studies have used simple empirical formulas equating recharge to a certain percentage of the annual precipitation (Watson et al., 1976; Mandel and Shiftan, 1981; Sinha and Sharma, 1988; Nielsen and Widjaya, 1989; Perez, 1997). Others have used changes in the temperature profile to quantify recharge rates (Suzuki, 1960; Stallman, 1960, 1963, 1965; Bredehoeft and Papadopulos, 1965; Sorey, 1971; Nightingale, 1975; Boyle and Saleem, 1979; Lapham, 1989; Taniguchi and Sharma, 1990, 1993; Taniguchi, 1993, 1994; Silliman and Booth, 1993; Constantz et al., 1994; Silliman et al., 1995; Constantz and Thomas, 1996; Hunt et al., 1996; Ronan et al., 1998; Taniguchi et al., 1999). Cook and Kilty (1992) and Rosen et al. (1999) used electromagnetic methods to estimate recharge. Although many of these methods show promise, none has been shown to be widely applicable.

(6) Natural and Artificial Chemical Tracers: Environmental geochemical tracers are commonly used to estimate recharge rates (Sharma and Hughes, 1985; O'Brien et al., 1996; Sukhija et al., 1996; Bromley et al., 1997; Wood, 1999). Most tracer techniques provide point measurements of recharge which are insufficient for mapping regional recharge distributions. In addition, many of these techniques were designed for arid settings and are inadequate for humid environments where recharge rates are much higher.

THE RECHARGE MODEL

Approach

We have developed a practical, physically-based model that uses readily available data to estimate the spatial distribution of groundwater recharge at the watershed scale for humid areas like Wisconsin. Of all the techniques discussed in the previous section, the water balance approach offers the greatest ability to estimate and account for recharge heterogeneity. Consequently, our model uses a water balance technique to estimate recharge on a grid cell - by - grid cell basis.

Specifically, we estimate recharge using a modified Thornthwaite – Mather approach (Thornthwaite and Mather, 1957; Eaton, 1995; Swanson, 1996) coupled to a digital elevation model (DEM). Our model uses typically available soil, land cover, topographic, and climatic data to calculate the spatial distribution of annual groundwater recharge.

For each model grid cell, a simple mass balance is calculated for a specified time period:

Changes in Soil Moisture Storage = Precipitation - Runoff – Evapotranspiration

The mass balance quantitatively accounts for soil water conditions on a cell-by-cell basis, based on the spatial and temporal distribution of climatic, soil, and vegetation characteristics. These characteristics dictate the amount of water potentially available for recharge.

The model operates on a monthly time step and is designed to be used at the watershed scale for watersheds in humid regions. The code is written in Visual Basic and requires Microsoft Excel 2000 to run.

The model requires three input grids: (1) soil texture, (2) land cover, and (3) surface flow direction. The coding details for each of these grids are discussed in the subsequent section on 'Model Input Parameters'. Each grid is input to the model as an Ascii file in ARCINFO Ascii Grid format (See Appendix A for the proper input format).

In addition to the land surface data, the model requires daily meteorological data. At a bare minimum, the model needs daily precipitation (in inches) and daily average temperature (in °F), but may require additional climatic data (daily average wind speed (m/sec), daily average relative humidity (%), daily percent sunshine (%)) depending on which evapotranspiration equation the user selects for the water budget calculations. The user is queried at the onset to select one of four equations to calculate evapotranspiration in the model (Thornthwaite – Mather (1957), Turc (1961), Jensen – Haise (1963), or Blaney – Criddle (1966)). The specific requirements for each of the four methods are discussed in Appendix B. The model does not account for spatial variability of meteorological parameters and assumes that all meteorological data are uniform across the model area. Meteorological data are input to the model via an Excel worksheet.

Conceptual Model

Figure 1 is a simplified model flow chart. A brief description of the model flow chart follows, with each component discussed in detail in subsequent sections.

Precipitation data are input at a daily time step. Surface runoff is generated for each grid cell in the model domain for each precipitation event using a Soil Conservation Service (SCS) Curve Number approach (1964). In the SCS approach, runoff is calculated as a function of the soil texture, land cover, and antecedent moisture, all of which are inputs to the model. The estimated runoff is routed downslope on a cell-by-cell basis using a digital elevation model (DEM). Runoff from each cell is routed to the nearest downgradient cell where it is treated as additional "precipitation" and, using an SCS approach, either infiltrates or continues downslope as runoff. Accounting for runoff in this fashion is a conceptual improvement over the original Thornthwaite - Mather model (1957) in which runoff simply exited the model without the possibility of downslope reinfiltration. Runoff is routed iteratively this way for each precipitation event until all the precipitation either infiltrates or exits the model domain. Water that infiltrates goes towards satisfying each grid cell's maximum soil moisture storage capacity, which is calculated as a function of the cell's soil texture and land cover type. Potential evapotranspiration, computed from climatic variables, removes moisture from soil storage. Once the evapotranspirative demands are fulfilled and the maximum storage capacity is satisfied, any excess water percolates down to the water table and is considered recharge.

The output from the model is an annual net percolation map that serves as a surrogate for the potential annual groundwater recharge. This coupled soil-water balance - DEM approach provides estimates of potential annual recharge rates, but does not incorporate the groundwater flow system and thus is unable to differentiate recharge from discharge areas.

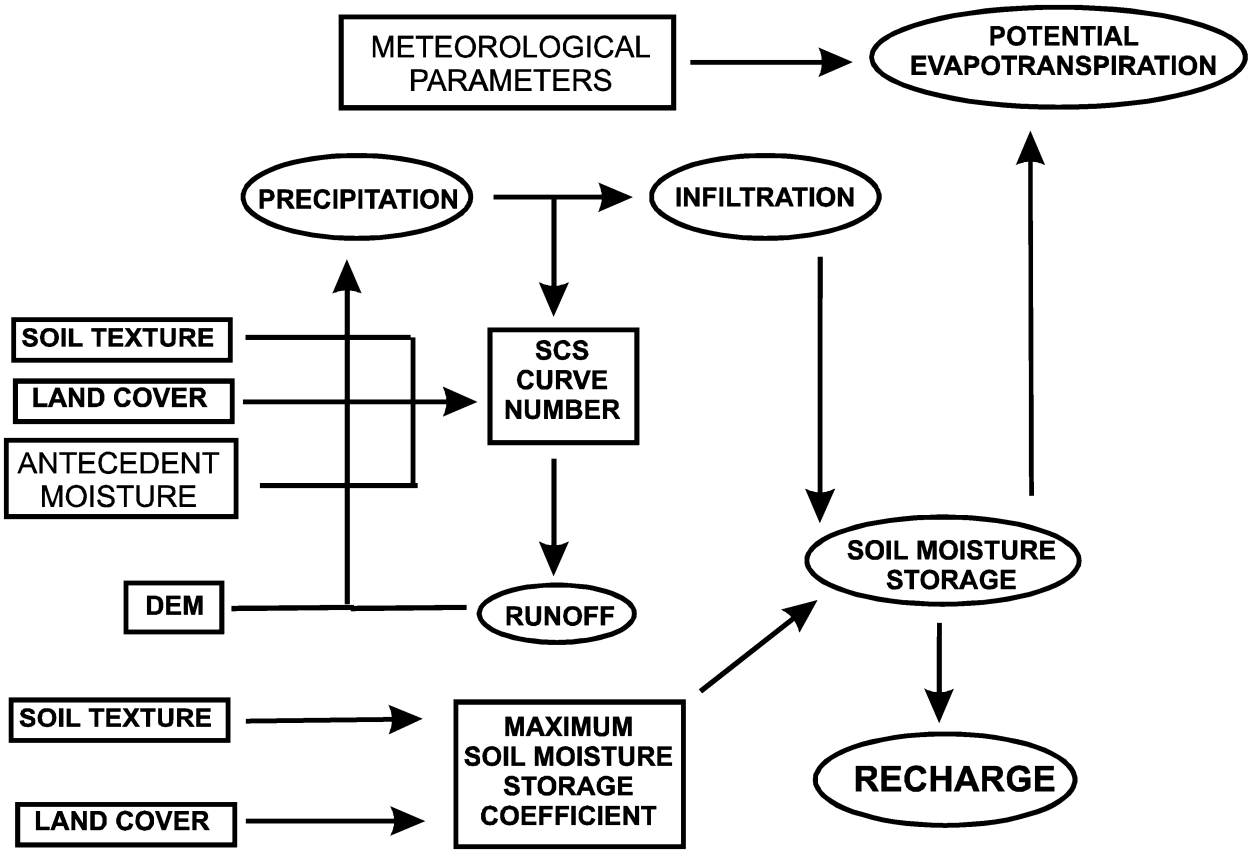

Figure 1: Simplified model flowchart

COMPONENTS OF THE HYDROLOGIC BUDGET

Precipitation

Precipitation is the source of groundwater recharge. Precipitation data are collected at most weather stations and are readily available for almost all regions of the United States. Daily precipitation (in inches) is input into the model via the 'daily variables' worksheet in the 'precipitation' column. In the model, the form of the precipitation is determined by the average daily temperature. Precipitation that falls on a day when the average temperature is less than or equal to 32 ° F is assumed to fall as snow. Precipitation that falls on a day when the average temperature is greater than 32 ° F is assumed to fall as rain.

The model calculates and uses a 'daily net precipitation' as input. The daily net precipitation is the sum of the daily rainfall plus the snowmelt, if any, for that day. The model uses a temperature – index method to compute snowmelt. When snow is present, one millimeter of water-equivalent snow is assumed to melt per day per average degree Celsius when the daily average temperature is above the freezing point (Kim, 1996). Snow is accumulated and melted on a daily basis. Any snow that does not melt over the course of a day is carried over to the following day.

Runoff

One of the major shortcomings of most water balance models is that they do not allow for the routing and potential downslope infiltration of surface runoff. Runoff is generated and either directly dumped into the nearest downgradient water body or simply removed from the model. In reality, runoff may infiltrate as it proceeds downslope.

Our model uses the SCS Curve Number approach (US Soil Conservation Service, 1964) to calculate surface runoff and then uses a DEM to route this runoff through the model domain. The model allows for infiltration into downgradient cells as runoff proceeds downslope. The SCS method was selected because computationally it is simple, it uses readily available data, and there are few other practical methods that are known to be better.

The SCS Curve Number approach is the most widely used runoff method in the United States (Dingman, 1994). It was developed in the 1960s by the U.S. Soil Conservation Service to classify the runoff potential for different combinations of soil and land cover. The method relates runoff (R) to total rainfall (P) and each cell's storage capacity (S_{max}) via the empirical equation:

$$R = (P - 0.2S_{max})^2 / (P + 0.8S_{max}) \text{ for } P > .2\ S_{max}$$

The precipitation (in inches) is measured, and S_{max} is calculated as a function of a curve number (CN) where:

$$S_{max} = (1000 / CN) - 10$$

Curve numbers range from 0 to 100 and are a function of the soil texture, the land cover, and the antecedent soil moisture conditions. The lower the curve number, the lower the runoff potential. To assign a curve number to a grid cell, the cell's soil type is first assigned to one of four hydrologic soil groups (A – D) based on the soil's infiltration capacity (Table 1). Since infiltration capacity data are typically unavailable for all soils, the soil texture is used to assign each soil type to an SCS soil group. Saturated hydraulic conductivity data are used as a proxy for minimum infiltration capacity (Table 2).

We used data from the literature to assign curve numbers to all the possible soil and land cover combinations (Table 3 and Appendix C). Beaches (72), other sandy areas (73), exposed bedrock (74), quarries (75), and gravel pits (75) are assumed to have essentially no runoff (curve number = 5). All water bodies (51 – 54) and wetlands (61 – 62) are assumed to be fully saturated and have complete runoff (curve number = 100).

Antecedent wetness affects the runoff potential. The wetter the antecedent conditions, the higher the runoff potential. There are three antecedent soil moisture conditions (conditions I, II, and III). The curve numbers in Table 3 are for Condition II, which is considered an average wetness. Condition I is for very dry conditions, and condition III is for very wet conditions. The model adjusts the curve numbers on a daily basis depending on the antecedent wetness and the time of year (growing verse dormant season) (Tables 4 and 5).

Frost data are used to define the growing and the dormant seasons. The last frost of the winter / spring marks the beginning of the growing season and the first frost of the fall marks the end of the growing season. The user is queried for frost data for the model area. Table 6 contains average frost data for select areas across the US Midwest.

The model uses empirical equations to adjust the curve numbers to the proper condition on a daily basis. We derived these equations by fitting an exponential curve to the SCS curve number data. Surprisingly, all the digits in the equations are significant.

To adjust the curve number from condition II (CNII) to condition I (CNI) or condition III (CNIII):

$$CNI = (1.44206581732462 \times 10^{-6})(CNII)^4 - (2.54340415305462 \times 10^{-4})(CNII)^3 + (2.07018739405394 \times 10^{-2})(CNII)^2 - (7.67877072822852 \times 10^{-3})(CNII) + 2.09678222732103$$

$$CNIII = (-6.20352282661163 \times 10^{-7})(CNII)^4 + (1.60650096926368 \times 10^{-4})(CNII)^3 - (2.03362629006156 \times 10^{-2})(CNII)^2 + (2.01054923513527)(CNII) + 3.65427885962651$$

Runoff is then calculated at a daily time step for each cell within the watershed. Each day, the daily precipitation, if any, is uniformly applied across the surface of the watershed. The SCS approach is used to calculate an initial runoff. This runoff is routed to the appropriate downgradient cell using the flow direction grid generated from the DEM. Incoming runoff from an upgradient cell is treated as "additional precipitation" and is added to the original precipitation to yield a net input for each grid cell (original precipitation plus incoming runoff). The model

Table 1

Hydrologic Soil Groups

(as defined by the US Soil Conservation Service (1964))

Soil Group	Characteristics
A	**Low overland flow potential; high minimum infiltration capacity even when thoroughly wetted (infiltration capacity > 0.76 cm/h)**
B	**Moderate minimum infiltration capacity when thoroughly wetted. (infiltration capacity = 0.38 to 0.76 cm/h)**
C	**Low minimum infiltration capacity when thoroughly wetted. (infiltration capacity = 0.13 - 0.38 cm/h)**
D	**High overland flow potential; very low minimum infiltration capacity when thoroughly wetted (infiltration capacity < 0.13 cm/h)**

Table 2

Texture Class	Saturated Hydraulic Conductivity (cm/h)	SCS Soil Group
Sand	**21.00**	**A**
Loamy Sand	**6.11**	**A**
Sandy Loam	**2.59**	**A**
Fine Sandy Loam	**-----**	**A**
Very Fine Sandy Loam	**-----**	**A**
Loam	**1.32**	**A**
Silt Loam	**0.68**	**B**
Silt	**-----**	**B**
Sandy Clay Loam	**0.43**	**B**
Silty Clay Loam	**0.15**	**C**
Clay Loam	**-----**	**C**
Sandy Clay	**0.12**	**C**
Silty Clay	**0.09**	**D**
Clay	**0.06**	**D**

(Adapted from the Handbook of Soil Science, 2000)

Table 3
SCS Curve Numbers for all Soil / Land Cover Combinations
Antecedent Wetness Condition II

		Hydrologic Soil Group			
	Land Use Description	A	B	C	D
Urban or Built Up Land					
11	**Residential (1/3 acre lots)[1]**	**57**	**72**	**81**	**86**
12	**Commercial and Services[1]**	**89**	**92**	**94**	**95**
13	**Industrial[1]**	**81**	**88**	**91**	**93**
14	**Transportation / Communication[1]**	**91**	**94**	**95**	**96**
15	**Industrial / Commercial Complex[1]**	**85**	**90**	**92**	**94**
16	**Mixed Urban or Built Up[1]**	**81**	**88**	**91**	**93**
17	**Other Urban or Built Up[1]**	**39**	**61**	**74**	**80**
Agricultural Land					
21	**Cropland and Pasture[1]**	**62**	**71**	**78**	**81**
22	**Orchards, Groves, Vineyards[2]**	**39**	**53**	**67**	**71**
23	**Confined Feeding Operations[2]**	**59**	**74**	**82**	**86**
24	**Other Agricultural Land[2]**	**59**	**74**	**82**	**86**
Rangeland					
31	**Herbaceous Rangeland[1]**	**39**	**61**	**74**	**80**
32	**Shrub and Brush Rangeland[1]**	**39**	**61**	**74**	**80**
33	**Mixed Rangeland[1]**	**39**	**61**	**74**	**80**
Forest Land					
41	**Deciduous Forest Land[1]**	**25**	**55**	**70**	**77**
42	**Evergeen Forest Land[1]**	**25**	**55**	**70**	**77**
43	**Mixed Forest Land[1]**	**25**	**55**	**70**	**77**
Water					
51	**Streams and Canals**	**100**	**100**	**100**	**100**
52	**Lakes**	**100**	**100**	**100**	**100**
53	**Reservoirs**	**100**	**100**	**100**	**100**
54	**Bays and Estuaries**	**100**	**100**	**100**	**100**
Wetland					
61	**Forested Wetland**	**100**	**100**	**100**	**100**
62	**Nonforested Wetland**	**100**	**100**	**100**	**100**
Barren Land					
72	**Beaches**	**5**	**5**	**5**	**5**
73	**Sandy Areas Other than Beaches**	**5**	**5**	**5**	**5**
74	**Bare Exposed Rock**	**5**	**5**	**5**	**5**
75	**Strip Mines, Quarries, Gravel Pits**	**5**	**5**	**5**	**5**
76	**Transitional Areas[2]**	**77**	**86**	**91**	**94**
77	**Mixed Barren Land[2]**	**77**	**86**	**91**	**94**

[1] taken from Handbook of Hydrology, 1993.
[2] taken from U.S. SCS, 1964.

Table 4

Condition	Soil Wetness	Total Rain from 5 Previous Days (inches) Dormant Season	Growing Season
I	Dry	< 0.05	< 1.4
II	Average	0.5 – 1.1	1.4 – 2.1
III	Near Saturation	> 1.1	> 2.1

Table 5

Curve Number Conversions for the Three Antecedent Wetness Conditions

CN I	CN II	CN III	CN I	CN II	CN III
100	100	100	42	62	79
97	99	100	41	61	78
94	98	99	40	60	78
91	97	99	39	59	77
89	96	99	38	58	76
87	95	98	37	57	75
85	94	98	36	56	75
83	93	98	35	55	74
81	92	97	34	54	73
80	91	97	33	53	72
78	90	96	32	52	71
76	89	96	31	51	70
75	88	95	31	50	70
73	87	95	30	49	69
72	86	94	29	48	68
70	85	94	28	47	67
68	84	93	27	46	66
67	83	93	26	45	65
66	82	92	25	44	64
64	81	92	25	43	63
63	80	91	24	42	62
62	79	91	23	41	61
60	78	90	22	40	60
59	77	89	21	39	59
58	76	89	21	38	58
57	75	88	20	37	57
55	74	88	19	36	56
54	73	87	18	35	55
53	72	86	18	34	54
52	71	86	17	33	53
51	70	85	16	32	52
50	69	84	16	31	51
48	68	84	15	30	50
47	67	83	12	25	43
46	66	82	9	20	37
45	65	82	6	15	30
44	64	81	4	10	22
43	63	80	2	5	13

Table 6

Frost Data for the US Midwest

Illinois

	Last Frost		First Frost	
City	Date	Julian Day	Date	Julian Day
Aledo	**8-May**	**128**	**25-Sep**	**268**
Cairo	**6-Apr**	**96**	**29-Oct**	**302**
Chicago	**25-Apr**	**115**	**22-Oct**	**295**
East St. Louis	**1-May**	**121**	**5-Oct**	**278**
Peoria	**8-May**	**128**	**6-Oct**	**279**
Rockford	**13-May**	**133**	**25-Sep**	**268**
Springfield	**1-May**	**121**	**6-Oct**	**279**
Windsor	**7-May**	**127**	**7-Oct**	**280**

Indiana

	Last Frost		First Frost	
City	Date	Julian Day	Date	Julian Day
Evansville	**23-Apr**	**113**	**12-Oct**	**285**
Fort Wayne	**15-May**	**135**	**25-Sep**	**268**
Gary	**17-May**	**137**	**2-Oct**	**275**
Indianapolis	**9-May**	**129**	**7-Oct**	**280**
Muncie	**15-May**	**135**	**1-Oct**	**274**
Princeton	**30-Apr**	**120**	**4-Oct**	**277**
Scottsburg	**10-May**	**130**	**1-Oct**	**274**

Iowa

	Last Frost		First Frost	
City	Date	Julian Day	Date	Julian Day
Ames	**12-May**	**132**	**26-Sep**	**269**
Cedar Rapids	**13-May**	**133**	**25-Sep**	**268**
Clarinda	**10-May**	**130**	**24-Sep**	**267**
Davenport	**25-Apr**	**115**	**13-Oct**	**286**
Decorah	**26-May**	**146**	**18-Sep**	**261**
Des Moines	**9-May**	**129**	**21-Sep**	**264**
Le Mars	**18-May**	**138**	**17-Sep**	**260**
Mason City	**20-May**	**140**	**16-Sep**	**259**
Ottumwa	**3-May**	**123**	**5-Oct**	**278**

Michigan

	Last Frost		First Frost	
City	Date	Julian Day	Date	Julian Day
Cheboygan	**30-May**	**150**	**25-Sep**	**268**
Detriot	**12-May**	**132**	**9-Oct**	**282**
Evart	**14-Jun**	**165**	**28-Aug**	**240**
Kalamazoo	**15-May**	**135**	**29-Sep**	**272**
Lansing	**31-May**	**151**	**18-Sep**	**261**

Marquette	**25-May**	**145**	**4-Oct**	**277**
Muskegon	**24-May**	**144**	**24-Sep**	**267**
Pontiac	**16-May**	**136**	**29-Sep**	**272**
Sault Ste. Marie	**10-Jun**	**161**	**12-Sep**	**255**
Traverse City	**9-Jun**	**160**	**17-Sep**	**260**

Minnesota

	Last Frost		First Frost	
City	Date	Julian Day	Date	Julian Day
Canby	**23-May**	**143**	**16-Sep**	**259**
Detriot Lakes	**10-Jun**	**161**	**31-Aug**	**243**
Duluth	**4-Jun**	**155**	**10-Sep**	**253**
Faribault	**24-May**	**144**	**15-Sep**	**258**
Hallock	**9-Jun**	**160**	**10-Sep**	**253**
International Falls	**9-Jun**	**160**	**4-Sep**	**247**
Marshall	**19-May**	**139**	**24-Sep**	**267**
Minneapolis	**21-May**	**141**	**15-Sep**	**258**
St. Paul	**21-May**	**141**	**15-Sep**	**258**
Warroad	**6-Jun**	**157**	**4-Sep**	**247**

Nebraska

	Last Frost		First Frost	
City	Date	Julian Day	Date	Julian Day
Ainsworth	**21-May**	**141**	**24-Sep**	**267**
Falls City	**3-May**	**123**	**3-Oct**	**276**
Grand Island	**16-May**	**136**	**26-Sep**	**269**
Lincoln	**9-May**	**129**	**30-Sep**	**273**
North Platte	**25-May**	**145**	**10-Sep**	**253**
Omaha	**12-May**	**132**	**23-Sep**	**266**
Scottsbluff	**25-May**	**145**	**14-Sep**	**257**
York	**10-May**	**130**	**30-Sep**	**273**

North Dakota

	Last Frost		First Frost	
City	Date	Julian Day	Date	Julian Day
Bismark	**26-May**	**146**	**7-Sep**	**250**
Cavelier	**2-Jun**	**153**	**8-Sep**	**251**
Crosby	**5-Jun**	**156**	**31-Aug**	**243**
Dickinson	**9-Jun**	**160**	**28-Aug**	**240**
Fargo	**25-May**	**145**	**12-Sep**	**255**
Linton	**10-Jun**	**161**	**1-Sep**	**244**
Minot	**31-May**	**151**	**2-Sep**	**245**
Wahpeton	**23-May**	**143**	**14-Sep**	**257**

South Dakota

	Last Frost		First Frost	
City	Date	Julian Day	Date	Julian Day
Castlewood	**30-May**	**150**	**4-Sep**	**247**

Custer	**3-Jul**	**184**	**17-Aug**	**229**
Gettysburg	**23-May**	**143**	**14-Sep**	**257**
Huron	**27-May**	**147**	**15-Sep**	**258**
Ludlow	**6-Jun**	**157**	**31-Aug**	**243**
Mobridge	**19-May**	**139**	**20-Sep**	**263**
Pierre	**2-Jun**	**153**	**8-Sep**	**251**
Rapid City	**26-May**	**146**	**14-Sep**	**257**
Sioux Falls	**24-May**	**144**	**17-Sep**	**260**

Wisconsin

	Last Frost		First Frost	
City	Date	Julian Day	Date	Julian Day
Ashland	**18-Jun**	**169**	**6-Sep**	**249**
Eau Claire	**26-May**	**146**	**15-Sep**	**258**
Green Bay	**26-May**	**146**	**18-Sep**	**261**
Lacrosse	**15-May**	**135**	**29-Sep**	**272**
Madison	**13-May**	**133**	**25-Sep**	**268**
Milwaukee	**20-May**	**140**	**26-Sep**	**269**
Solon Springs	**10-Jun**	**161**	**7-Sep**	**250**
Wausau	**22-May**	**142**	**6-Sep**	**249**

recalculates runoff based on the new net input and then routes the resulting runoff downslope. This iterative process propagates runoff downgradient and continues until the net precipitation to the system either infiltrates into the soil or exits the model domain as runoff, typically via a stream or other water body. Once the precipitation for a given day has been separated into a runoff and infiltration component for each grid cell, the model proceeds to the next day. The model assumes that all the precipitation that enters the system on a given day moves completely through the system within that day. The model does not account for a runoff time lag. The daily runoff is summed to yield a monthly net runoff for each cell, which is then used in the monthly water budget calculations.

Infiltration

Infiltration is defined as the entry of water from the ground surface into the soil profile. For each grid cell and each month, the model calculates infiltration as the difference between the monthly net precipitation (actual precipitation plus incoming runoff) and the monthly total runoff. The model assumes one-dimensional vertical infiltration.

Evapotranspiration

Evapotranspiration is the conversion of water to vapor and the transport of that vapor away from the watershed surface back into the atmosphere. Solar radiation provides the energy necessary to evaporate water from plants, soils, and water bodies. Since direct measurement of solar radiation and other variables like vapor and heat flux is difficult and typically not available, most techniques for estimating potential evapotranspiration are based on one or more atmospheric variables like air temperature. We have selected four commonly used empirical methods for calculating potential evapotranspiration: Thornthwaite – Mather (1957), Turc (1961), Jensen – Haise (1963), and Blaney-Criddle (1966). The user must select one of the four methods at the outset of a model run. The choice of method may depend on what climatic data are available. All four methods produce a single estimate of potential evapotranspiration that is uniformly applied to the entire model area. Although evapotranspiration varies spatially, a single estimate is often adequate for small area applications. We recognize that more sophisticated approaches like the Penman-Monteith equation (Monteith, 1965) exist to calculate evapotranspiration, but the data requirements for these techniques are often substantial, making them prohibitive for the typical watershed where the available data are limited.

The Thornthwaite - Mather equation is the simplest of the four techniques, based solely on average monthly temperature data that are typically available from any U.S. weather station. The Blaney – Criddle method is also a temperature- based approach although it requires additional climatic parameters including the daily average wind speed, the minimum relative humidity, and the daily percent sunshine, all of which are also usually available from any U.S. weather station. The other two techniques, the Turc and Jensen – Haise methods, are radiation-based approaches, requiring estimates or measurements of the daily net solar radiation. Net solar radiation is measured at some weather stations, but can otherwise be estimated as a function of cloud cover, surface albedo, latitude, and time of year. Both the Turc and Jensen-Haise methods additionally require daily average temperature measurements, and the Turc equation requires daily relative humidity data. A brief summary of each of the four methods can be found in Appendix B.

Changes in Soil Moisture

Once the monthly estimates of precipitation, runoff, infiltration, and evapotranspiration are calculated, the model proceeds to track changes in soil moisture for each grid cell at a monthly time step. In order to determine periods of moisture excess and deficiency, the model calculates the monthly difference between the potential evapotranspiration and the net infiltration, hereafter referred to as the SM value (Net Infiltration – Potential Evapotranspiration). A positive SM value indicates an excess of water available towards satisfying the soil moisture holding capacity. A negative SM value indicates the inability of the infiltrating water to satisfy the evapotranspirative needs and requires the removal of soil moisture from the system.

A starting point must be specified in order to track monthly changes in the soil moisture budget. The model tallies the annual net potential evapotranspiration and subtracts it from the annual net infiltration. If the difference is positive, indicating a net annual input to the system, the model assumes that the soil is fully saturated (at its maximum holding capacity) for the month before evapotranspiration begins in the spring. This assumption is reasonable for most humid areas where either the spring snowmelt or winter rains have saturated the soil system. For those sites with year round evapotranspiration, the model assumes the system is at full saturation for the month of April following the usual spring rains. If the difference is negative, indicating a net annual moisture loss from the system, the model uses a successive approximation technique to specify a starting soil moisture value (Appendix D).

Once a starting soil moisture value has been specified, moisture is either removed or added to the system on a month-to-month basis. For those months with a net input to the soil, the gain is simply added to the existing soil moisture value from the previous month. If the net exceeds the cell's maximum soil moisture storage capacity, the excess is considered to be recharge and the soil is assumed to be at full moisture capacity. For those months with a net output from the soil, the loss is added to any existing deficit and the net accumulated water loss is used to calculate the soil moisture via the appropriate moisture retention equation (Appendix E).

MODEL INPUT PARAMETERS

Soil Texture

The soil texture or the size of the soil particles influences a soil's ability to transmit and retain water. Sandy soils have a high infiltration capacity and a low water holding capacity, making them conducive to rapid vertical throughflow and subsequently favorable for groundwater recharge. In contrast, silty and clay-rich soils possess low infiltration rates and high water holding capacities and are thus less favorable for groundwater recharge.

The model uses soil textural information, together with land cover information, to calculate surface runoff and assign a maximum soil moisture holding capacity to each grid cell. Soil classifications, which include the requisite textural information, are typically available through the state soil conservation service office. Each soil series must be classified into one of fourteen different soil texture types (Figure 2). ARCINFO or ArcView can be used to code and generate the ascii soil texture input file (see Appendix A for an example ascii input file). In this study we used soil texture data from the USGS and from the U.S. Department of Agriculture's Soil Conservation Service's Soil Survey of Dane County (USDA, 1978).

Land Cover

Land cover affects infiltration rates and dictates the subsurface zone over which evapotranspiration occurs. The less pervious the cover type, the larger the runoff, the less the infiltration, the less the recharge. Urban areas are typically less pervious and thus less favorable for groundwater recharge compared to more permeable cover types like forests or rangelands. Countering this trend is the fact that some of the more permeable cover types like forests have deeper root systems and subsequently higher moisture holding capacities that must be satisfied before recharge can occur.

The model uses land cover information, together with the soil textural information, to calculate surface runoff and assign a maximum soil moisture holding capacity for each grid cell. The model requires an Anderson Level II Land Cover Classification (Anderson et al., 1976) in which each grid cell is classified into one of twenty-nine different land cover types (Table 7). Definitions for each of the cover types are provided in Appendix F.

Land cover classifications are typically available through state and/or federal agencies. If no land cover classification exists for the study area, air photos, satellite images, and/or field surveys can be used to generate a digital land cover map. ARCINFO or ArcView can then be used to code and generate the ascii land cover input file (see Appendix A for an example ascii input file). In this study we used land cover data available from the USGS.

Surface Flow Direction

The model uses a digital elevation model (DEM) to route runoff on a cell-by-cell basis. Runoff is generated for each precipitation event using the SCS Curve Number approach and is iteratively transferred downslope to the next downgradient cell. The incoming runoff to a cell either

Soil Texture Classification

Texture
Sand
Loamy Sand
Sandy Loam
Fine Sandy Loam
Very Fine Sandy Loam
Loam
Silt Loam
Silt
Sandy Clay Loam
Silty Clay Loam
Clay Loam
Sandy Clay
Silty Clay
Clay

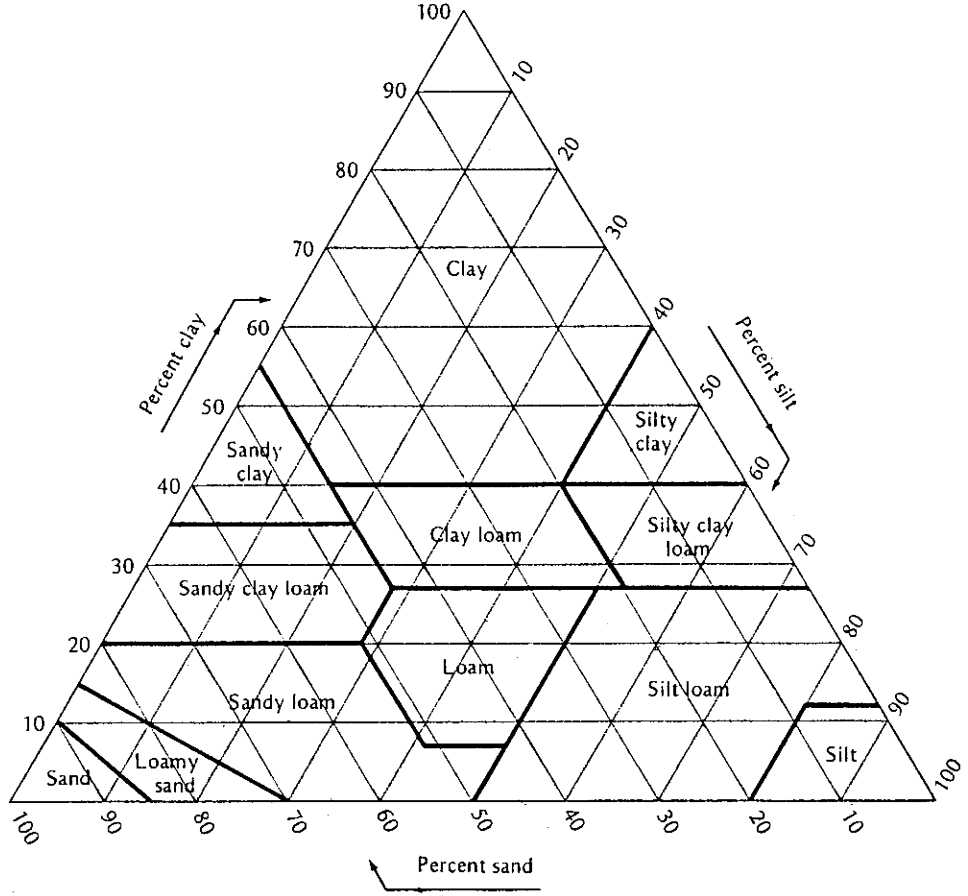

Figure 2: Soil Texture Classification Scheme

Table 7: Land Cover Classes

Level I	Level II
Urban or Built Up Land	**Residential (11)**
	Commercial and Services (12)
	Industrial (13)
	Transportation, Communications, and Utilities (14)
	Industrial and Commercial Complexes (15)
	Mixed Urban or Built Up Land (16)
	Other Urban or Built Up Land (17)
Agricultural Land	**Cropland and Pasture (21)**
	Orchards, Groves, Nurseries (22)
	Confined Feeding Areas (23)
	Other Agricultural Land (24)
Rangeland	**Herbaceous Rangeland (31)**
	Shrub and Brush Rangeland (32)
	Mixed Rangeland (33)
Forest Land	**Deciduous Forest Land (41)**
	Evergreen Forest Land (42)
	Mixed Forest Land (43)
Water	**Streams and Canals (51)**
	Lakes (52)
	Reservoirs (53)
	Bays and Estuaries (54)
Wetland	**Forested Wetland (61)**
	Non-forested Wetland (62)
Barren Land	**Beaches (72)**
	Sandy Areas other then Beaches (73)
	Bare Exposed Rock (74)
	Strip Mines, Quarries, and Gravel Pits (75)
	Transitional Area (76)
	Mixed Barren Land (77)

infiltrates or continues downslope as runoff, depending on the soil texture, the land cover, and the antecedent soil moisture of the cell.

30 meter digital elevation models are available for the entire United States through the USGS. Digital aerial photographs can be used to make higher resolution DEMs if necessary. The 'flowdirection' command in ARCINFO is used to generate a flow direction grid from the DEM (Appendix A and Figure 3). Each cell is assigned to one of eight values (1, 2, 4, 8, 16, 32, 64, 128) depending on the cell's topography. The model is coded to use these numbers to route surface runoff. If the cell resides in a closed depression, ARCINFO assigns the cell a value other than one of the eight. The model recognizes these alternative values as closed depressions and assumes that all incoming runoff to these depressions infiltrates. In this study we generated flow directions from a 30 m DEM available from the USGS.

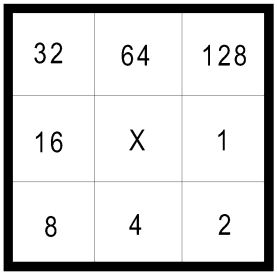

Figure 3: Each grid cell is assigned a number based on the digital elevation model. This number specifies the direction of surface flow. For example, a "1" in a cell would route runoff to the cell to the right; a "4" would route runoff to the cell below; and so on.

Meteorological Inputs

The model uses typically available meteorological data. At a bare minimum, the model requires daily precipitation (inches) and daily average temperature data (° F), but may require additional climatic data (daily average wind speed (m/sec), daily average relative humidity (%), daily percent sunshine(%)) depending on how the user chooses to calculate evapotranspiration. The model does not account for spatial variability of meteorological parameters and assumes that all meteorological data are uniform across the model area. Meteorological data are input into the model via the "daily variables" worksheet within the model. The requisite daily data should be pasted into the appropriate data columns within the worksheet. The spreadsheet automatically generates the weekly and monthly model input data from the daily data. For our study we downloaded climatic data from NCDC from the world-wide-web.

Maximum Soil Moisture Storage Coefficient

Each grid cell is assigned a maximum soil moisture storage coefficient based on the soil texture and the land cover type. The maximum soil moisture storage coefficient represents the amount of water a particular soil / land cover combination is capable of retaining. This amount needs to be satisfied before recharge can occur. Different soil textures have different retention and storage properties. Sandy soils are typically well drained and have a limited ability to retain water while clay-rich soils are poorly drained and retain water well. Estimates of available water (inches of

water per foot of strata) were interpolated from Thornthwaite and Mather (1957) to accommodate the fourteen possible soil texture types (Figure 2).

Rooting depths indicate the depth to which plant roots actively retain water. Any water that percolates below this depth is assumed to be recharge and continue down to the water table. We are assuming that below the root zone the moisture content is at the specific yield. Rooting depths vary as a function of land cover type and soil texture. Plants and trees have a tendency to have longer roots in sandier soils relative to clay-rich soils. Where possible, root zone depths were interpolated from Thornthwaite and Mather (1957) for the various land cover / soil texture combinations. The remaining combinations were taken from the literature and from discussions with foresters and soil scientists. Water holding capacity tables (Table 8 and Appendix G) were generated for all soil texture and land cover combinations by multiplying the available water by the associated root zone depth.

Table 8: Maximum Soil Moisture Storage Coefficients
(Adapted from Thornthwaite and Mather, 1957)

Urban or Built-Up Land Categories (Cover Types 11, 24) … 2/3 trees + 1/3 grass

Texture	Available Water (in/ft)	Root Zone (ft)	Water Holding Capacity (in)
sand	1.20	6.08	7.3
loamy sand	1.40	5.67	7.9
sandy loam	1.60	5.26	8.4
fine sandy loam	1.80	4.86	8.7
very fine sandy loam	2.00	4.83	9.7
loam	2.20	4.79	10.5
silt loam	2.40	4.77	11.5
silt	2.55	4.53	11.6
sandy clay loam	2.70	4.29	11.6
silty clay loam	2.85	4.05	11.5
clay loam	3.00	3.80	11.4
sandy clay	3.20	3.46	11.1
silty clay	3.40	3.12	10.6
clay	3.60	2.78	10.0

Urban or Built-Up Land Categories (Cover Types 16) …1/3 tree and 2/3 grass

Texture	Available Water (in/ft)	Root Zone (ft)	Water Holding Capacity (in)
sand	1.20	3.75	4.5
loamy sand	1.40	3.50	4.9
sandy loam	1.60	3.25	5.2
fine sandy loam	1.80	3.00	5.4
very fine sandy loam	2.00	2.93	5.9
loam	2.20	2.87	6.3
silt loam	2.40	2.83	6.8
silt	2.55	2.68	6.8
sandy clay loam	2.70	2.53	6.8
silty clay loam	2.85	2.38	6.8
clay loam	3.00	2.23	6.7

sandy clay	3.20	2.03	6.5
silty clay	3.40	1.82	6.2
clay	3.60	1.62	5.8

Urban or Built-Up Land Categories (Cover Types 12, 15, 17) …1/4 tree and 3/4 grass

Texture	Available Water (in/ft)	Root Zone (ft)	Water Holding Capacity (in)
sand	1.20	3.21	3.8
loamy sand	1.40	2.99	4.2
sandy loam	1.60	2.78	4.4
fine sandy loam	1.80	2.57	4.6
very fine sandy loam	2.00	2.49	5.0
loam	2.20	2.42	5.3
silt loam	2.40	2.37	5.7
silt	2.55	2.24	5.7
sandy clay loam	2.70	2.12	5.7
silty clay loam	2.85	1.99	5.7
clay loam	3.00	1.86	5.6
sandy clay	3.20	1.69	5.4
silty clay	3.40	1.52	5.2
clay	3.60	1.35	4.9

Urban or Built-Up Land Categories (Cover Types 13, 14) …all grass

Texture	Available Water (in/ft)	Root Zone (ft)	Water Holding Capacity (in)
sand	1.20	1.50	1.8
loamy sand	1.40	1.40	2.0
sandy loam	1.60	1.30	2.1
fine sandy loam	1.80	1.20	2.2
very fine sandy loam	2.00	1.10	2.2
loam	2.20	1.00	2.2
silt loam	2.40	0.94	2.3
silt	2.55	0.88	2.2
sandy clay loam	2.70	0.82	2.2
silty clay loam	2.85	0.76	2.2
clay loam	3.00	0.70	2.1
sandy clay	3.20	0.64	2.0
silty clay	3.40	0.57	1.9
clay	3.60	0.50	1.8

Cropland and Pastures (Cover Type 21) … 3/4 moderate + 1/4 deep

Texture	Available Water (in/ft)	Root Zone (ft)	Water Holding Capacity (in)
sand	1.20	2.71	3.2
loamy sand	1.40	2.92	4.1
sandy loam	1.60	3.13	5.0
fine sandy loam	1.80	3.33	6.0
very fine sandy loam	2.00	3.40	6.8
loam	2.20	3.47	7.6
silt loam	2.40	3.54	8.5
silt	2.55	3.36	8.6

sandy clay loam	2.70	3.19	8.6
silty clay loam	2.85	3.02	8.6
clay loam	3.00	2.84	8.5
sandy clay	3.20	2.49	8.0
silty clay	3.40	2.15	7.3
clay	3.60	1.81	6.5

Orchards, Groves, Vineyards, Nurseries (Cover Type 22)

Texture	Available Water (in/ft)	Root Zone (ft)	Water Holding Capacity (in)
sand	1.20	5.00	6.0
loamy sand	1.40	5.18	7.3
sandy loam	1.60	5.36	8.6
fine sandy loam	1.80	5.55	10.0
very fine sandy loam	2.00	5.36	10.7
loam	2.20	5.18	11.4
silt loam	2.40	5.00	12.0
silt	2.55	4.58	11.7
sandy clay loam	2.70	4.16	11.2
silty clay loam	2.85	3.74	10.7
clay loam	3.00	3.33	10.0
sandy clay	3.20	2.96	9.5
silty clay	3.40	2.59	8.8
clay	3.60	2.22	8.0

Rangeland (Cover Types 31 - 33)

Texture	Available Water (in/ft)	Root Zone (ft)	Water Holding Capacity (in)
sand	1.20	3.33	4.0
loamy sand	1.40	3.33	4.7
sandy loam	1.60	3.33	5.3
fine sandy loam	1.80	3.33	6.0
very fine sandy loam	2.00	3.61	7.2
loam	2.20	3.89	8.6
silt loam	2.40	4.17	10.0
silt	2.55	3.96	10.1
sandy clay loam	2.70	3.75	10.1
silty clay loam	2.85	3.54	10.1
clay loam	3.00	3.33	10.0
sandy clay	3.20	2.96	9.5
silty clay	3.40	2.59	8.8
clay	3.60	2.22	8.0

Forest Land (Cover Types 41 - 43)

Texture	Available Water (in/ft)	Root Zone (ft)	Water Holding Capacity (in)
sand	1.20	8.33	10.0
loamy sand	1.40	7.77	10.9
sandy loam	1.60	7.21	11.5
fine sandy loam	1.80	6.66	12.0
very fine sandy loam	2.00	6.66	13.3

loam	2.20	6.66	14.7
silt loam	2.40	6.66	16.0
silt	2.55	6.33	16.1
sandy clay loam	2.70	6.00	16.2
silty clay loam	2.85	5.67	16.2
clay loam	3.00	5.33	16.0
sandy clay	3.20	4.85	15.5
silty clay	3.40	4.37	14.9
clay	3.60	3.90	14.0

Barren Lands, Confined Feeding Operations (Cover Types 23, 72, 73, 76, 77)

Texture	**Available Water (in/ft)**	**Root Zone (ft)**	**Water Holding Capacity (in)**
sand	1.20	0.50	0.6
loamy sand	1.40	0.50	0.7
sandy loam	1.60	0.50	0.8
fine sandy loam	1.80	0.50	0.9
very fine sandy loam	2.00	0.50	1.0
loam	2.20	0.50	1.1
silt loam	2.40	0.50	1.2
silt	2.55	0.50	1.3
sandy clay loam	2.70	0.50	1.4
silty clay loam	2.85	0.50	1.4
clay loam	3.00	0.50	1.5
sandy clay	3.20	0.50	1.6
silty clay	3.40	0.50	1.7
clay	3.60	0.50	1.8

MODEL APPLICATION

Selection of Model Test Area

We selected the Pheasant Branch Creek watershed, located in rural south central Wisconsin (Figure 4), as a test watershed to apply our recharge model. The Pheasant Branch Creek area has received increasing attention due to concerns over the potential hydrologic impacts associated with increasing development and urbanization within the watershed. It was the focus of recent watershed studies completed by Jeff Steuer and Randy Hunt of the Water Resources Division of the USGS in Middleton, Wisconsin (Steuer, 1999; Hunt and Steuer, 2000). Steuer used the precipitation runoff modeling system (PRMS) (Leavesley et al., 1983) to quantify groundwater recharge rates for the Pheasant Branch Creek watershed. Subsequently, Hunt and Steuer (2000) used these recharge rates in a calibrated groundwater flow model of part of the watershed.

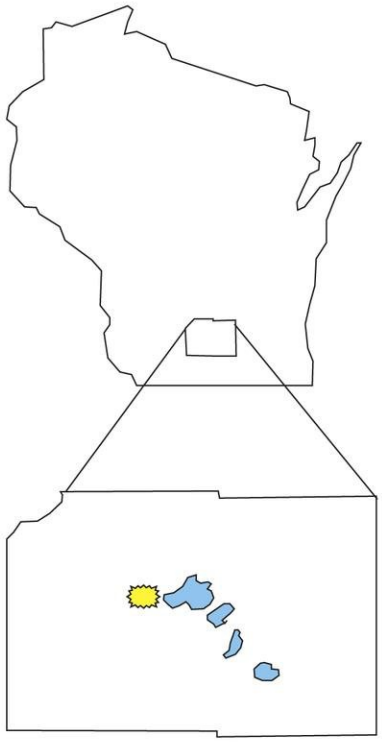

Figure 4: Location of the Pheasant Branch Creek Watershed.

Comparison to the USGS Groundwater Flow Model

Hunt and Steuer (2000) used recharge rates derived from Steuer's PRMS model (Steuer, 1999) in a calibrated steady-state, groundwater flow model of part of the Pheasant Branch Creek watershed. Their flow model, based on a subset of a regional Dane County groundwater model (Krohelski et al., 1999), showed improved calibration compared to the regional model. Their calibrated model used an average recharge rate of 7.96 inches per year.

As an initial test of our model, we used data from a representative year, and compared the average potential recharge estimate to that used in the USGS model.

Monthly precipitation data from the weather station closest to the Pheasant Branch Creek watershed (the Madison airport station) are summarized for 1969 – 1999 in Table 9. The average annual precipitation for the thirty-year period is 32.53 inches. Statistically, the monthly precipitation data in 1977 is the closest to the 30-year monthly and annual averages. Consequently, we used the 1977 data to calculate recharge for the watershed for an average year (Figure 5). The watershed has a mean potential recharge of 7.87 inches per year (or roughly 24% of the annual precipitation) with a standard deviation of 3.6 inches per year. Our mean annual recharge estimate of 7.87 inches compares extremely well with Hunt and Steuer's estimate of 7.96 inches.

Comparison to the USGS PRMS Model

Steuer (1999) used the precipitation runoff modeling system (PRMS) (Leavesley et al., 1983) to model the hydrologic response of the Pheasant Branch Creek area as well as to quantify groundwater recharge rates under the current land cover configuration.

As an additional test of our model, using what we considered to be the most reasonable model parameters, we compared our model output to the results from Steuer's calibrated, more data intensive PRMS model for 1993 – 1995 (Figures 6, 7, and 8). We used the Thornthwaite – Mather equation to calculate the potential evapotranspiration for the three model runs. The recharge patterns for the two models are quite similar, but our recharge estimates are consistently higher than those from the PRMS model for the three years. Our 1994 and 1995 annual estimates exceed the PRMS estimates by 2 – 3 inches, and our 1993 estimates exceed the PRMS estimates by as much as 6 – 7 inches. It should be noted that 1993 was the wettest year in the past thirty years. Although 6 – 7 inches of additional recharge represents a significant quantity of recharge, on a percent basis, it is not significantly larger than the differences between the two models for 1994 and 1995. Without actual field measurements of recharge, it is impossible to determine which of the two models, if either, yields a correct result. The PRMS model was calibrated to streamflow data and the recharge array was used in the groundwater flow model whereas our model, as presented, is completely uncalibrated. This suggests that the PRMS model estimates are more realistic although further testing is clearly needed. Consequently, we are currently making field measurements of recharge across a small watershed in northern Wisconsin where we plan to apply and further test our model to assess both its applicability and validity.

If we are to assume that the PRMS recharge estimates are more realistic, our model either underestimates runoff, underestimates evapotranspiration, or underestimates the soil moisture holding capacity. We modified the model input parameters within reasonable and defensible limits so as to minimize recharge and reran the model for the three years (see Appendix H for a listing of the parameters). We again compared our model output to the PRMS output. The average potential annual recharge dropped from 18.3 inches to 15.6 inches for 1993, from 6.2 inches to 5.7 inches for 1994, and from 10.6 inches to 9.2 inches for 1995. Although these parameters improved the differences between the two models, the new parameters did not change

Table 9

Monthly Precipitation Data for Madison Airport (inches)

	30 year										
Month	**Averages**	**1969**	**1970**	**1971**	**1972**	**1973**	**1974**	**1975**	**1976**	**1977**	**1978**
Jan	1.23	2.26	0.44	1.48	0.40	1.54	2.45	0.98	0.56	0.53	1.03
Feb	1.21	0.18	0.16	2.59	0.42	1.20	1.17	1.54	1.72	1.44	0.24
March	2.30	1.47	1.17	1.52	2.23	5.04	3.43	3.09	4.75	3.03	0.28
April	3.33	2.72	2.53	2.42	2.02	7.11	4.24	4.19	4.80	2.59	3.50
May	3.15	3.45	6.09	0.98	2.83	5.27	5.77	4.57	1.95	2.52	3.96
June	3.78	7.96	2.26	2.27	1.65	0.81	3.86	4.30	1.38	2.63	9.95
July	3.91	4.28	2.42	1.65	3.49	2.68	2.69	6.05	1.46	6.63	4.54
August	4.16	0.96	0.97	3.96	7.47	2.53	4.60	5.25	1.99	5.19	1.63
Sept	3.27	1.35	8.82	1.87	5.26	3.59	1.08	0.84	0.50	2.84	5.44
Oct	2.22	2.65	2.65	1.30	2.42	2.30	3.18	0.64	1.49	1.41	1.11
Nov	2.27	0.70	1.06	3.48	0.86	1.48	1.79	2.79	0.11	2.12	3.05
Dec	1.70	1.66	2.12	3.64	1.91	1.98	1.80	0.29	0.37	1.60	1.71
Annual	32.53	29.64	30.69	27.16	30.96	35.53	36.06	34.53	21.08	32.53	36.44
	30 Year										
Month	**Averages**	**1980**	**1981**	**1982**	**1983**	**1984**	**1985**	**1986**	**1987**	**1988**	**1989**
Jan	1.23	1.11	0.14	1.42	0.53	0.36	1.43	1.02	0.68	1.82	0.61
Feb	1.21	0.64	2.47	0.17	2.26	1.26	1.89	2.72	0.62	0.46	0.57
March	2.30	0.68	0.33	2.11	2.70	1.15	3.13	1.55	1.99	1.20	1.69
April	3.33	2.36	3.42	3.26	2.23	3.86	1.52	2.27	2.46	2.65	1.69
May	3.15	2.08	0.64	4.34	4.21	3.32	3.35	1.97	3.90	0.92	1.72
June	3.78	3.43	4.99	3.40	1.85	7.01	3.06	3.24	1.17	2.06	1.67
July	3.91	2.67	4.81	3.47	1.92	1.96	4.48	4.31	3.26	2.44	4.97
August	4.16	9.49	7.06	2.67	5.05	1.89	2.98	4.38	5.85	2.95	6.46
Sept	3.27	7.84	3.10	1.42	2.85	2.79	5.00	6.82	3.61	3.33	0.89
Oct	2.22	1.13	2.68	1.46	2.59	5.63	4.58	1.85	1.24	1.60	1.88
Nov	2.27	1.33	1.71	4.21	3.18	1.83	5.13	1.03	3.24	3.58	0.98
Dec	1.70	1.62	0.75	3.65	2.30	2.66	2.39	0.69	4.09	1.56	0.26
Annual	32.53	34.38	32.10	31.58	31.67	33.72	38.94	31.85	32.11	24.57	23.39
	30 Year										
Month	**Averages**	**1990**	**1991**	**1992**	**1993**	**1994**	**1995**	**1997**	**1998**	**1999**	
Jan	1.23	1.60	1.17	0.78	1.60	1.46	2.12	1.21	2.24	2.10	
Feb	1.21	0.99	0.44	1.34	1.18	2.76	0.06	2.52	1.44	0.91	
March	2.30	4.18	4.24	1.90	3.29	0.46	2.17	1.54	5.46	0.47	
April	3.33	1.90	4.89	3.17	5.33	2.57	4.14	2.50	4.10	6.91	
May	3.15	5.35	2.20	1.12	3.81	1.33	3.92	1.94	4.58	3.72	
June	3.78	4.88	3.75	1.53	6.67	5.66	1.22	5.23	7.46	5.57	
July	3.91	2.61	5.18	5.54	9.34	4.10	4.36	6.23	2.50	4.49	
August	4.16	6.03	2.34	2.48	5.57	4.56	5.58	2.33	4.24	3.26	
Sept	3.27	1.64	3.96	5.99	3.74	6.14	1.78	1.38	2.48	1.55	
Oct	2.22	2.25	5.35	1.06	0.91	0.65	4.29	1.23	3.20	0.88	
Nov	2.27	1.65	3.86	4.83	1.55	2.77	3.17	1.25	1.95	1.21	
Dec	1.70	3.46	1.71	2.39	0.35	1.08	0.77	1.25	0.29	0.86	
Annual	32.53	36.54	39.09	32.13	43.34	33.54	33.58	28.61	39.94	31.93	

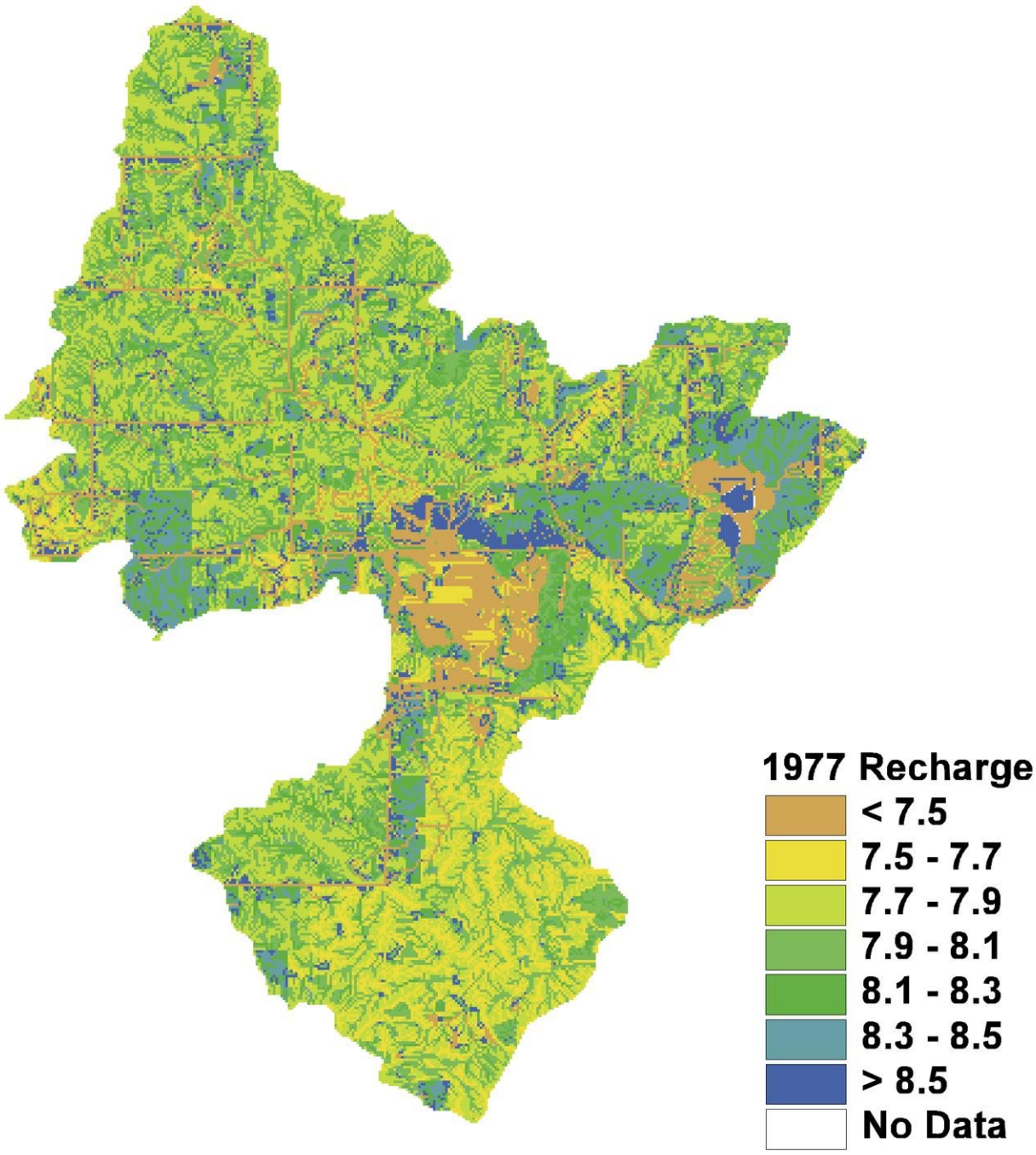

Figure 5: Recharge distribution (in inches) for the Pheasant Branch Creek Watershed for an average year (1977 data).

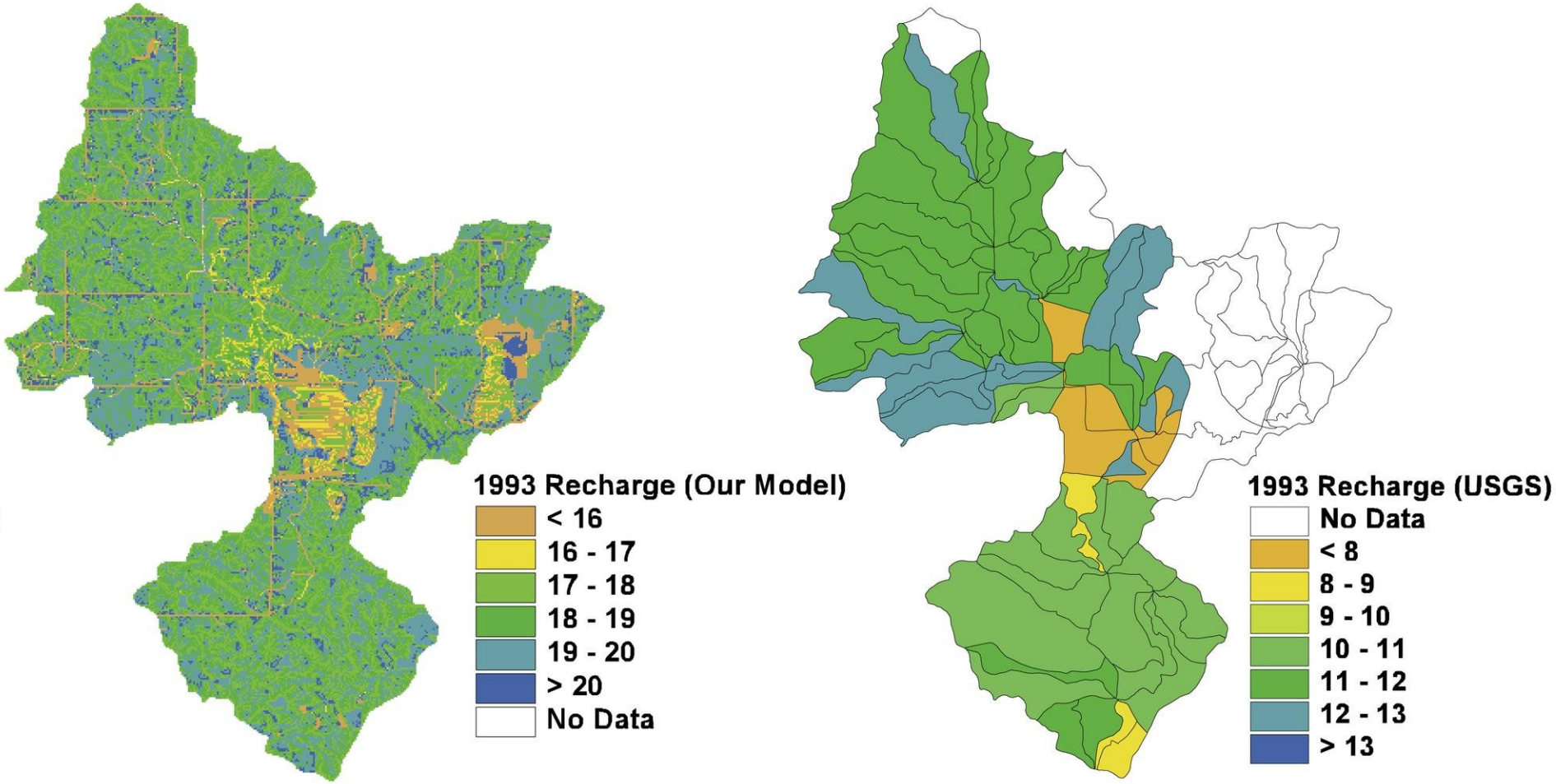

Figure 6: Comparison between the recharge estimates from our model and the estimates from the USGS model for 1993. (Recharge is in inches)

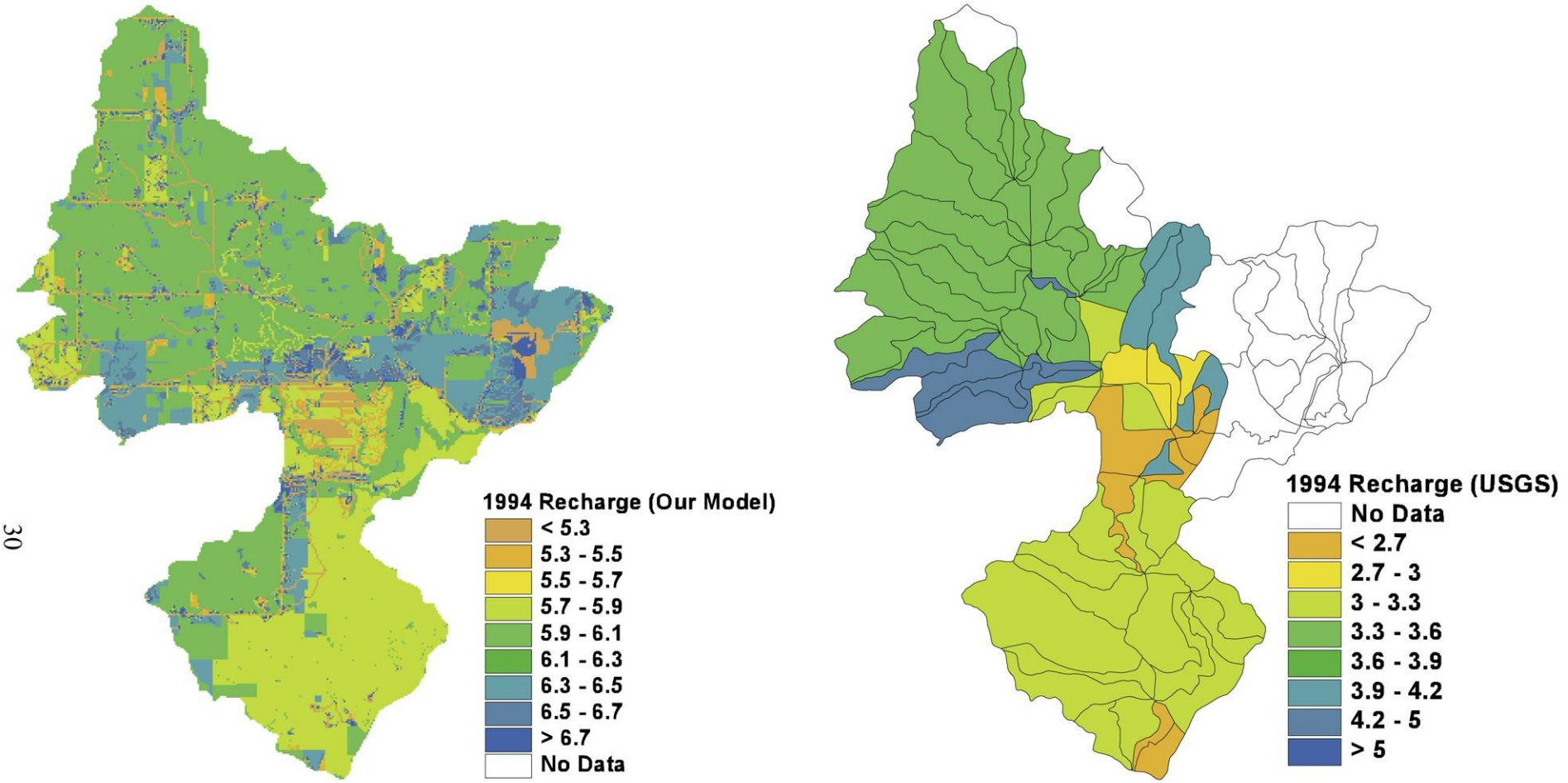

Figure 7: Comparison between the recharge estimates from our model and the estimates from the USGS model for 1994. (Recharge is in inches)

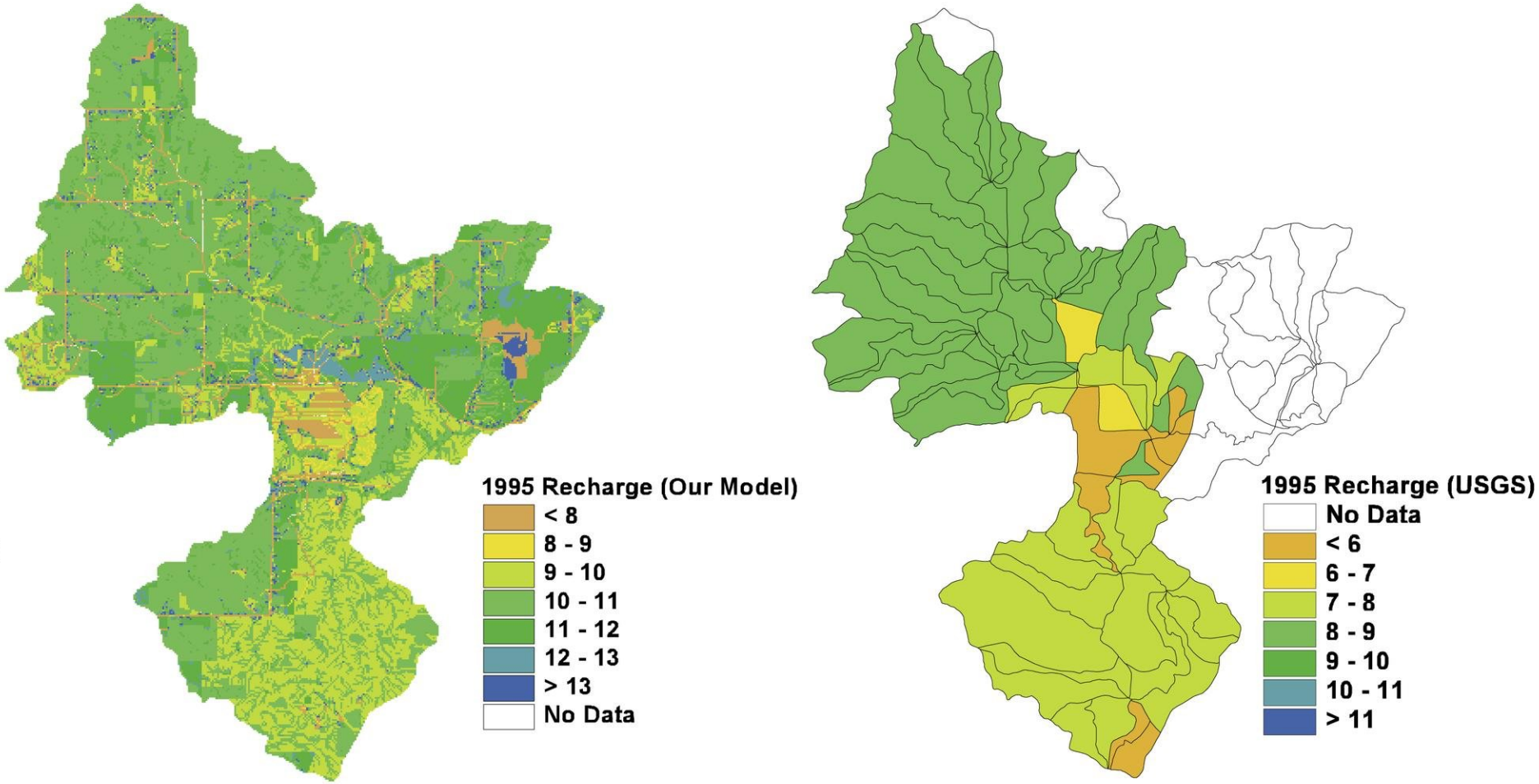

Figure 8: Comparison between the recharge estimates from our model and the estimates from the USGS model for 1995. (Recharge is in inches)

the results significantly, and the model still yields slightly higher recharge estimates relative to the USGS estimates.

We believe our original model parameters are the most reasonable, and for an uncalibrated model, our model still compares reasonably well with the PRMS model and provides similar spatial recharge arrays for the watershed and comparable ballpark estimates of groundwater recharge. The rest of the model discussion is based on model runs that use these original model parameters and use the Thornthwaite – Mather equation to calculate evapotranspiration unless otherwise specified.

Range of Recharge Rates for the Pheasant Branch Creek watershed

In Wisconsin, groundwater modelers sometimes assume an empirical relationship between rainfall and recharge and have found, through calibration, that a recharge estimate on the order of 25 – 33.3 % of the annual precipitation typically provides a reasonable fit for matching stream discharge data in their models. Modelers treat recharge simply as a calibration parameter and adjust it to match streamflow without any other physically-based constraints. If the model discharge estimates are too low and more water is needed in the system, recharge is increased. If the model discharge estimates are too high and less water is needed, recharge is decreased. Our 1977 model results support an empirical estimate of 25% of the precipitation and provide potentially a physical basis to justify using this "rule of thumb" for estimating recharge for a "typical" year in this watershed. The mean potential recharge of 7.9 inches is 24% of the annual precipitation.

We also ran our model using data from the wettest (1993) and the driest (1976) year of the past thirty years in an effort to quantify the potential range of recharge that planners, policy makers, and modelers might expect for the watershed. This type of information could be critical for future water resource planning and could be used by a watershed commission to help establish a management plan that accommodates the range of feasible recharge scenarios. The additional model runs also allowed us to test the 25% empirical estimate over the likely range of annual precipitation**.** According to the model, the mean potential recharge for the wettest year is 18.2 inches per year (or roughly 42 % of the annual precipitation) with a standard deviation of 5.6 inches per year (Figure 9). The mean potential recharge for the driest year is 3.9 inches per year (or roughly 18 % of the annual precipitation) with a standard deviation of 2.4 inches per year (Figure 10). Based on the model, annual recharge has varied substantially over the past thirty years, ranging from less than 4 inches to greater than 18 inches a year. The model provides a means for water resource planners to quantify groundwater recharge on an annual basis and potentially use the model output to help guide and modify yearly water management practices to ensure adequate water supplies and sustainable water practices.

The model results suggest that a 25% fixed percentage empirical relationship between precipitation and recharge for Wisconsin may be inappropriate. Although the 25% estimate appears reasonable for the "typical" year, it might significantly underestimate recharge for a wet year (as much as 18% according to the model) and overestimate recharge for a dry year (as much as 6% according to the model). Not only does the amount of recharge increase with increasing

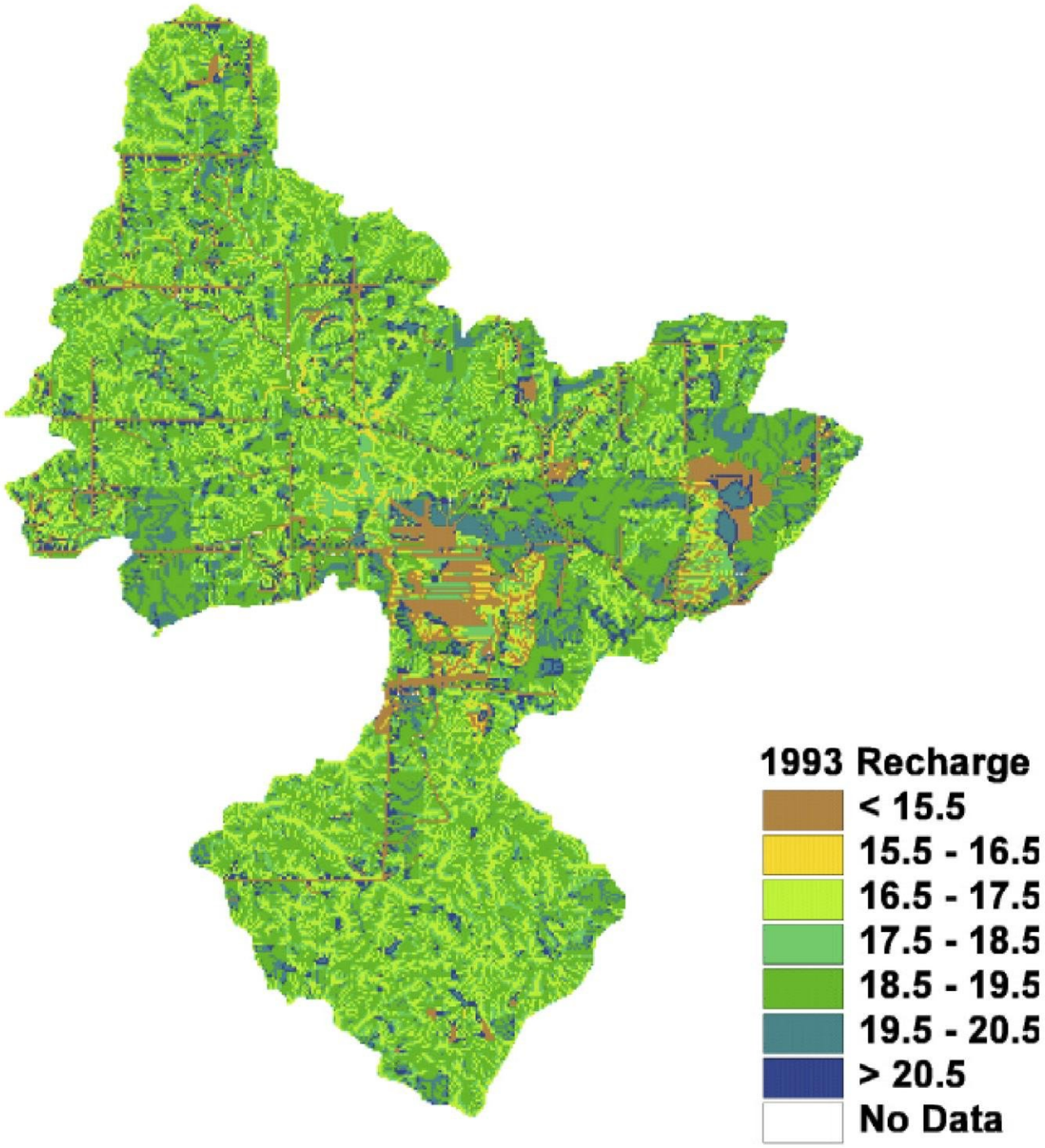

Figure 9: Recharge distribution (in inches) for the Pheasant Branch Creek Watershed for the wettest year in the past thirty years (1993 data).

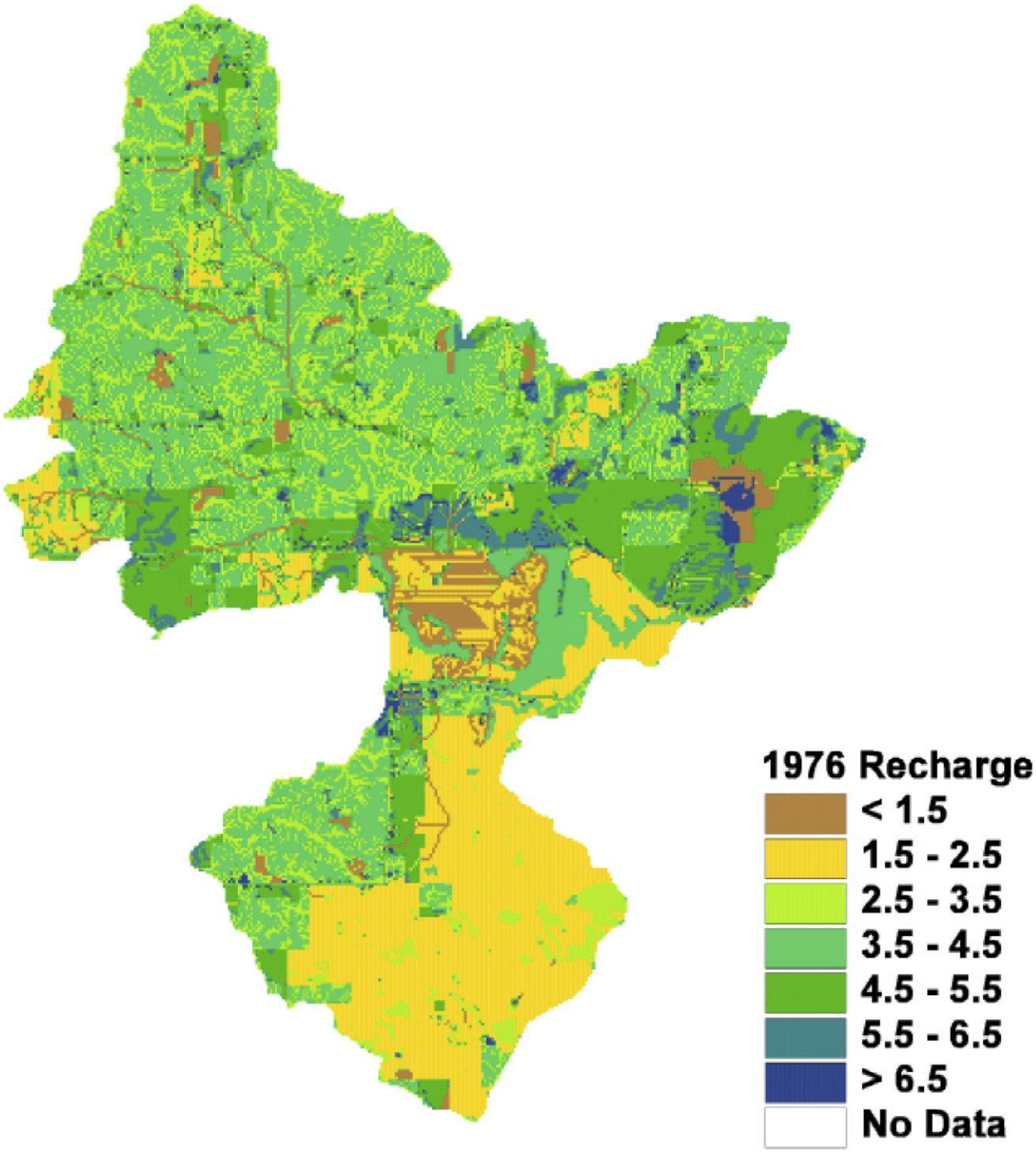

Figure 10: Recharge distribution (in inches) for the Pheasant Branch Creek Watershed for the driest year in the past thirty years (1976 data).

precipitation, which is to be expected, but the percentage of rainfall that becomes recharge also seems to increase with increasing precipitation. It should be noted that we are modeling "potential recharge" and not necessarily "actual recharge". There will be discharge areas as well as certain areas within a watershed with a shallow water table where the potential recharge fully saturates the system and causes the water table to meet the land surface. In these regions, some or all of the recharge will be "refused" and become runoff, and the actual recharge will be less than the potential recharge. Our model does not consider the depth to the water table or the presence of discharge areas in our recharge estimates.

The watershed requires a certain threshold volume of water that must be satisfied before recharge occurs. In a dry year, the majority of the precipitation goes towards satisfying that threshold, and subsequently a smaller percentage of the precipitation becomes recharge. In a wet year, the reverse holds true; the same volume of water, which represents a smaller percentage of the total precipitation, goes towards satisfying the threshold such that a larger percentage of the annual precipitation becomes recharge. Using a fixed percent estimate for recharge is thus both unreliable and in many cases inaccurate.

Recharge is one of the most complex components of the hydrologic budget and is dependent on a large number of variable, interactive parameters. Although there is a general correlation between the annual precipitation and the annual recharge, it is simply inappropriate to use a fixed percentage to estimate recharge. Physically-based models, like the one we have developed, are necessary to provide accurate recharge estimates. Although not as straightforward as using a fixed percentage, our model is easy to use, utilizes readily available data, and can provide results within a timely manner.

Spatial Variability

Due to the complexity and uncertainty of estimating recharge distributions, groundwater modelers usually disregard recharge heterogeneity and use a single estimate of groundwater recharge for their model area. The recharge estimate is often either empirically derived, is a fitted parameter determined by calibration, or is calculated using stream baseflow as a surrogate.

Recharge is influenced by a wide variety of factors including the vegetation, topography, climate, and the soils. Since the distribution, rate, and timing of recharge are dictated by the interaction of these variable parameters, recharge will vary at the watershed scale such that the use of a single estimate for an entire watershed may be inappropriate.

Our model computes recharge on a grid cell - by - grid cell basis and is thus capable of representing the spatial distribution of recharge within a watershed. Figure 11 presents the 1977 model recharge array expressed as an absolute percent deviation from the mean recharge. The mean deviation for all model grid cells is 9 %, with the majority of the grid cells within 5% of the mean. The lack of significant variability suggests that the use of a single recharge estimate for the entire watershed may be acceptable in this case, particularly for more regionally based studies. The modeled recharge array for the wettest year (1993) (Figure 12) yields a similar result, with a mean deviation of 10% and the majority of the grid cells within 5% of the mean.

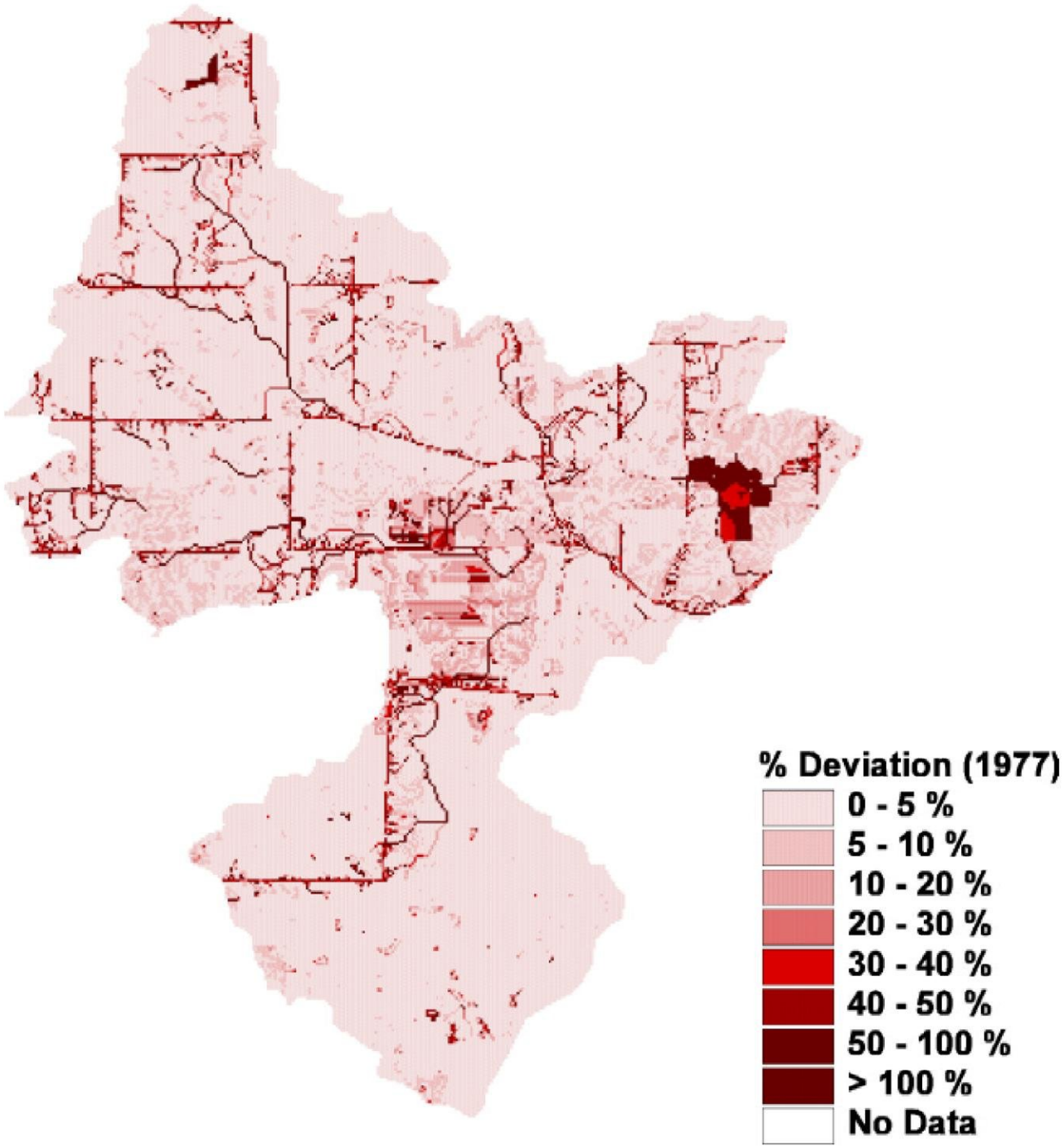

Figure 11: Absolute value of the percent deviation from the mean recharge value for the 1977 data.

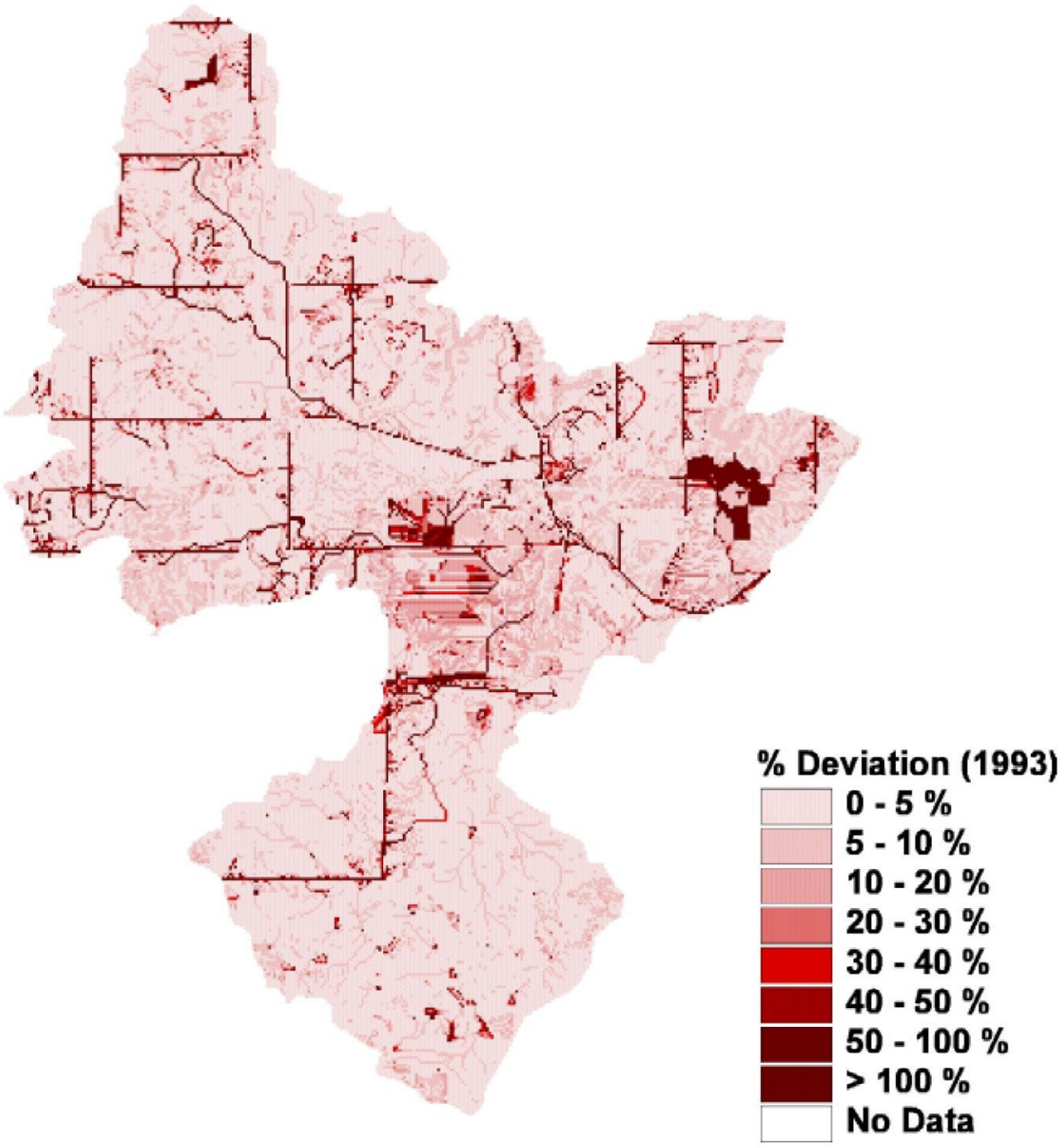

Figure 12: Absolute value of the percent deviation from the mean recharge value for the 1993 data.

There are, however, select areas within the 1977 and 1993 recharge arrays (Figures 11 and 12) where the deviation exceeds 100%. Standard, single estimate recharge techniques are not able to identify these areas. For site-specific analyses that involve nutrient cycling, contaminant transport, or detailed water budgets, use of the mean recharge in these select areas would produce erroneous results. Although it appears for a regional study that we may be able to ignore recharge variability in the Pheasant Branch Creek watershed for the "typical" and wetter years, recharge does vary within the watershed (Figures 11 and 12), and in certain areas and instances the variability is significant such that it can not be ignored.

The dry scenario (1976) yields a very different result (Figure 13). The mean deviation is 28%, with a large number of the grid cells in excess of a 30% difference. In this case, it is inappropriate to use a single estimate of recharge for the watershed, given the recharge variability present. Results from a study that ignores this variability become suspect.

The increase in variability for the drier year is expected. In drier years, the soil system is infrequently saturated such that differences in the soil moisture holding capacity of the various land cover and soil texture combinations play a more critical role in controlling the recharge distribution. In wetter years, when the system is saturated more frequently, these differences are less relevant, and the recharge distribution becomes more homogeneous.

Our model not only provides a means to identify those areas within a watershed that differ from the mean, but also produces recharge estimates for all grid cells within the watershed. The resulting spatial distribution of groundwater recharge can be input directly into a groundwater flow model. The use of a spatially variable recharge array in flow models is both a conceptual and physical improvement on how recharge is often represented in groundwater models.

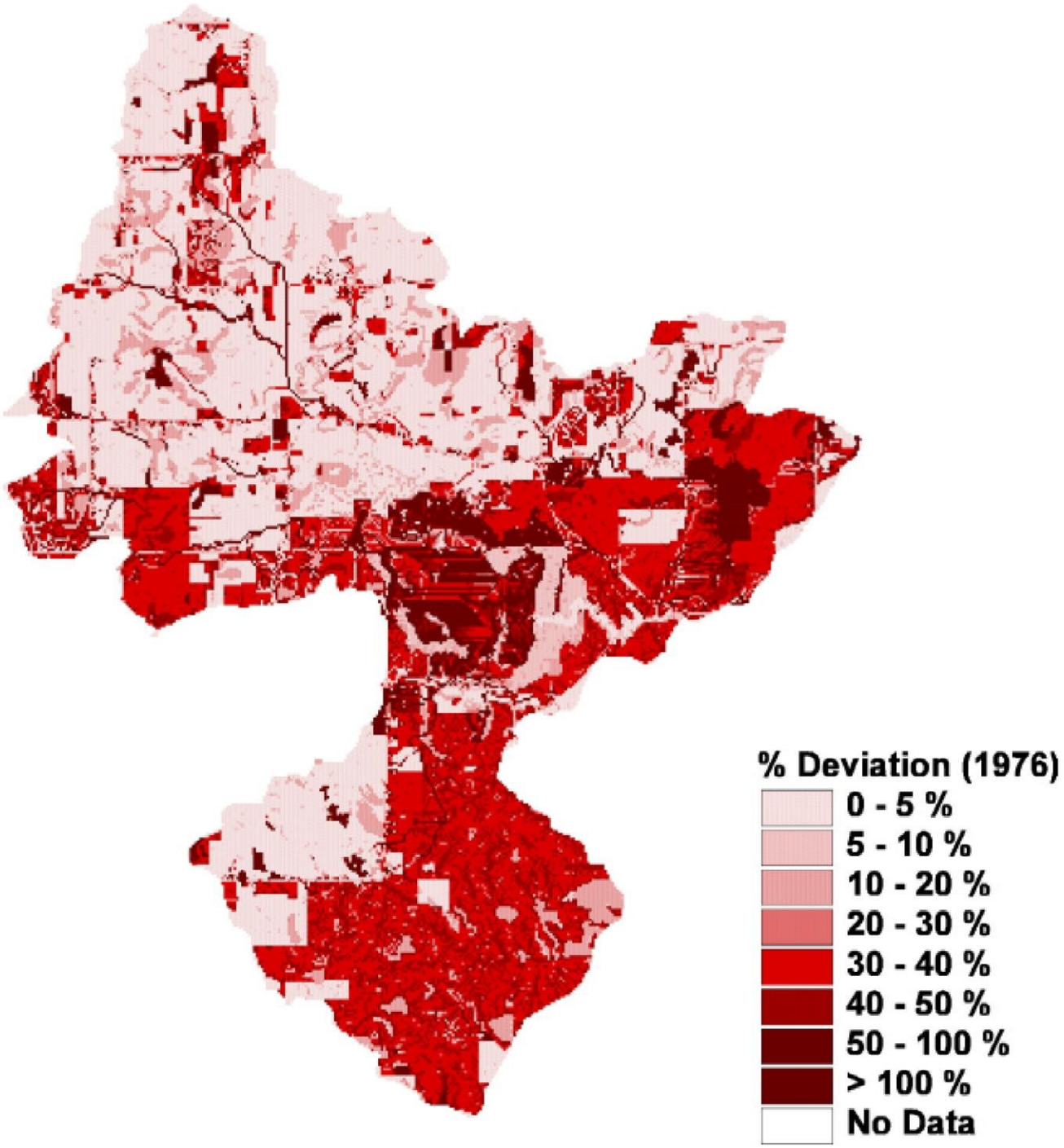

Figure 13: Absolute value of the percent deviation from the mean recharge value for the 1976 data.

SENSITIVITY ANALYSIS

We ran a number of model scenarios to assess the sensitivity of our model to various model parameters including the soil moisture storage coefficient, the curve number, and the grid cell size. In addition, we calculated and compared recharge estimates using the four different evapotranspiration equations. We assumed that the soil texture, land cover, and digital elevation data are correct and did not assess the sensitivity of the model to potential errors in these inputs.

Soil Moisture Storage Coefficients

The model is not very sensitive to changes in the soil moisture storage coefficients. The coefficients used in the model were modified from tables presented in Thornthwaite and Mather (1957). We ran two model scenarios using the 1977 data to test the sensitivity. In one model, we increased all the soil moisture storage coefficients by one inch, and in the other we decreased the coefficients by one inch. We felt a ± 1 inch sensitivity range was reasonable for this parameter. This span represents a range of at least ± 10% of the original value for all soil and land cover combinations except for select soil textures in the forest cover type where it is only 6%.

We compared the output arrays from the two model runs to the original recharge array by calculating a percent difference for each cell and then plotted the average of the absolute differences between the modified and original arrays (Figure 14). The recharge pattern and estimates for all but a few tiny areas of the watershed are essentially unaffected by the change (< 5% difference).

SCS Curve Numbers

The model is not particularly sensitive to changes in the SCS curve numbers. Using the 1977 data, we ran two model scenarios: one in which we increased all the curve numbers by 5, and another in which we decreased all the curve numbers by 5. Curve numbers cannot be negative or exceed 100. If the addition or subtraction of 5 yielded a number outside the acceptable bounds, the curve number was modified to the appropriate upper or lower bound. The original curve number estimates used in the model are taken from the literature and are well established. These estimates are fairly consistent between sources, with disparities between references for various land cover / soil texture combinations rarely exceeding 5. Consequently, we felt a span of ± 5 was a reasonable range to test.

We compared the output arrays from the two model runs to the original recharge array and plotted the average of the absolute differences between the modified and original arrays (Figure 15). All but a small portion of the watershed is essentially unaffected by the change (< 5% difference). Those areas with changes greater than 5 % are areas of low recharge where a small change in quantity converts to a more marked change in percentage. In addition, the low recharge areas typically have high curve numbers, and the ± 5 change for a high curve number in a low recharge area translates to a larger change in the recharge value relative to the same ± 5 change for a lower curve number (Figure 16).

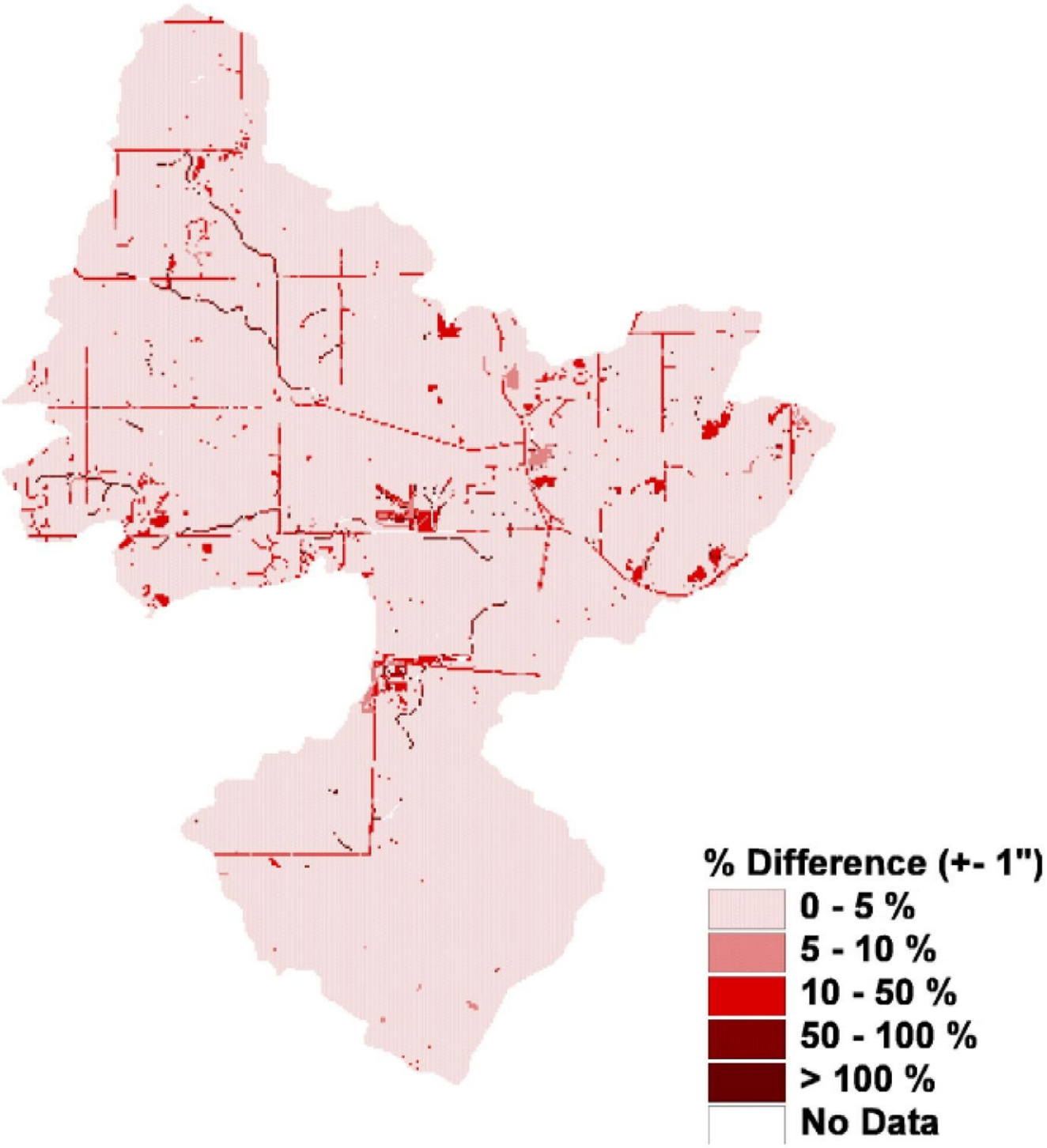

Figure 14: Sensitivity of recharge estimates to changes in the maximum soil moisture storage parameters. Absolute value of the average difference for a change of plus or minus 1 inch.

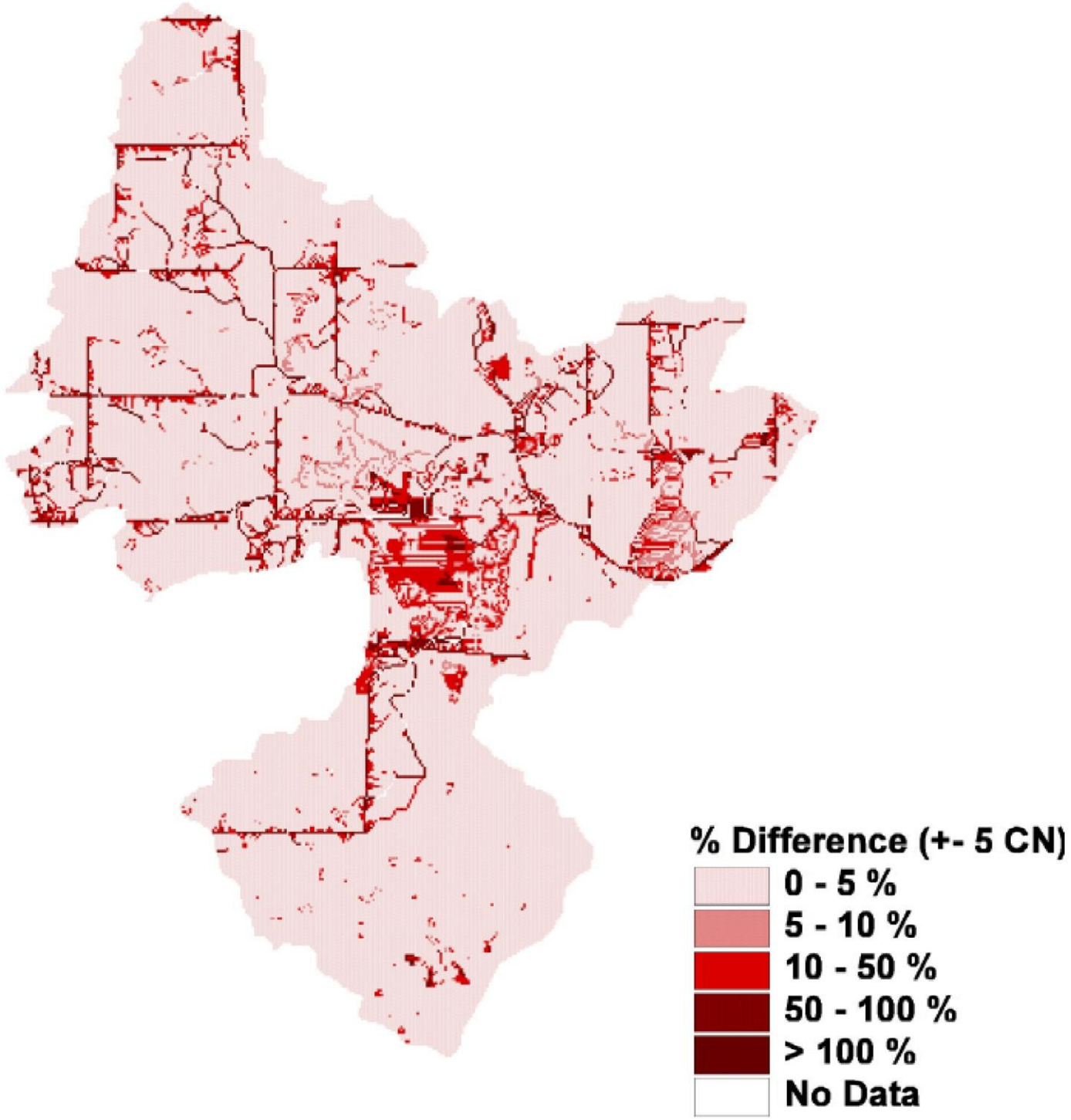

Figure 15: Sensitivity of recharge estimates to changes in curve number. Absolute value of the average difference for a change of plus or minus 5.

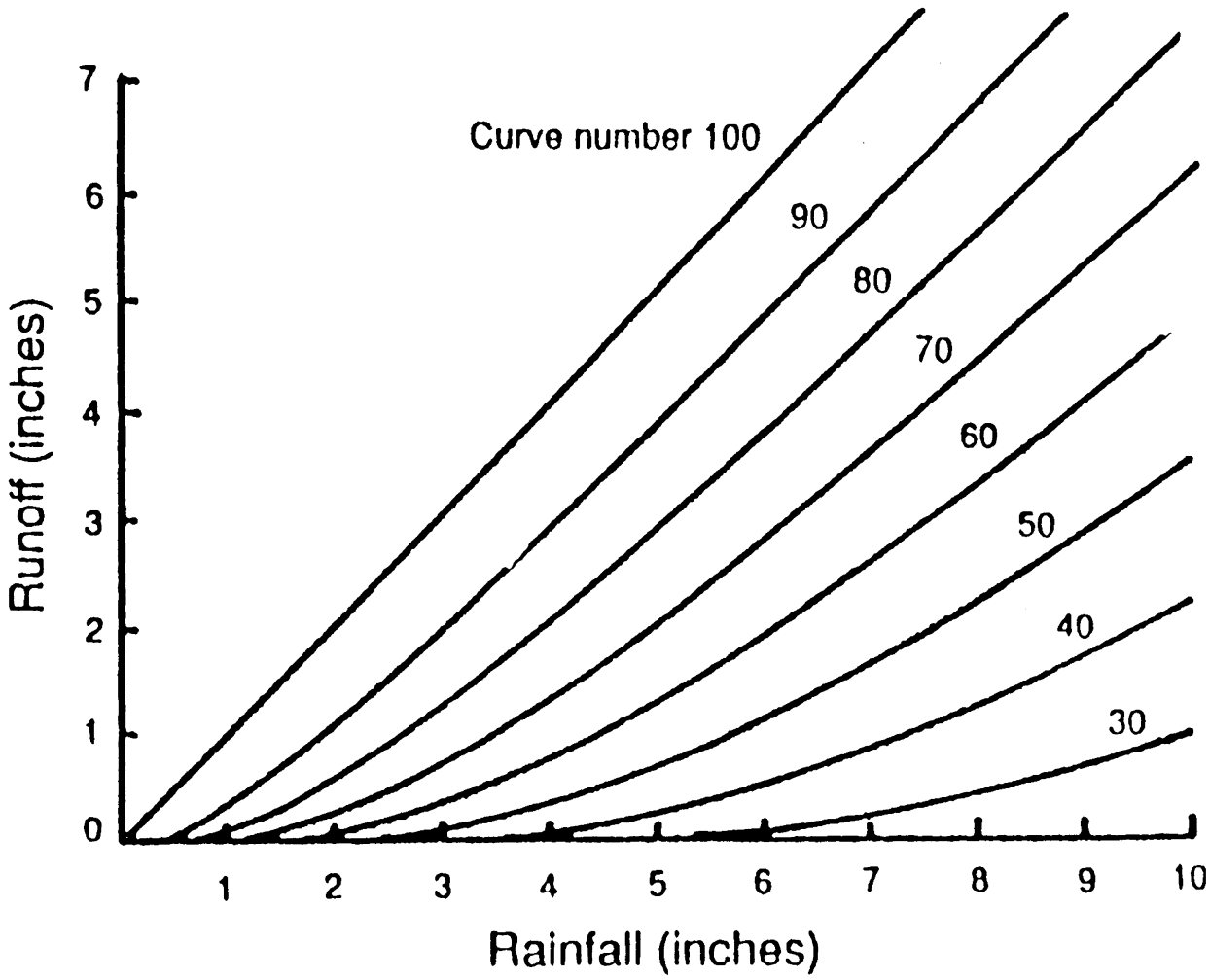

Figure 16: Graphical form of the SCS Curve Number Method (Maidment, 1993)

Model Grid Cell Size

We ran the model for three common grid spacings (30 meters, 75 meters, and 500 meters) using the 1977 data to assess the impact, if any, of the cell size on the recharge estimates and distribution. We did not expect the model to be particularly sensitive to the grid spacing although some previous recharge models (Stoertz and Bradbury, 1989) have been shown to be sensitive to the model cell size, with recharge estimates increasing with decreasing grid spacing (Anderson et al., 1997).

For our model, the cell size does not have a significant impact on either the estimates or the distribution of recharge. The 75 meter recharge array is almost identical to the 30 meter array (Figure 17). Differences between the two arrays are likely due to the resampling algorithm used to generate the grids in ArcView, and not a function of the model design. There is no consistent increase or decrease in the recharge estimates with changing cell size; some of the cells show a slight increase while others show a slight decrease. The mismatches between the arrays occur in the more heterogeneous regions of the watershed where different land cover / soil texture combinations are in close proximity. ArcView re-samples using a nearest neighbor approach which typically does a poor job characterizing heterogeneous regions. The differences are more accentuated in the 500 meter array in which a single nearest neighbor node, and not a statistical average, is being used to characterize a larger area (Figure 18). Ideally, the model should be run at a spacing consistent with the coarsest grid spacing of the model input grids (DEM, soil texture, land cover) to ensure reliable output.

Model Time Step

Previous researchers (Howard and Lloyd, 1979; Houston, 1982; Steenhuis, 1986; Taylor and Howard, 1996) have found that using a monthly time step for recharge modeling can lead to an underestimation of the net recharge. Short periods of recharge are often masked by the averaging effect of long time steps. We are in the process of modifying the model to run at a weekly, instead of a monthly, time step to see what impact the time step has, if any, on our recharge estimates.

Evapotranspiration

We ran our recharge model using each of four different evapotranspiration equations for a one-year period. Initially, we wanted to use data from 1977 (representative of a typical year), but many of the climatic parameters required for the various equations were unavailable for that year. Instead, we used data from 1994, which climatically also was a relatively typical year for the area (Table 9). Figure 19 is a plot of monthly potential evapotranspiration (pET) in 1994 calculated using the four methods. The overall patterns of monthly pET are similar for the four equations (fairly symmetric curves with pET peaking during the summer months), but the magnitude of the estimates vary between methods. The Blaney – Criddle estimates are significantly higher than the other three estimates, particularly during the summer months. We are more inclined to use the pET estimates from either the Turc, Thornthwaite – Mather, or Jensen – Haise equations for our water budget calculations since they produce similar estimates. The Thornthwaite - Mather estimates lag slightly behind the Jensen – Haise and Turc estimates

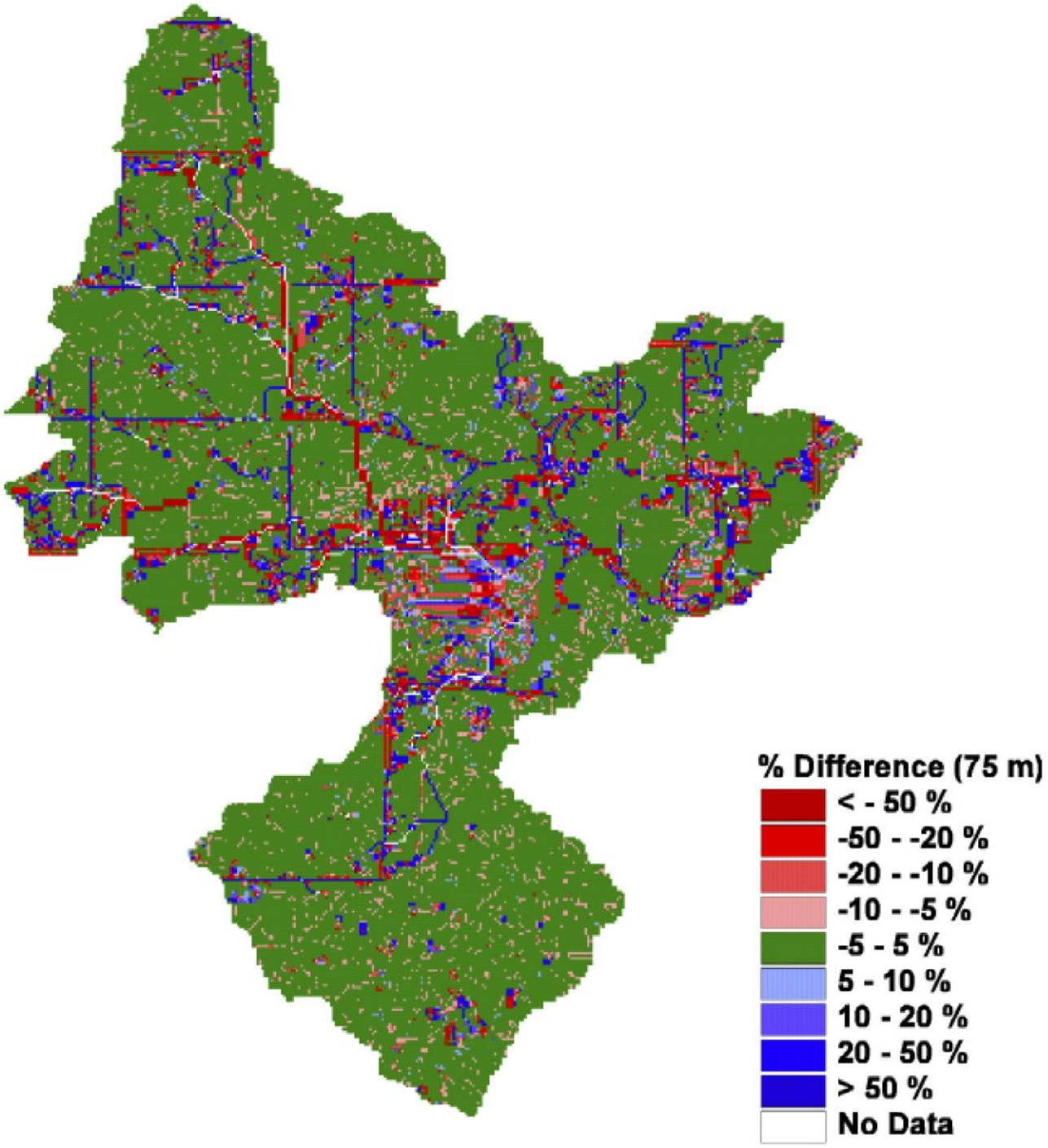

Figure 17: Difference in modeled recharge values between a 30 m grid spacing and a 75 m grid spacing

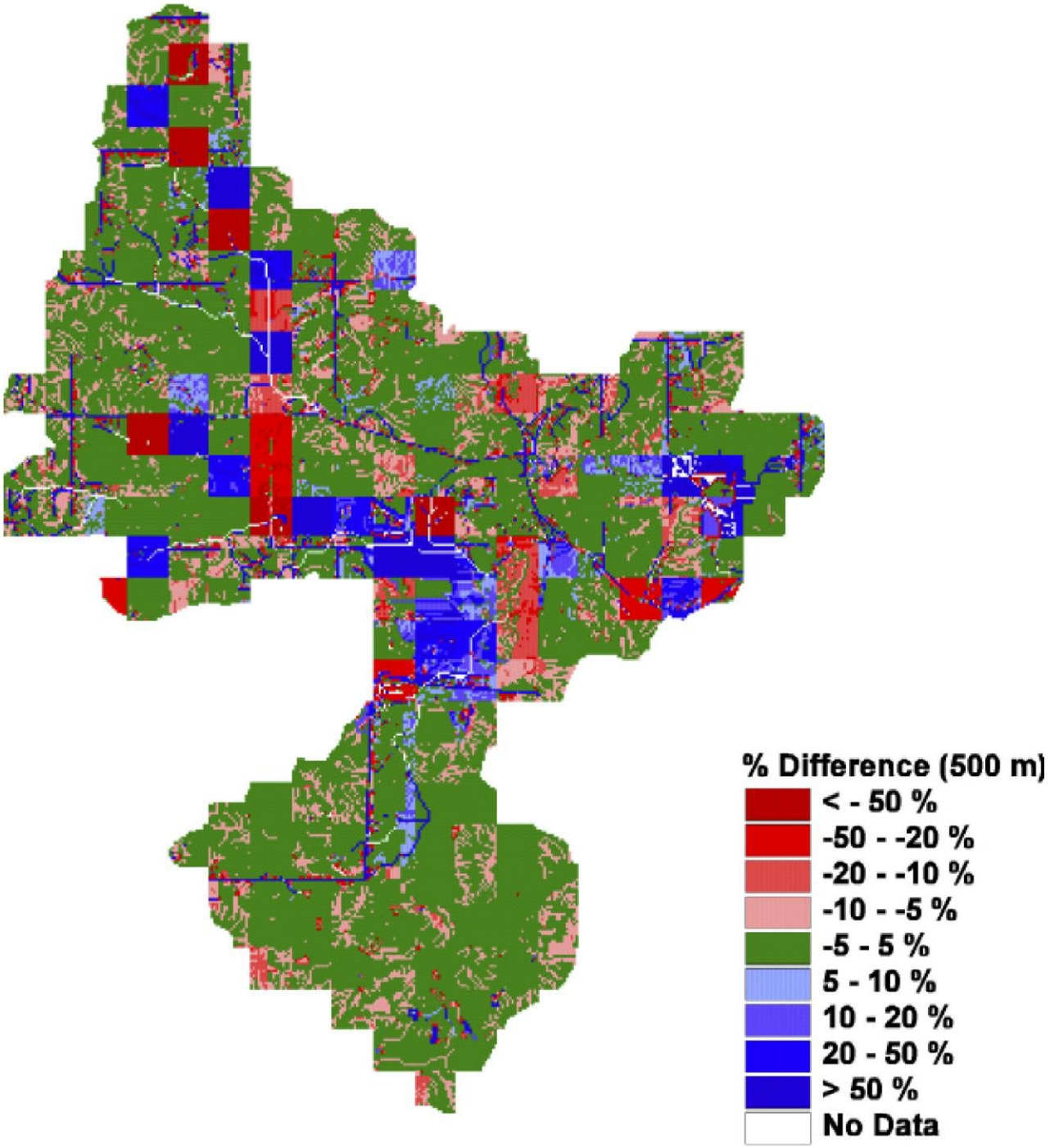

Figure 18: Difference in modeled recharge values between a 30 m grid spacing and a 500 m grid spacing

(Figure 19), which may be attributed to the fact that temperature lags seasonally behind solar radiation (Federer et al., 1996). Federer et al. (1996) also found that the Jensen – Haise method tends to give slightly higher estimates than both the Thornthwaite – Mather and Turc methods which agrees with our findings (Figure 19). Despite the subtle differences, the pET estimates are quite comparable among the Thornthwaite – Mather, Jensen – Haise, and Turc techniques.

The average annual recharge for the watershed using the four methods (Thornthwaite – Mather, Turc, Jensen – Haise, and Blaney – Criddle) is 6.19 inches (21% of the annual precipitation), 6.88 inches (23% of the annual precipitation), 5.29 inches (18% of the annual precipitation), and 0.66 inches (2% of the annual precipitation) respectively. The first three methods give comparable, seemingly reasonable results; the Blaney Criddle method yields ostensibly unrealistic recharge estimates that are dramatically lower than other three. Due to its unreasonably low estimates and inconsistency with the other results, we do not include the Blaney – Criddle method in the rest of our analysis and discussion.

We selected the Thornthwaite – Mather pET equation as the model default based on its ease of use, limited data requirements, and its ability to provide consistently reasonable pET estimates. Although the magnitude of the average recharge value varies among the three methods (from 18 – 23% of the annual precipitation), the recharge pattern generated by the Thornthwaite – Mather, Turc, and Jensen – Haise methods is essentially identical. We created a variability array for each of the three methods by plotting the difference between each grid cell's recharge estimate and the mean recharge for the entire watershed. We then compared the spatial recharge patterns among the methods by plotting the difference between the variability arrays of both the Thornthwaite – Mather and Turc scenarios and the Thornthwaite – Mather and Jensen – Haise scenarios (Figures 20 and 21). For all but a few cells, the differences are less than ± 5 %.

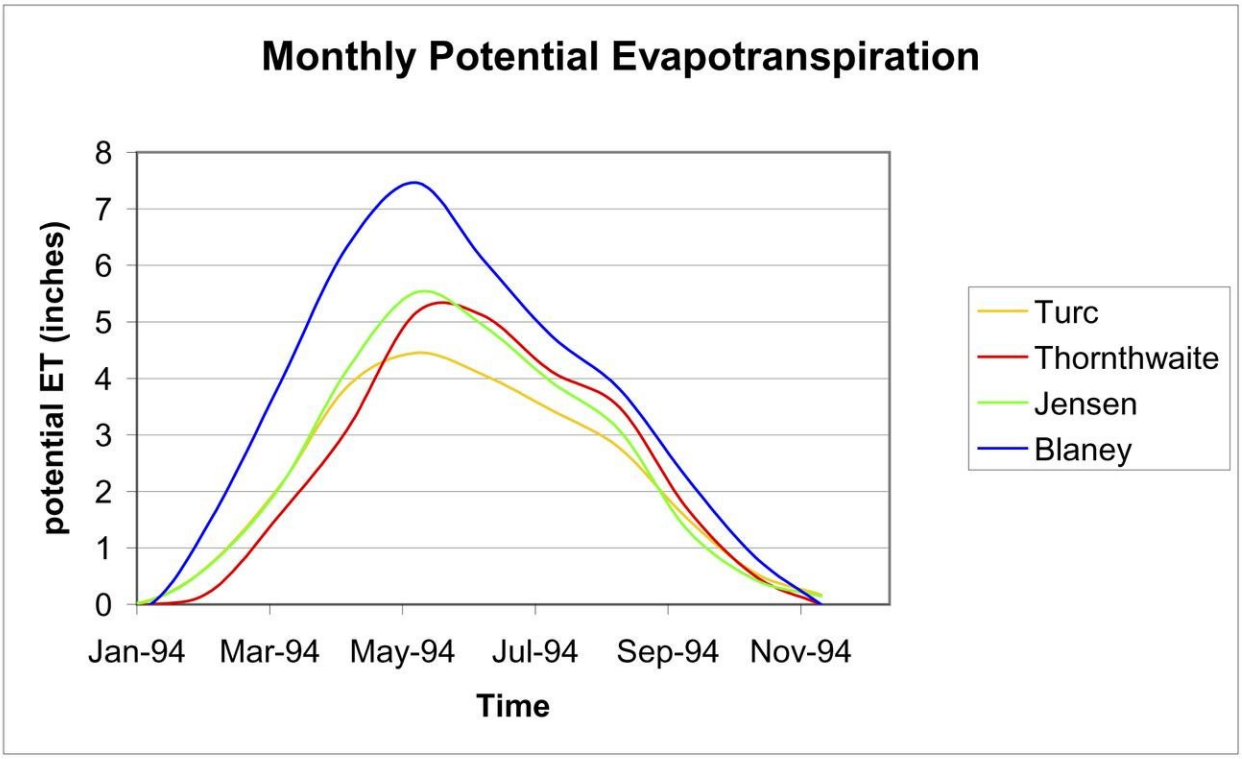

Figure 19: Estimates of potential evapotranspiration for 1994 using four different evapotranspiration equations.

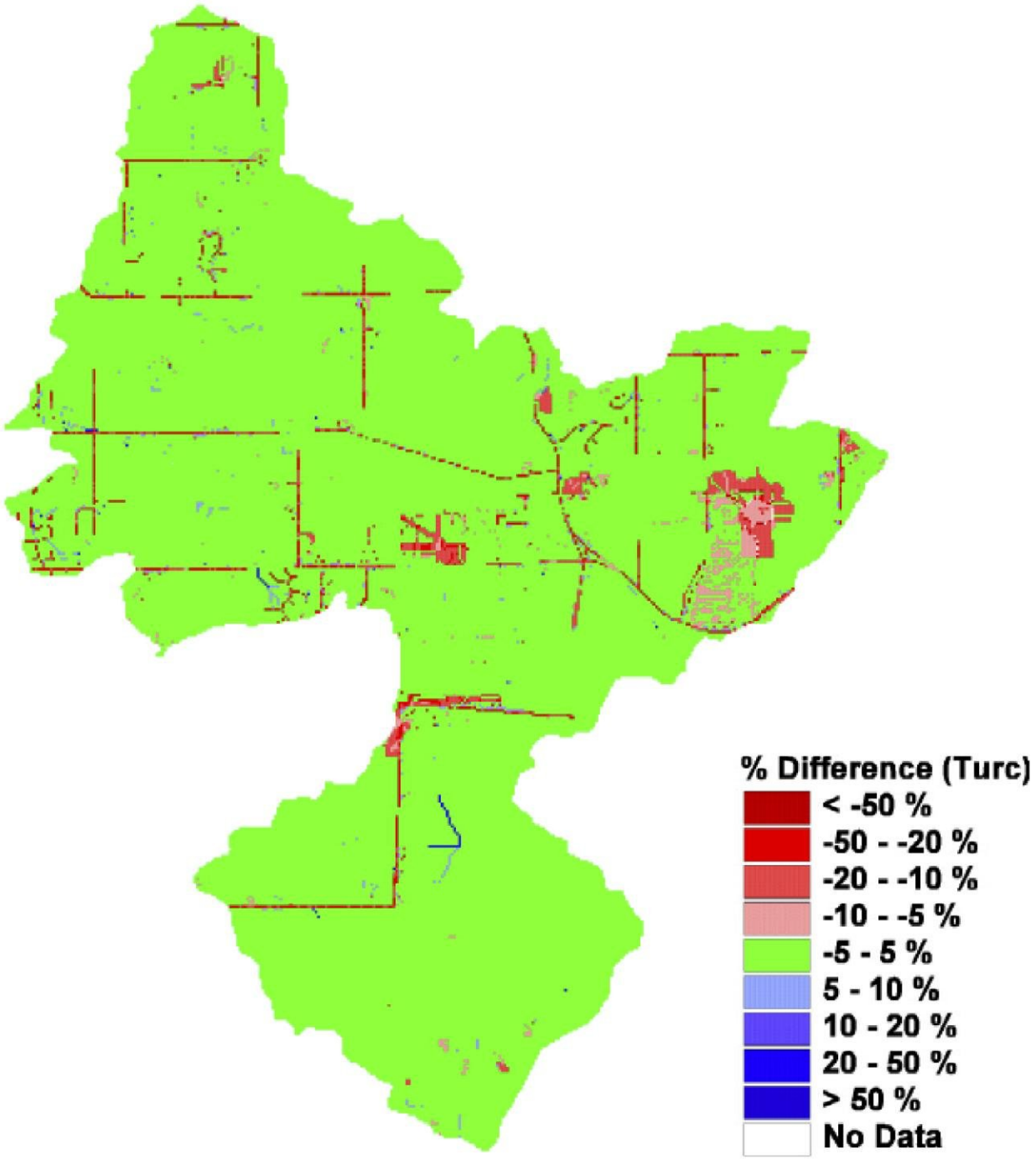

Figure 20: Comparison between the Thornthwaite - Mather spatial recharge variability and the Turc spatial recharge variability. Expressed as a percent difference between the two variability plots.

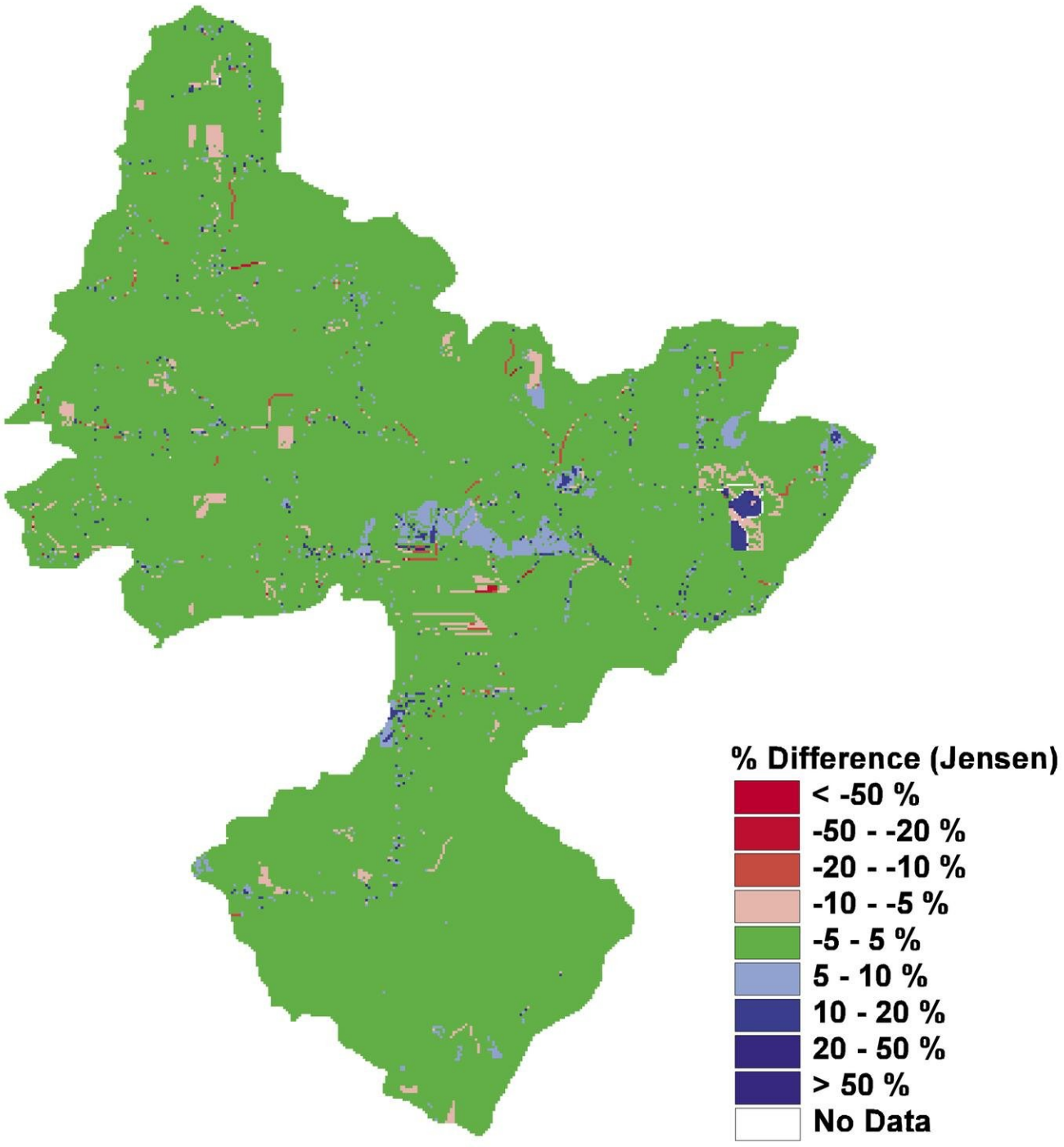

Figure 21: Comparison between the Thornthwaite - Mather spatial recharge variability and the Jensen - Haise spatial recharge variability. Expressed as a percent difference between the two variability plots.

SUMMARY

Synopsis

We have developed a new recharge model to estimate the annual spatial distribution of groundwater recharge for watersheds in humid areas. The model operates on a monthly time step and couples a modified Thornthwaite – Mather soil-water balance with a digital elevation model.

We applied the model to the Pheasant Branch Creek watershed in Middleton, Wisconsin. The output compares reasonably well with that of more rigorous USGS models, and, in most instances, provides similar spatial recharge arrays for the watershed and comparable ballpark estimates of groundwater recharge. The following key points summarize our findings:

- Conceptually, our model is a marked improvement over existing water balance models as it allows for routing and downslope infiltration of surface runoff.

- Our model calculates recharge on a cell-by-cell basis, and consequently can represent the spatial distribution of recharge, which few other models consider.

- The model is physically-based, does not require extensive parameterization, uses typically available data, and can be practically applied in a relatively short time frame.

- The model output was not particularly sensitive to the soil moisture storage coefficient, the SCS curve numbers, or the grid spacing.

- Our model results suggest that a common approach of estimating recharge in Wisconsin using a fixed percentage empirical relationship between precipitation and recharge may be inappropriate in many instances. Not only does the amount of recharge increase with increasing precipitation, which is to be expected, but the percentage of rainfall that becomes recharge also seems to increase with increasing precipitation.

- The model results show that recharge can vary across a watershed such that the use of single estimate of recharge for an entire watershed may be inappropriate. This variability appears to be larger for drier years.

Overall, this new model presents modelers, planners, and policy makers with a practical tool for generating spatially-distributed recharge estimates for modeling and water resource planning purposes. The use of a spatially variable recharge array in flow models is both a conceptual and physical improvement on how recharge is typically represented in groundwater models.

Suggestions for Future Work

We have identified a number of areas of suggested future work that would help improve the model:

1. The model currently does not account for the spatial variability of meteorological parameters and assumes that all meteorological data are uniform across the model area. Since our estimates of evapotranspiration (ET) are based on these meteorological parameters, we further assume that ET does not vary across the watershed. The model could be refined to account for ET variability. Specifically, the Turc and Jensen-Haise methods are radiation-based approaches that require an estimate of albedo to calculate ET. In the current model we assign a single albedo estimate of 0.23 to the entire watershed. In reality, albedo is a function of the land surface and will vary spatially and temporally with changing land cover type and snow cover. The model could be refined to accommodate both differences and changes in albedo.

2. The model currently operates at a monthly time step. Previous researchers (Howard and Lloyd, 1979; Houston, 1982; Steenhuis, 1986; Taylor and Howard, 1996) have found that using a monthly time step for recharge modeling can lead to an underestimation of the net recharge. We are in the process of refining our model to run at a weekly time step to test the sensitivity of the model to the model time step. If the model appears to be sensitive to the time step, the model could also be modified to run at a daily time step as well.

3. The model has only been tested at one test site. Although it performed reasonably well, the model still needs to be tested at other sites. We are in the process of applying the model to the Allequash Watershed of Vilas County in Northern Wisconsin where we have independent field estimates of recharge. We also hope to apply the model to all of Dane County some time in the near future. Others have expressed interest in possibly using the model to estimate recharge for the Central Sand Plains region.

REFERENCES

Adar, E.M., Neuman, S.P., and Woolhiser, D.A., 1988. Estimation of Spatial Recharge Distribution Using Environmental Isotopes and Hydrochemical Data, I. Mathematical Model and Application to Synthetic Data. *J. of Hydro*. 97: 251-277.

Adar, E.M. and Neuman, S.P., 1988. Estimation of Spatial Recharge Distribution Using Environmental Isotopes and Hydrochemical Data, II. Application to Aravaipa Valley in Southern Arizona. *J. of Hydro*. 97: 279-302.

Anderson, J.R., Hardy, E.E., Roach, J.T., and Witmer, R.E., 1976. A Land Use and Land Cover Classification System for Use with Remote Sensor Data. *USGS Professional Paper* 964, 28 p.

Anderson, M.P., Bradbury, K.R., and Riemersma, P.E., 1997. Improved Estimation of Groundwater Recharge Rates. Univ. of Wisconsin Groundwater Research Program.

Barnes, C.J., Jacobson, G., and Smith, G.D., 1994. The Distributed Recharge Mechanism in an Australian Arid Zone. *Soil Sci. Soc. Am. J.* 58, 31-40.

Blaney, H.F. and Criddle, W.D., 1966. Determining Consumptive Use for Water Developments. ASCE Irrig. And Drain. Spec. Conf., Proc. Nov. 2-4, 1-34.

Boyle, J.M. and Saleem, Z.A., 1979. Determination of Recharge Rates Using Temperature Depth Profiles in Wells. *Water Resour. Res.* 15(6), 1616-1622.

Bredehoeft, J.D. and Papadopulos, I.S., 1965. Rates of Vertical Groundwater Movement Estimated from the Earth's Thermal Profile. *Water Resour. Res.* 1(2), 325-328.

Bromley, J., Edmunds, W.M., Fellman, E., Brouwer, J., Gaze, S.R., Sudlow, J., and Taupin, J.D., 1997. Estimation of Rainfall Inputs and Direct Recharge to the Deep Unsaturated Zone of Southern Niger Using Chloride Profile Method. *J. of Hydro.* 188-189, 139-154.

Cherkauer, D.S. and Ansari, S.A., 1999. Controls on the Spatial Distribution of Ground-Water Recharge in Southeastern Wisconsin. (in preparation)

Chiew, F.H.S. and McMahon, T.A., 1990. Estimating Groundwater Recharge Using a Surface Watershed Modeling Approach. *J. of Hydro.* 114, 285-304.

Constantz, J., Thomas, C.L., and Zellweger, G., 1994. Influence of Diurnal Variations in Stream Temperature on Streamflow Loss and Groundwater Recharge. *Water Resour. Res.* 30(12), 3253-3264.

Constantz, J. and Thomas, C.L., 1996. The Use of Streambed Temperature Profiles to Estimate the Depth, Duration, and Rate of Percolation Beneath Arroyos. *Water Resour. Res.* 32(12), 3597-3602.

Cook, P.G., Walker, G.R., and Jolly, I.D., 1989. Spatial Variability of Groundwater Recharge in a Semiarid Region. *J. of Hydro.* 111: 195-212.

Cook, P.G. and Kilty, S., 1992. A Helicopter-Borne Electromagnetic Survey to Delineate Groundwater Recharge Rates. *Water Resour. Res.* 28(11), 2953-2961.

Davidson, M.R., 1985. Numerical Calculation of Saturated - Unsaturated Infiltration in a Cracked Soil. *Water Resour. Res.* 21, 709-714.

Dingman, S.L., 1994. Physical Hydrology.

Eaton, T.T., 1995. Estimating Groundwater Recharge Using a Modified Soil-Water Budget Method, in Landscape-Level Assessment of Water Quality [abs]. AWRA Wisconsin Nineteenth Annual Meeting, Abstracts, p.18.

Edmunds, W.M. and Gaye, C.B., 1994. Estimating the Spatial Variability of Groundwater Recharge in the Sahel Using Chloride. *J. of Hydro.* 156, 47-59.

Faustini, J.M., 1985. Delineation of Groundwater Flow Patterns in a Portion of the Central Sand Plain of Wisconsin. Univ. of Wisconsin, Madison. M.S. Thesis, 117 p.

Federer, C.A., Vorosmarty, C., and Fekete, B., 1996. Intercomparison of Methods for Calculating Potential Evaporation in Regional and Global Water Balance Models. *Water Resour. Res.* 32(7), 2315-2321.

Freeze, R.A., 1969. The Mechanism of Natural Ground-Water Recharge and Discharge 1. One Dimensional, Vertical, Unsteady, Unsaturated Flow Above a Recharging or Discharging Ground-Water Flow System. *Water Resour. Res*. 5(1), 153-171.

Freeze, R.A. and Banner, J., 1970. The Mechanism of Natural Ground-Water Recharge and Discharge. 2. Laboratory Column Experiments and Field Measurements. *Water Resour. Res.* 6(1), 138-155.

Gee, G.W., Wierenga, P.J., Andraski, B.J., Young, M.H., Fayer, M.J., and Rockhold, M.L., 1994. Variations in Water Balance and Recharge Potential at Three Western Desert Sites. *Soil Sci. Soc. Am. J.* 58, 63-72.

Gillham, R.W., 1984. The Capillary Fringe and Its Effect on Water Table Response. *J. of Hydro.* 67, 307-324.

Gleick, P.H., 1987. The Development and Testing of a Water Balance Model for Climate Change Impact Assessment: Modeling the Sacramento Basin. *Water Resour. Res.* 23(6), 1049-1061.

Graham, W.D. and Tankersley, C.D., 1994. Optimal Estimation of Spatially Variable Recharge

and Transmissivity Fields Under Steady-State Groundwater Flow. Part I. Theory. *J. of Hydro.* 157, 247 – 266.

Graham, W.D. and Neff, C.R., 1994. Optimal Estimation of Spatially Variable Recharge and Transmissivity Fields Under Steady-State Groundwater Flow. Part II. Case Study. *J. of Hydro.* 157, 267-285.

Gupta, A.D. and Paudyal, G.N., 1988. Estimating Aquifer Recharge and Parameters From Water Level Fluctuations. *J. of Hydro.* 99, 103-116.

Hoos, A.B., 1990. Recharge Rates and Aquifer Hydraulic Characteristics for Selected Drainage Basins in Middle and East Tennessee. *USGS Water Resour. Invest. Report* 90-4015.

Houston, J.F., 1982. Rainfall and Recharge to a Dolomitic Aquifer in a Semi-Arid Climate at Kabwe, Zambia. *J. of Hydro.* 59, 173-187.

Houston, J.F., 1988. Rainfall – Runoff – Recharge Relationships in the Basement Rocks of Zimbabwe. In Simmers, Estimation of Natural Groundwater Recharge, 349-366.

Howard, K.W.F. and Lloyd, J.W., 1979. The Sensitivity of Parameters in the Penman Evaporation Equations and Direct Recharge Balance. *J. of Hydro.* 41, 329-344.

Hunt, R.J., Krabbenhoft, D.P., and Anderson, M.P., 1996. Groundwater Inflow Measurements in Wetland Systems. *Water Resour. Res.* 32(3), 495-507.

Hunt, R.J. and Steuer, J., 2000. Delineating a Spring's Recharge Area Using Numerical Groundwater Flow Modeling and Geochemical Investigation. Wisconsin Dept. of Natural Resources.

Jansson, P.E. and Halldin, S., 1979. Model for Annual Water and Energy Flow in a Layered Soil, in Halldin, *Comparison of Forest Water and Energy Exchange Models*. Int. Soc. For Ecological Modeling, Copenhagen.

Jansson, P.E. and Halldin, S., 1980. Soil Water and Heat Model. Technical Description. Swedish Coniferous Forest Project, Upssala, Tech. Rep. 26, 81 p.

Jensen, M.E. and Haise, R.H., 1963. Estimating Evapotranspiration from Solar Radiation. ASCE Proc. 89(IR4), 15-41.

Johansson, P., 1987. Estimation of Groundwater Recharge in Sandy Till with Two Different Methods Using Groundwater Level Fluctuations. *J. of Hydro.* 90, 183-198.

Johansson, P., 1988. Methods for Estimation of Natural Groundwater Recharge Directly From Precipitation – Comparative Studies in Sandy Till. In Simmers, Estimation of Natural Groundwater Recharge, 239-270.

Kafri, U. and Asher, B., 1978. Computer Estimates of Natural Recharge through Soils of Southern Arizona. *J. of Hydro*. 38, 125-138.

Kennett-Smith, A., Cook, P.G., and Walker, G.R., 1994. Factors Affecting Groundwater Recharge Following Clearing in the South Western Murray Basin. *J. of Hydro.* 154, 85-105.

Kim, K., 1996. A Geochemical and Flow Modeling Study on Groundwater in a Sandy, Silicate Aquifer, Northern Wisconsin, USA. Ph.D. Thesis, University of Wisconsin – Madison, Dept. of Geology and Geophysics, 213 p.

Kim, C.P., Stricker, N.M., and Torfs, P.J., 1996. An Analytical Framework for the Water Budget of the Unsaturated Zone. *Water Resour. Res.* 32(12), 3475-3484.

Kitching, R. and Bridge, L.R., 1974. Lysimeter Installation in Sandstone at Styrrup, Nottingham. *J. of Hydro.* 23, 219-232.

Kitching, R. and Day, J.B., 1979. Two Day Meeting on Lysimeters. Rep. Inst. Geol. Sci. 79/6, 50 p.

Kitching, R., Edmunds, W.M., Shearer, T.R., Walton, N.R., and Jacovides, J., 1980. Assessment of Recharge to Aquifers. *Hydrol. Sci. Bull.* 25, 217-235.

Kitching, R. and Shearer, T.R., 1982. Construction and Operation of a Large Undisturbed Lysimeter to Measure Recharge to the Chalk Aquifer, England. *J. of Hydro.* 58, 267-277.

Kitching, R., Shearer, T.R., and Shedlock, S.L., 1977. Recharge to the Bunter Sandstone Determined from Lysimeters. *J. of Hydro.* 33, 217-232.

Krishnamurthi, N., Sunada, D.K., and Longenbaugh, R.A., 1977. Mathematical Modeling of Natural Groundwater Recharge. *Water Resour. Res.* 13, 720-724.

Krohelski, J.T., Bradbury, K.R., Hunt, R.J., and Swanson, S.K., 2000. Numerical Simulation of Groundwater Flow in Dane County, Wisconsin. Wisconsin Geological and Natural History Survey Informational Circular. 44 p.

Lapham, W.W., 1989. Use of Temperature Profiles Beneath Streams to Determine Rates of Vertical Ground-Water Flow and Vertical Hydraulic Conductivity. *US Geological Survey Water Supply Paper 2337,* 35p.

Leavesley, G.H., Lichty, R.W., Troutman, B.M., and Saindon, L.G., 1983. Precipitation-runoff modeling system; user's manual. *USGS Water Resour. Invest. Report* #4238, 207p.

Leduc, C., Bromley, J., and Schroeter, P., 1997. Water Table Fluctuation and Recharge in Semi Arid Climate: Some Results of the HAPEX-Sahel Hydrodynamic Survey. *J. of Hydro.* 188-189, 123-138.

Lerner, D.N., A.S. Issar, and I. Simmers, 1990. Groundwater Recharge: A Guide to Understanding and Estimating Natural Recharge. International Association of Hydrogeologists vol. 8, 345 p.

Levine, J.B. and Salvucci, G.D., 1999. Equilibrium Analysis of Groundwater – Vadose Zone Interactions and the Resulting Spatial Distribution of Hydrologic Fluxes Across a Canadian Prairie. *Water Resour. Res.* 35(5), 1369-1383.

Liu, Y. And Zhang, C., 1993. A Comparative Study of Calculation Methods for Recharge of Rainfall Seepage to Ground Water in Plain Area. *Ground Water* 31(1), 12 -18.

Maidment, D.R., 1993. Handbook of Hydrology.

Mandel, S. And Shiftan, Z.L., 1981. Groundwater Resources: Investigation and Development. Academic Press, London.

Mau, D.P. and Winter, T.C., 1997. Estimating Ground Water Recharge from Streamflow Hydrographs for a Small Mountain Watershed in a Temperate Humid Climate, NH. *Ground Water* 35(2), 291 - 304.

Meyboom, P., 1961. Estimating Ground-Water Recharge from Stream Hydrographs. *J. Geophys. Res.* 66(4), 1203-1214.

Monteith, J.L., 1965. Evaporation and the Environment. *Symp. Soc. Expl. Biol.,* vol. 19, p 205 – 234.

Morell - Seytoux, H.J. and Billica, J.A., 1985. A Two Phase Numerical Model for Prediction of Infiltration: Application to a Semi-infinite Soil Column. *Water Resour. Res.* 21, 607-615.

Nathan, R.J. and McMahon, T.A., 1990. Evaluation of Automated Techniques for Base Flow and Recession Analyses. *Water Resour. Res.* 26(7), 1465-1473.

Nielsen, G.L., and Widjaya, J.M., 1989. Modeling of Ground Water Recharge in Southern Bali, Indonesia. *Ground Water* 27(4), 473-480.

Nightingale, H.I., 1975. Ground Water Recharge Rates from Thermometry. *Ground Water* 13(4), 340-344.

O'Brien, R., Keller, C.K., and Smith, J.L., 1996. Multiple Tracers of Shallow Ground Water Flow and Recharge in Hilly Loess. *Ground Water* 34(4), 675 - 682.

Perez, E., 1997. Estimation of Basin Wide Recharge Rates Using Spring Flow, Precipitation, and Temperature Data. *Ground Water* 35(6), 1058 - 1065.

Ragab, R., Finch, J., and Harding, R., 1997. Estimation of Groundwater Recharge to Chalk and

Sandstone Aquifers Using Simple Soil Models. *J. of Hydro.* 190, 19-41.

Rai, S.N. and Singh, R.N., 1992. Water Table Fluctuations in an Aquifer System Owing to Time Varying Surface Infiltration and Canal Recharge. *J. of Hydro.* 136, 381-387.

Rehm, B.W., Moran, S.R., and Groenewold, G.H., 1982. Natural Groundwater Recharge in an Upland Area of Central North Dakota, USA. *J. of Hydro.* 59, 293-314.

Rennolls, K., Carnell, R., and Tee, V., 1980. A Descriptive Model of the Relationship Between Rainfall and Soil Water Table. *J. of Hydro.* 47, 103-114.

Ronan, A.D., Prudic, D.E., Thodal, C.E., and Constantz, J., 1998. Field Study and Simulation of Diurnal Temperature Effects on Infiltration and Variably Saturated Flow Beneath an Ephemeral Stream. *Water Resour. Res.* 34(9), 2137-2153.

Rosen, M.R., Bright, J., Carran, P., Stewart, M.K., and Reeves, R., 1999. Estimating Rainfall Recharge and Soil Water Residence Times in Pukekohe, New Zealnd, by Combining Geophysical, Chemical, and Isotopic Methods. *Ground Water* 37(6), 836-844.

Ross, P.J., 1990. Efficient Numerical Methods for Infiltration Using Richards' Equation. *Water Resour. Res.* 26(2), 279-290.

Rushton, K.R. and Ward, C., 1979. The Estimation of Groundwater Recharge. *J. of Hydro.* 41, 345-361.

Rushton, K.R., 1988. Numerical and Conceptual Models for Recharge Estimation in Arid and Semi-Arid Zones. in Simmers, Estimation of Natural Groundwater Recharge, 223-238.

Rutledge, A.T. and Daniel, C.C., 1994. Testing an Automated Method to Estimate Ground Water Recharge from Streamflow Records. *Ground Water* 32(2), 180 - 189.

Salama, R.B., Tapley, I., Ishii, T., and Hawkes, G., 1994. Identification of Areas of Recharge and Discharge Using Landsat-TM Satellite Imagery and Aerial Photography Mapping Techniques. *J. of Hydro.* 162, 119-141.

Senarath, D.C.H., 1988. Estimation of Recharge of Sand Aquifer of the Island of Mannar Sri Lanka. In Simmers, Estimation of Natural Groundwater Recharge, 423-434.

Sharma, M.L. And Hughes, M.W., 1985. Groundwater Recharge Estimation using Chloride, Deuterium, and Oxygen-18 Profiles in the Deep Coastal Sands of Western Australia. *J. of Hydro.* 81, 93-109.

Silliman, S.E. and Booth, D.F., 1993. Analysis of Time Series Measurements of Sediment Temperatures for Identification of Gaining Verses Losing Portions of Juday Creek, Indiana. *J. Hydro.* 146, 131-148.

Silliman, S.E., Ramirez, J., and McCabe, R., 1995. Quantifying Downflow through Creek Sediments Using Temperature Time Series: One Dimensional Solution Incorporating Measured Surface Temperature. *J. Hydro.* 167, 99-119.

Simmers, I., 1988. Estimation of Natural Groundwater Recharge. NATO ASI Series C, vol. 222.

Sinha, B.P. and Sharma, S.K., 1988. Natural Groundwater Recharge Methodologies in India. In I. Simmers, 301-311.

Sophocleous, M. and Perry, C.A., 1985. Experimental Studies in Natural Groundwater Recharge Dynamics: The Analysis of Observed Recharge Events. *J. of Hydro.* 81, 297-332.

Sophocleous, M. and McAllister, J.A., 1987. Basinwide Water-Balance Modeling With Emphasis on Spatial Distribution of Ground Water Recharge. *Water Resour. Bull.* 23(6), 997-1010.

Sophocleous, M., 1991. Combining the Soilwater Balance and Water Level Fluctuation Methods to Estimate Natural Groundwater Recharge: Practical Aspects. *J. of Hydro.* 124, 229-241.

Sophocleous, M., 1992. Groundwater Recharge Estimation and Regionalization: The Great Bend Prairie of Central Kansas and its Recharge Statistics. *J. of Hydro.* 137, 113-140.

Sorey, M.L., 1971. Measurement of vertical Groundwater Velocity from Temperature Profiles in Wells. *Water Resour. Res.* 7(4), 963-970.

Stallman, R.W., 1960. Notes on the Use of Temperature Data for Computing Ground-Water Velocity, Societe Hydrotechnique de France, Nancy, France, 6^{th} *Assembly* on Hydraulics, *Rapport 3,* 1-7.

Stallman, R.W., 1963. Computation of Groundwater Velocity From Temperature Data. *USGS Water Supply Paper* 1544-H, 36-46.

Stallman, R.W., 1965. Steady One-Dimensional Fluid Flow in a Semi-Infinite Porous Medium with Sinusoidal Surface Temperature. *J. Geophys. Res.* 70(12), 2821-2827.

Steenhuis, T., Jackson, C., Kung, S., and Brutsaert, W., 1985. Measurement of Ground Water Recharge on Eastern Long Island, New York, USA. *J. of Hydro.* 79, 145-169.

Steenhuis, T. and Van Der Molen, W., 1986. The Thornthwaite-Mather Procedure as a Simple Engineering Method to Predict Recharge. *J. of Hydro.* 84, 221-229.

Stephens, D.B. and Knowlton, R., 1986. Soil Water Movement and Recharge Through Sand at a Semi-Arid Site in New Mexico. *Water Resour. Res.* 22(6), 881-889.

Steuer, J.J., 1999. A Precipitation-Runoff Model for Pheasant Branch Creek, Middleton, WI. USGS Water Resources Division, Middleton, WI. (in preparation)

Stoertz, M.W. and Bradbury, K.R., 1989. Mapping Recharge Areas Using a Groundwater Flow Model - A Case Study. *Ground Water* 27(2), 220-229.

Stoertz, M.W., 1989. A New Method for Mapping Groundwater Recharge Areas and for Zoning Recharge for an Inverse Model. University of Wisconsin, Madison, Department of Geology and Geophysics, Ph.D. dissertation, 178 p.

Sukhija, B.S., Reddy, D.V., Nagabhushanam, P., Hussain, S., Giri, V.Y., and Patil, D.J., 1996. Environmental and Injected Tracers Methodology to Estimate Direct Precipitation Recharge to a Confined Aquifer. *J. of Hydro.* 177, 77-97.

Suzuki, S., 1960. Percolation Measurements Based on Heat Flow through Soil With Special Reference to Paddy Fields. *J. Geophys. Res* 65(9), 2883-2885.

Swanson, S.K., 1996. A Comparison of Two Methods Used to Estimate Groundwater Recharge in Dane County, Wisconsin. University of Wisconsin, Madison, Department of Geology and Geophysics, Master's thesis, 123 p.

Taniguchi, M. and Sharma, M.L., 1990. Solute and Heat Transport Experiments for Estimating Recharge Rates. *J. Hydro.* 119(1), 57-69.

Taniguchi, M. and Sharma, M.L., 1993. Determination of Groundwater Recharge Using the Change in Soil Temperature. *J. Hydro.* 148, 219-229.

Taniguchi, M., 1993. Evaluation of Vertical Groundwater Fluxes and Thermal Properties of Aquifers Based on Transient Temperature Depth Profiles. *Water Resour. Res.* 29(7), 2021-2026.

Taniguchi, M., 1994. Estimated Recharge Rates From Groundwater Temperatures in the Nara Basin, Japan. *Applied Hydrogeology* 2, 7-13.

Taniguchi, M., Shimada, J., Tanaka, T., Kayane, I., Sakura, Y., Shimano, Y., Dapaah-Siakwan, S., and Kawashima, S., 1999. Disturbances of Temperature-Depth Profiles Due to Surface Climate Change and Subsurface Water Flow: 1. An Effect of Linear Increase in Surface temperature Caused by Global Warming and Urbanization in the Tokyo, Metropolitan Area, Japan. *Water Resour. Res.* 35(5), 1507-1517.

Taniguchi, M., Williamson, D.R., and Peck, A.J., 1999. Disturbances of Temperature-Depth Profiles Due to Surface Climate Change and Subsurface Water Flow: 2. An Effect of Step Increase in Surface Temperature Caused by Forest Clearing in Southwest Western Australia. *Water Resour. Res.* 35(5), 1519-1529.

Taylor, R.G. and Howard, K.W., 1996. Groundwater Recharge in the Victoria Nile Basin of East Africa: Support for the Soil Moisture Balance Approach Using Stable Isotope Tracers and Flow Modeling. *J. of Hydro.* 180, 31-53.

Thornthwaite, C.W. and Mather, J.R., 1957. Instructions and Tables for Computing Potential Evapotranspiration and the Water Balance. *Publications in Climatology* 10(3).

Turc, L., 1961. Evaluation Des Besoins en Eau d'irrigation, evapotranspiration potentielle. *Ann. Agron.* 12(1), 13-49.

U.S. Department of Agriculture, Soil Conservation Service, 1978. Soil Survey of Dane County, Wisconsin.

U.S. Soil Conservation Service, 1964. SCS National Engineering Handbook. Hydrology. Section 4. Washington DC: US Soil Conservation Service.

Viswanathan, M.N., 1984. Recharge Characteristics of an Unconfined Aquifer from the Rainfall Water Table Relationship. *J. of Hydro.* 233-250.

Watson, K.K., 1980. Numerical Analysis of Natural Groundwater Recharge Under Intermittent Surface Inputs. AWRC Groundwater Recharge Conference, Townsville, Australia, 98-107.

Watson, P., Sinclair, P., and Waggonner, R., 1976. Quantitative Evaluation of a Method for Estimating Recharge to the Desert Basins of Nevada. *J. of Hydro.* 31, 335-357.

Winter, T.C., 1986. Effect of Ground-Water Recharge on Configuration of the Water Table Beneath Sand Dunes and on Seepage in Lakes in the Sandhills of Nebraska, USA. *J. of Hydro.* 86, 221-237.

Wood, W.W., 1999. Use and Misuse of the Chloride Mass-Balance Method in Estimating Ground Water Recharge. *Ground Water* 37(1), 2-3.

Wu, J., Zhang, R., and Yang, J., 1996. Analysis of Rainfall - Recharge Relationships. *J. of Hydro.* 177, 143-160.

Wu, J., Zhang, R., and Yang, J., 1997. Estimating Infiltration Recharge Using a Response Function Model. *J. of Hydro.* 198, 124-139.

Appendix A

Example of an input grid:
(an Ascii file in Arc/Info Ascii Grid format)

```
ncols         5
nrows         5
xllcorner     551771.08505427
yllcorner     285382.21453446
cellsize      30
NODATA_value  -9999
11 21 41 21 15
11 13 14 51 12
42 22 74 17 11
16 31 43 21 21
14 12 11 17 16
```

Annotation:

ncols	# of columns in the input grid
nrows	# of rows in the input grid
xllcorner	spatial location
yllcorner	spatial location
cellsize	size of grid cell
NODATA value	value assigned to a No-Data cell

To generate the grids for the soil-water balance model:

1. Bring up all three model layers (soil texture, land cover, DEM) into one view in ArcView. It is best if the soil texture and land cover layers are cut to fit the watershed boundary.
2. Under Theme, use the 'convert to grid' command to generate the model grids. Start with the coverage of largest extent (in most cases the DEM). The model requires a rectangular or square grid. Make sure for the other two grids that you specify the 'grid extent' and 'grid cell size' be the same as the first grid you generated. For discussion sake, we will refer to these three grids as 'soilsgrd', 'landgrd', and 'demgrd'.
3. Assuming the DEM covered a larger area than the other two coverages, there will be a number of 'No Data' values around the fringes of the latter two grids. Our model will not recognize these 'No Data' values so these values must be modified before the model can be run. Use the 'con' and 'isnull' commands in ARC INFO to modify the soils and land cover grids. At the Arc prompt type *grid*. At the grid prompt type:

   "name of new grid" = con(isnull("grid to be modified"), new value, otherwise)

   For example: to get rid of the 'No Data' values in the soilsgrd, the command would be:

   soils = con(isnull(soilsgrd), 7, soilsgrd)

This command generates a new grid 'soils' from the original grid 'soilsgrd'. If the value of the original grid was 'No Data', then assign this node a new value of 7; otherwise, use the value from the original grid 'soilsgrd'. Although the 'new value' is a dummy value since we don't have data for these points and they are out of the study watershed, make sure that the value

you choose is one that is recognizable by the model. In this case we used '7' which represents a 'Silt Loam' soil texture which is the average texture for the watershed. There will be a similar expression for the land cover grid:

land = con(isnull(landgrd), 21, landgrd)

4. To generate the flow direction grid from 'demgrd' use the 'flowdirection' command in ARC INFO. At the grid prompt type:

   flow = flowdirection(demgrd)

5. Finally you need to convert all three grids into an Ascii file. Use the 'gridascii' command in ARC INFO:

   soil_text = gridascii(soils)
   land_cov = grdiascii(land)
   fl_dir = gridascii(flow)

Make sure these three files are in the folder that contains the model code and are named exactly as above.

Appendix B

Thornthwaite - Mather

The Thornthwaite - Mather equation for estimating potential evapotranspiration was developed in the 1940s and 1950s by Thornthwaite and Mather at the Laboratory of Climatology in Centerton, NJ. They made measurements of evapotranspiration around the world and noticed that potential evapotranspiration appeared to be a function of the average temperature, the latitude of the measurement, and the length of the day. They developed an empirical equation that uses monthly average temperature as a measure of the energy available for evapotranspiration. Although they felt that the method was not mathematically fully developed, they considered it a good approximation for potential evapotranspiration. The method is still widely used. The equation has no correction for different vegetation types and is commonly stated as:

$$pET = .63[50(T-32)/(9I)]^{a} \times lcf$$

Where: pET = potential evapotranspiration (in/month)
T = average monthly temperature (°F)
I = annual thermal index
a = calculated constant
lcf = latitude correction factor

For each month, a monthly heat index (i) is calculated as a function of the average monthly temperature (T): $i = ((T - 32)/9)^{1.514}$. The monthly heat indices are summed to give an annual thermal index (I). "a" is calculated as a function of the annual thermal index (I):

$$a = (6.75 \times 10^{-7})I^3 - (7.71 \times 10^{-5})I^2 + (1.79 \times 10^{-2})I + .49239$$

Finally, the latitude correction factor (lcf) is based on the number of daylight hours per month which is a function of the solar declination and the latitude of the study site:

lcf = (daylight hours for entire month) / (12 * number of days in the month)
daylight hours per day = (24 / π) * (Arccos(-Tan(latitude) * Tan(solar declination)))
latitude (in radians) = (2π * (latitude (in degrees))) / 360
solar declination (in radians) = 0.4093 * Sin(((2πJ) / 365) - 1.405)
J = Julian day number

The empirical equation holds for temperatures between 32° and 79.7° F. If the temperature is less than 32° F, the potential evapotranspiration is zero. If the temperature is greater than 79.7° F, then potential evapotranspiration is given by:

$$PET = lcf\,(((-5.25625072726565E\text{-}03 * T^2) + (1.04170341298537 * T) - 44.3259754866234)).$$

Turc

The Turc equation is an empirical radiation-based equation for calculating potential evapotranspiration. The method has been shown to perform well in humid climates. The equation requires estimates or measurements of net solar radiation (Sn), average daily temperature (T), and daily relative humidity (RH):

If the relative humidity is less than 50%, then:

$$pET = (0.313 / 25.4) (T / (T + 15)) (Sn + 2.1) (1 + ((50 - RH) / 70))$$

If the relative humidity is greater than or equal to 50%, then:

$$pET = (0.313 / 25.4) (T / (T + 15)) (Sn + 2.1)$$

where: pET = potential evapotranspiration (inches/day)
T = daily average temperature (C)
RH = daily relative humidity (%)
Sn = daily net solar radiation (mm/day)

Our model assumes that solar radiation data are not available and calculates the daily net solar radiation as a function of the daily extraterrestrial radiation (So), the surface albedo (α), and the number of daily measured sunshine hours (n/N):

$$Sn = (So) (1 - \alpha) (a_s + (b_s)(n/N))$$

Where: So = extraterrestrial radiation (MJ/m^2day)
α = albedo = .23 is recommended in absence of knowledge of land cover
a_s = 0.25 for average climates
b_s = 0.50 for average climates
n = bright sunshine hours per day (hours)
N = total day length (hours)

The daily extraterrestrial radiation (So) is calculated as a function of the sunset hour angle (ω_s), the latitude (ϕ), and the solar declination (δ):

$$So = 15.392\ d_r\ (\omega_s\ Sin(\phi)\ Sin(\delta) + Cos(\phi)\ Cos(\delta)\ Sin(\omega_s))$$

Where: So = daily extraterrestrial radiation (mm/day)
d_r = relative distance between the earth and sun
ω_s = sunset hour angle (radians)
ϕ = latitude (radians)
δ = solar declination (radians)

The relative distance between the earth and sun (d_r) is given by:

$$d_r = 1 + (0.033\ (\text{Cos}(2\pi J) / 365))$$

Where: J = Julian day number

The sunset hour angle (ω_s) is given by:

$$\omega_s = \text{Arccos}(-\ \text{Tan}(\phi)\ \text{Tan}(\delta))$$

The solar declination (δ) is given by:

$$\delta = 0.4093\ \text{Sin}((2\pi J) / 365) - 1.405)$$

Where: J = Julian day number

To convert the daily extraterrestrial radiation from mm/day to MJ/m^2day, multiply So by the density of water (0.001 g/mm^3) and the latent heat of vaporization (2447.22 J/g) and convert to meters.

The total day length (N) can be calculated from:

$$N = (24 / \pi)\ \omega_s$$

Like the Thornthwaite equation, if the temperature is less than 32° F, the potential evapotranspiration is assumed to be zero; otherwise, the equation holds.

Jensen-Haise

The Jensen - Haise equation is an empirical radiation-based equation for calculating potential evapotranspiration. The equation requires estimates or measurements of net solar radiation (Sn) and average daily temperature (T):

$$pET = (0.41 / 25.4)\ Sn\ ((0.025\ T) + 0.078)$$

where: pET = potential evapotranspiration (inches/day)
T = daily average temperature (°C)
Sn = daily net solar radiation (mm/day)

As with the Turc method described above, the model assumes that solar radiation data are not available and calculates the daily net solar radiation as a function of the daily extraterrestrial radiation (So), the surface albedo (α), and the number of daily measured sunshine hours (n/N):

$$Sn = So\ (1 - \alpha)\ (a_s + b_s\ (n/N))$$

Where: So = extraterrestrial radiation (MJ/m^2day)
α = albedo = .23 is recommended in absence of knowledge of land cover
a_s = 0.25 for average climates
b_s = 0.50 for average climates

n = bright sunshine hours per day (hours)
N = total day length (hours)

The daily extraterrestrial radiation (So) is calculated as a function of the sunset hour angle (ω_s), the latitude (ϕ), and the solar declination (δ):

$$So = 15.392\ d_r\ (\omega_s\ \ Sin(\phi)\ \ Sin(\delta) + Cos(\phi)\ \ Cos(\delta)\ \ Sin(\omega_s))$$

Where: So = daily extraterrestrial radiation (mm/day)
d_r = relative distance between the earth and sun
ω_s = sunset hour angle (radians)
ϕ = latitude (radians)
δ = solar declination (radians)

The relative distance between the earth and sun (d_r) is given by:

$$d_r = 1 + (0.033\ \ (Cos(2\pi J) / 365))$$

Where: J = Julian day number

The sunset hour angle (ω_s) is given by:

$$\omega_s = Arccos(- Tan(\phi)\ \ Tan(\delta))$$

The solar declination (δ) is given by:

$$\delta = 0.4093\ \ Sin((2\pi J) / 365) - 1.405)$$

Where: J = Julian day number

To convert the daily extraterrestrial radiation from mm/day to MJ/m^2day, multiply So by the density of water (0.001 g/mm^3) and the latent heat of vaporization (2447.22 J/g) and convert to meters.

The total day length (N) can be calculated from:

$$N = (24 / \pi)\ \ \omega_s$$

Like the Thornthwaite equation, if the temperature is less than 32° F, the potential evapotranspiration is assumed to be zero; otherwise, the equation holds.

Blaney-Criddle Equation

The Blaney – Criddle equation is primarily a temperature-based approach for estimating potential evapotranspiration. The equation was originally developed in 1950 and has been widely

applied for irrigation designs in the western United States. The method is still in common use and is stated in its most modern complex form as:

$$E = a_{BC} + b_{BC}f$$

With: $f = p(.46T + 8.13)$

$a_{BC} = 0.0043RH_{min} - (n/N) - 1.41$

$b_{BC} = 0.81917 - 0.0040922(RH_{min}) + 1.0705(n/N) + 0.065649(U_d)$
$- 0.0059684(RH_{min})(n/N) - 0.0006967(RH_{min})(U_d)$

where: p = ratio of monthly daytime hours to annual daytime hours (%)
T = average monthly air temperature (°C)
(n/N) = ratio of the actual to possible monthly sunshine hours
RH_{min} = average minimum monthly relative humidity (%)
U_d = average monthly daytime wind speed at 2 meters height (m/sec)

The total day length (N) can be calculated from:

$$N = (24 / \pi)\ \omega_s$$

Where: ω_s = sunset hour angle (in radians)

The sunset hour angle (ω_s) is given by:

$$\omega_s = \text{Arccos}(- \text{Tan}(\phi)\ \text{Tan}(\delta))$$

Where: ϕ = latitude (in radians)
δ = solar declination (in radians)

The solar declination (δ) is given by:

$$\delta = 0.4093\ \text{Sin}((2\pi J) / 365) - 1.405)$$

Where: J = Julian day number

Like the Thornthwaite equation, if the temperature is less than 32° F, the potential evapotranspiration is assumed to be zero; otherwise, the equation holds.

Appendix C

SCS Curve Numbers

We used data from the literature to assign curve numbers to all the possible soil and land cover combinations (Table 5):

1. We assume a $^1/_3$ acre lot size or 30% impervious area for all Residential (11) plots.
2. Curve numbers for Commercial and Services (12) and Industrial (13) lots are taken directly from the Handbook of Hydrology (Maidment, 1993).
3. Transportation and Communication (14) curve numbers are modified from the Commercial and Service estimates.
4. Industrial and Commercial Complex (15) curve numbers are the average of the Commercial and Services and the Industrial cover type estimates.
5. Mixed Urban (16) numbers are based on a 72% impervious surface.
6. We assume that the majority of the Other Urban (17) lots are open spaces, parks, cemeteries, golf courses, etc. with grass cover on 75% or more of the area.
7. We used the 'cultivated land with conservation treatment' curve numbers for our Cropland and Pasture (21) category.
8. We used curve number estimates from an orchard in California for the Orchard (22) cover type.
9. Curve numbers for Farmsteads are used for the Confined Feeding Operation (23) and Other Agricultural (24) cover types.
10. The Rangeland (31-33) plots are assumed to be in good condition. The Forest (41-43) plots are assumed to have good cover. The curve numbers for these categories are taken directly from the Handbook of Hydrology (Maidment, 1993)
11. All water bodies (51 – 54) and wetlands (61 – 62) are assumed to be fully saturated and have complete runoff (curve number = 100).
12. Beaches (72), Other Sandy Areas (73), Exposed Bedrock (74), and Quarries and Gravel Pits (75) are assumed to have essentially no runoff (curve number = 5).
13. Curve numbers for fallow land are used for the Transitional Area (76) and Mixed Barren Land (77) cover types.

Appendix D

Successive Approximation Method

If the net annual input to the soil system is negative (i.e., there is more water being removed from than input to the soil system), the model uses a successive approximation method to specify a starting soil moisture value. First, the model sums the SM values for the water deficit months (those with a negative SM value) and calculates the soil moisture retention for this total loss using the equations in Appendix E. This estimate would be the soil moisture storage at the end of the deficit months assuming the soil was at full moisture capacity at the beginning of the dry season. Next, the model sums the SM values for the water surplus months (those with a positive SM value) and adds this net gain to the soil moisture retention calculated above. This new sum represents the estimated soil moisture storage predicted at the end of the spring wet season. The model calculates the associated loss for this new sum using the equations in Appendix E. The associated loss is then added to the sum of the negative SM values, and the process is repeated until the system converges and the difference between cycles is less than .01 inches. The result is a starting soil moisture storage and associated starting water loss for those years with a net annual water deficiency. (See Thornthwaite – Mather 1957 for an example)

Appendix E

Accumulated Water Loss and Monthly Net Soil Moisture

Once a starting soil moisture storage has been determined, changes in soil moisture are tracked on a month by month basis. Monthly estimates of soil moisture retention are based on an accumulated monthly water loss. The model begins with the month in which we specified or calculated a starting soil moisture storage value. If the system is saturated, the starting water loss is zero. If the system is not saturated, the successive approximation method (Appendix D) is used to define a starting water loss. If the following month has a negative SM value (moisture loss), the loss is added to the net loss from the previous month, and the equations below are used to convert the accumulated monthly deficit into an associated soil moisture value. This process is repeated for successive months that have a negative SM value. When months with a positive SM value (moisture gain) are encountered, the gain is simply added to the previous month's soil moisture value to define a new moisture value. The same equations below can be used to calculate the accumulated loss associated with this new soil moisture value. In this fashion, the accumulated water loss is tracked from month to month and is used to determine the monthly net soil moisture value. (See Thornthwaite – Mather 1957 for examples)

Exponential Curve Equations for Estimating Soil Moisture Retention

All equations have the form: $y = a * e^{bx}$

Max. Soil Moisture Capacity = 0.5	$y = 0.5432 * e^{1.1845 * x}$
Max. Soil Moisture Capacity = 0.6	$y = 0.6519 * e^{1.1845 * x}$
Max. Soil Moisture Capacity = 0.7	$y = 0.7605 * e^{1.1845 * x}$
Max. Soil Moisture Capacity = 0.8	$y = 0.8692 * e^{1.1845 * x}$
Max. Soil Moisture Capacity = 0.9	$y = 0.9778 * e^{1.1845 * x}$
Max. Soil Moisture Capacity = 1.0	$y = 1.0865 * e^{1.1845 * x}$
Max. Soil Moisture Capacity = 1.1	$y = 1.0848 * e^{0.9630 * x}$
Max. Soil Moisture Capacity = 1.2	$y = 1.1697 * e^{0.8600 * x}$
Max. Soil Moisture Capacity = 1.3	$y = 1.2744 * e^{0.7965 * x}$
Max. Soil Moisture Capacity = 1.4	$y = 1.3870 * e^{0.7526 * x}$
Max. Soil Moisture Capacity = 1.5	$y = 1.5081 * e^{0.7223 * x}$
Max. Soil Moisture Capacity = 1.6	$y = 1.5821 * e^{0.6576 * x}$
Max. Soil Moisture Capacity = 1.7	$y = 1.6732 * e^{0.6123 * x}$
Max. Soil Moisture Capacity = 1.8	$y = 1.7729 * e^{0.5784 * x}$
Max. Soil Moisture Capacity = 1.9	$y = 1.8774 * e^{0.5520 * x}$
Max. Soil Moisture Capacity = 2.0	$y = 1.9839 * e^{0.5300 * x}$
Max. Soil Moisture Capacity = 2.1	$y = 2.0207 * e^{0.4811 * x}$
Max. Soil Moisture Capacity = 2.2	$y = 2.0976 * e^{0.4483 * x}$
Max. Soil Moisture Capacity = 2.3	$y = 2.1928 * e^{0.4243 * x}$
Max. Soil Moisture Capacity = 2.4	$y = 2.2980 * e^{0.4058 * x}$
Max. Soil Moisture Capacity = 2.5	$y = 2.4091 * e^{0.3910 * x}$
Max. Soil Moisture Capacity = 2.6	$y = 2.5241 * e^{0.3788 * x}$
Max. Soil Moisture Capacity = 2.7	$y = 2.6417 * e^{0.3686 * x}$

Max. Soil Moisture Capacity = 2.8	$y = 2.7612 * e^{0.3598 * x}$
Max. Soil Moisture Capacity = 2.9	$y = 2.8820 * e^{0.3523 * x}$
Max. Soil Moisture Capacity = 3.0	$y = 3.0188 * e^{0.3475 * x}$
Max. Soil Moisture Capacity = 3.1	$y = 3.0911 * e^{0.3307 * x}$
Max. Soil Moisture Capacity = 3.2	$y = 3.1742 * e^{0.3169 * x}$
Max. Soil Moisture Capacity = 3.3	$y = 3.2648 * e^{0.3053 * x}$
Max. Soil Moisture Capacity = 3.4	$y = 3.3605 * e^{0.2953 * x}$
Max. Soil Moisture Capacity = 3.5	$y = 3.4602 * e^{0.2867 * x}$
Max. Soil Moisture Capacity = 3.6	$y = 3.5628 * e^{0.2791 * x}$
Max. Soil Moisture Capacity = 3.7	$y = 3.6676 * e^{0.2724 * x}$
Max. Soil Moisture Capacity = 3.8	$y = 3.7743 * e^{0.2664 * x}$
Max. Soil Moisture Capacity = 3.9	$y = 3.8824 * e^{0.2610 * x}$
Max. Soil Moisture Capacity = 4.0	$y = 3.9835 * e^{0.2554 * x}$
Max. Soil Moisture Capacity = 4.1	$y = 4.0701 * e^{0.2473 * x}$
Max. Soil Moisture Capacity = 4.2	$y = 4.1618 * e^{0.2401 * x}$
Max. Soil Moisture Capacity = 4.3	$y = 4.2575 * e^{0.2337 * x}$
Max. Soil Moisture Capacity = 4.4	$y = 4.3562 * e^{0.2280 * x}$
Max. Soil Moisture Capacity = 4.5	$y = 4.4574 * e^{0.2229 * x}$
Max. Soil Moisture Capacity = 4.6	$y = 4.5606 * e^{0.2182 * x}$
Max. Soil Moisture Capacity = 4.7	$y = 4.6654 * e^{0.2140 * x}$
Max. Soil Moisture Capacity = 4.8	$y = 4.7717 * e^{0.2101 * x}$
Max. Soil Moisture Capacity = 4.9	$y = 4.8791 * e^{0.2065 * x}$
Max. Soil Moisture Capacity = 5.0	$y = 4.9768 * e^{0.2027 * x}$
Max. Soil Moisture Capacity = 5.1	$y = 5.0756 * e^{0.1983 * x}$
Max. Soil Moisture Capacity = 5.2	$y = 5.1770 * e^{0.1944 * x}$
Max. Soil Moisture Capacity = 5.3	$y = 5.2804 * e^{0.1907 * x}$
Max. Soil Moisture Capacity = 5.4	$y = 5.3857 * e^{0.1874 * x}$
Max. Soil Moisture Capacity = 5.5	$y = 5.4925 * e^{0.1844 * x}$
Max. Soil Moisture Capacity = 5.6	$y = 5.6005 * e^{0.1815 * x}$
Max. Soil Moisture Capacity = 5.7	$y = 5.7097 * e^{0.1789 * x}$
Max. Soil Moisture Capacity = 5.8	$y = 5.8198 * e^{0.1764 * x}$
Max. Soil Moisture Capacity = 5.9	$y = 5.9308 * e^{0.1741 * x}$
Max. Soil Moisture Capacity = 6.0	$y = 6.0258 * e^{0.1714 * x}$
Max. Soil Moisture Capacity = 6.2	$y = 6.1849 * e^{0.1633 * x}$
Max. Soil Moisture Capacity = 6.3	$y = 6.2707 * e^{0.1597 * x}$
Max. Soil Moisture Capacity = 6.4	$y = 6.3598 * e^{0.1565 * x}$
Max. Soil Moisture Capacity = 6.5	$y = 6.4517 * e^{0.1534 * x}$
Max. Soil Moisture Capacity = 6.6	$y = 6.5460 * e^{0.1506 * x}$
Max. Soil Moisture Capacity = 6.7	$y = 6.6423 * e^{0.1480 * x}$
Max. Soil Moisture Capacity = 6.8	$y = 6.7403 * e^{0.1456 * x}$
Max. Soil Moisture Capacity = 6.9	$y = 6.8399 * e^{0.1433 * x}$
Max. Soil Moisture Capacity = 7.0	$y = 6.9409 * e^{0.1412 * x}$
Max. Soil Moisture Capacity = 7.1	$y = 7.0430 * e^{0.1392 * x}$
Max. Soil Moisture Capacity = 7.2	$y = 7.1462 * e^{0.1373 * x}$
Max. Soil Moisture Capacity = 7.3	$y = 7.2503 * e^{0.1355 * x}$
Max. Soil Moisture Capacity = 7.4	$y = 7.3553 * e^{0.1338 * x}$

Max. Soil Moisture Capacity = 7.5	$y = 7.4610 * e^{0.1322 * x}$
Max. Soil Moisture Capacity = 7.6	$y = 7.5674 * e^{0.1307 * x}$
Max. Soil Moisture Capacity = 7.7	$y = 7.6745 * e^{0.1293 * x}$
Max. Soil Moisture Capacity = 7.8	$y = 7.7820 * e^{0.1279 * x}$
Max. Soil Moisture Capacity = 7.9	$y = 7.8901 * e^{0.1266 * x}$
Max. Soil Moisture Capacity = 8.0	$y = 7.9976 * e^{0.1253 * x}$
Max. Soil Moisture Capacity = 8.1	$y = 8.0861 * e^{0.1233 * x}$
Max. Soil Moisture Capacity = 8.2	$y = 8.1771 * e^{0.1214 * x}$
Max. Soil Moisture Capacity = 8.3	$y = 8.2703 * e^{0.1196 * x}$
Max. Soil Moisture Capacity = 8.4	$y = 8.3656 * e^{0.1180 * x}$
Max. Soil Moisture Capacity = 8.5	$y = 8.4627 * e^{0.1164 * x}$
Max. Soil Moisture Capacity = 8.6	$y = 8.5613 * e^{0.1149 * x}$
Max. Soil Moisture Capacity = 8.7	$y = 8.6613 * e^{0.1135 * x}$
Max. Soil Moisture Capacity = 8.8	$y = 8.7625 * e^{0.1121 * x}$
Max. Soil Moisture Capacity = 8.9	$y = 8.8650 * e^{0.1109 * x}$
Max. Soil Moisture Capacity = 9.0	$y = 8.9684 * e^{0.1096 * x}$
Max. Soil Moisture Capacity = 9.1	$y = 9.0727 * e^{0.1085 * x}$
Max. Soil Moisture Capacity = 9.2	$y = 9.1780 * e^{0.1074 * x}$
Max. Soil Moisture Capacity = 9.4	$y = 9.3906 * e^{0.1053 * x}$
Max. Soil Moisture Capacity = 9.5	$y = 9.4980 * e^{0.1044 * x}$
Max. Soil Moisture Capacity = 9.6	$y = 9.6059 * e^{0.1034 * x}$
Max. Soil Moisture Capacity = 9.7	$y = 9.7144 * e^{0.1026 * x}$
Max. Soil Moisture Capacity = 9.8	$y = 9.8233 * e^{0.1017 * x}$
Max. Soil Moisture Capacity = 9.9	$y = 9.9328 * e^{0.1009 * x}$
Max. Soil Moisture Capacity = 10.0	$y = 10.0360 * e^{0.1000 * x}$
Max. Soil Moisture Capacity = 10.1	$y = 10.1243 * e^{0.0988 * x}$
Max. Soil Moisture Capacity = 10.2	$y = 10.2143 * e^{0.0977 * x}$
Max. Soil Moisture Capacity = 10.4	$y = 10.3985 * e^{0.0956 * x}$
Max. Soil Moisture Capacity = 10.5	$y = 10.4926 * e^{0.0946 * x}$
Max. Soil Moisture Capacity = 10.6	$y = 10.5877 * e^{0.0936 * x}$
Max. Soil Moisture Capacity = 10.7	$y = 10.6840 * e^{0.0927 * x}$
Max. Soil Moisture Capacity = 10.9	$y = 10.8792 * e^{0.0910 * x}$
Max. Soil Moisture Capacity = 11.0	$y = 10.9780 * e^{0.0902 * x}$
Max. Soil Moisture Capacity = 11.1	$y = 11.0776 * e^{0.0894 * x}$
Max. Soil Moisture Capacity = 11.2	$y = 11.1780 * e^{0.0886 * x}$
Max. Soil Moisture Capacity = 11.4	$y = 11.3805 * e^{0.0872 * x}$
Max. Soil Moisture Capacity = 11.5	$y = 11.4826 * e^{0.0866 * x}$
Max. Soil Moisture Capacity = 11.6	$y = 11.5853 * e^{0.0859 * x}$
Max. Soil Moisture Capacity = 11.7	$y = 11.6884 * e^{0.0853 * x}$
Max. Soil Moisture Capacity = 11.9	$y = 11.8961 * e^{0.0841 * x}$
Max. Soil Moisture Capacity = 12.0	$y = 11.9993 * e^{0.0835 * x}$
Max. Soil Moisture Capacity = 12.1	$y = 12.0924 * e^{0.0827 * x}$
Max. Soil Moisture Capacity = 12.2	$y = 12.1866 * e^{0.0819 * x}$
Max. Soil Moisture Capacity = 12.3	$y = 12.2817 * e^{0.0812 * x}$
Max. Soil Moisture Capacity = 12.4	$y = 12.3779 * e^{0.0804 * x}$
Max. Soil Moisture Capacity = 12.5	$y = 12.4749 * e^{0.0797 * x}$

Max. Soil Moisture Capacity = 12.6	$y = 12.5727 * e^{0.0791 * x}$
Max. Soil Moisture Capacity = 12.7	$y = 12.6713 * e^{0.0784 * x}$
Max. Soil Moisture Capacity = 13.0	$y = 12.9712 * e^{0.0766 * x}$
Max. Soil Moisture Capacity = 13.3	$y = 13.2764 * e^{0.0750 * x}$
Max. Soil Moisture Capacity = 13.7	$y = 13.6900 * e^{0.0730 * x}$
Max. Soil Moisture Capacity = 13.9	$y = 13.8993 * e^{0.0721 * x}$
Max. Soil Moisture Capacity = 14.0	$y = 13.9994 * e^{0.0716 * x}$
Max. Soil Moisture Capacity = 14.3	$y = 14.2831 * e^{0.0699 * x}$
Max. Soil Moisture Capacity = 14.5	$y = 14.4766 * e^{0.0688 * x}$
Max. Soil Moisture Capacity = 14.7	$y = 14.6732 * e^{0.0678 * x}$
Max. Soil Moisture Capacity = 14.9	$y = 14.8724 * e^{0.0669 * x}$
Max. Soil Moisture Capacity = 15.0	$y = 14.9730 * e^{0.0665 * x}$
Max. Soil Moisture Capacity = 15.1	$y = 15.0740 * e^{0.0660 * x}$
Max. Soil Moisture Capacity = 15.2	$y = 15.1757 * e^{0.0656 * x}$
Max. Soil Moisture Capacity = 15.5	$y = 15.4835 * e^{0.0644 * x}$
Max. Soil Moisture Capacity = 15.7	$y = 15.6909 * e^{0.0637 * x}$
Max. Soil Moisture Capacity = 15.9	$y = 15.8998 * e^{0.0630 * x}$
Max. Soil Moisture Capacity = 16.0	$y = 16.0048 * e^{0.0626 * x}$
Max. Soil Moisture Capacity = 16.1	$y = 16.1102 * e^{0.0623 * x}$
Max. Soil Moisture Capacity = 16.2	$y = 16.2158 * e^{0.0620 * x}$
Max. Soil Moisture Capacity = 16.5	$y = 16.5346 * e^{0.0611 * x}$
Max. Soil Moisture Capacity = 17.0	$y = 17.0710 * e^{0.0596 * x}$
Max. Soil Moisture Capacity = 17.1	$y = 17.1790 * e^{0.0594 * x}$
Max. Soil Moisture Capacity = 17.2	$y = 17.2870 * e^{0.0591 * x}$

Appendix F

Land Cover Categories
(from Anderson et al., 1976)

Residential (11)
Residential land ranges from high density housing, represented by the multiple-unit structures of urban cores, to low density housing, where houses are on lots of more than one acre, on the periphery of urban expansion.

Commercial and Services (12)
Commercial areas are those used predominantly for the sale of products and services. Components of the Commercial and Services category are urban central business districts; shopping centers, usually in suburban and outlying areas; commercial strip developments along major highways and access routes to cities; junkyards; resorts; and so forth. The main buildings, secondary structures, and areas supporting the basic use are all included. Institutional land uses, such as the various educational, religious, health, correctional, and military facilities are also components of this category.

Industrial (13)
Industrial areas include a wide array of land uses from light manufacturing to heavy manufacturing plants (mining industry, steel mills, lumber mills, electric power generating stations, oil refineries, chemical plants, etc …).

Transportation, Communications, and Utilities (14)
Transportation sites include major transportation routes (roads, highways, railways), airports, seaports, lakeports, etc … Communication and utilities areas such as those involved in processing, treatment, and transportation of water, gas, oil, and electricity and areas used for airwave communications are also included in this category.

Industrial and Commercial Complexes (15)
This category includes those industrial and commercial land uses that typically occur together or in close functional proximity. Such areas are commonly called “Industrial Parks”.

Mixed Urban or Built Up Land (16)
This category is used for a mixture of Level II Urban or Built Up uses when individual uses cannot be separated at mapping scale. When more than one-third intermixture of another use or uses occurs in a specific area, it is classified as Mixed Urban or Built-Up Land. This category typically includes developments along transportation routes and in cities, towns, and built up areas.

Other Urban or Built Up Land (17)
This category includes uses such as golf driving ranges, zoos, urban parks, cemeteries, waste dumps, water control structures and spillways, golf courses, and ski ways.

Cropland and Pasture (21)
This category includes all crop and pasture land (harvested and idle).

Orchards, Groves, Vineyards, Nurseries, and Ornamental Horticultural Areas (22)
This category includes orchards, groves, and vineyards which produce the various fruit and nut crops and nurseries and horticultural areas, which include floricultural and seed-and-sod areas and some greenhouses.

Confined Feeding Operations (23)
Confined feeding operations are large, specialized livestock production enterprises, chiefly beef cattle feedlots, dairy operations with confined feeding, and large poultry farms, but also including hog feedlots. These operations have large animal populations restricted to relatively small areas.

Other Agricultural Land (24)
Other land uses typically associated with the last three categories of Agricultural Land are the principal components of this category. They include farmsteads, holding areas for livestock such as corrals, breeding and training facilities on horse farms, farm lanes and roads, ditches and canals, small farm ponds, and similar uses.

Herbaceous Rangeland (31)
This category encompasses lands dominated by naturally occurring grasses and forbs as well as those areas of actual rangeland which have been modified to include grasses and forbs as their principal cover, when the land is managed for rangeland purposes and not managed using practices typical of pastureland.

Shrub and Brush Rangeland (32)
Rangeland typically found in arid and semiarid regions.

Mixed Rangeland (33)
When more than one-third intermixture of either herbaceous or shrub and brush rangeland species occurs in a specific area, the area is classified as mixed.

Deciduous Forest (41)
Category includes all forested areas having a predominance of trees that lose their leaves at the end of the frost season or at the beginning of the dry season.

Evergreen Forest (42)
Category includes all forested areas in which the trees are predominantly those which remain green throughout the year. Both coniferous and broad-leaved evergreens are included in this category.

Mixed Forest Land (43)
Category includes all forested areas where both evergreen and deciduous trees are growing and neither predominates.

Streams and Canals (51)
Category includes rivers, creeks, canals, and other linear water bodies.

Lakes (52)
Lakes are nonflowing, naturally enclosed bodies of water, including regulated natural lakes but excluding reservoirs.

Reservoirs (53)
Reservoirs are artificial impoundments of water used for irrigation, flood control, recreation, hydroelectric power generation, and so forth.

Bays and Estuaries (54)
Bays and estuaries are inlets or arms of the sea that extend inland.

Forested Wetland (61)
Forested wetlands are wetlands dominated by woody vegetation.

Nonforested Wetland (62)
Nonforested wetlands are wetlands dominated by wetland herbaceous vegetation or are nonvegetated. This category includes tidal and nontidal fresh, brackish, and salt marshes and nonvegetated flats and also freshwater meadows, wet prairies, and open bogs.

Beaches (72)
Beaches are the smooth sloping accumulations of sand and gravel along shorelines.

Sandy Areas Other Than Beaches (73)
This category is composed primarily of dunes.

Bare Exposed Rock (74)
Category includes areas of bedrock exposure, desert pavement, scarps, talus, slides, volcanic material, and other accumulations of rock without vegetative cover.

Strip Mines, Quarries, and Gravel Pits (75)
This category includes those extractive mining activities that have significant surface expression.

Transitional Area (76)
This category is intended for those areas which are in transition from one land use activity to another.

Mixed Barren Land (77)
This category is used when a mixture of Barren Land features occurs and the dominant land use occupies less than two-thirds the area.

Appendix G

Maximum Soil Moisture Storage Coefficients

The maximum soil moisture storage values used in our model were modified from Thornthwaite – Mather's original tables (1957). Water holding capacity tables were generated for all soil texture and land cover combinations by multiplying the available water (inches of water per foot of strata) by an associated root zone depth. The available water is a function of the soil texture; the root zone depth is a function of both the soil texture and the land cover type.

Thornthwaite and Mather presented available water holding capacities for five different soil texture types (fine sand, fine sandy loam, silt loam, clay loam, and clay). We linearly interpolated the values between these five categories to accommodate our fourteen soil texture types (figure 2). Where possible, root zone depths were also linearly interpolated from Thornthwaite and Mather (1957) for various land cover / soil texture combinations. The remaining combinations were taken from the literature, from discussions with foresters and soil scientists, and from visual assessment of the Madison area.

Root zones for many of the Urban Land Cover categories were assumed to be an intermediate between forests and lawn grass. We assumed the crown area of the trees reflected their lateral root extent. We conducted a visual inspection of the Madison area and concluded that:

1. $^{2}/_{3}$ of the Residential (11) and Other Agricultural Land (24) blocks is tree covered; the other $^{1}/_{3}$ is covered in grass
2. ¼ of Commercial and Services (12), Industrial and Commercial Complexes (15), and Other Urban (17) plots is tree covered; the other ¾ is covered in grass
3. $^{1}/_{3}$ of Mixed Urban (16) plots is tree covered; the other $^{2}/_{3}$ is grass
4. all of the Industrial (13) and Transportation, Communication, and Utility (14) blocks are covered in grass

Based on discussions with soil scientists, we estimated that grass rooting depths ranged from ½ a foot in clay rich soils to 1 ½ feet in sandy soils. We then used Thornthwaite and Mather's rooting depths for their Forest cover type and calculated a root zone depth for each category listed above by taking a weighted average of the two end members.

Thornthwaite and Mather subdivided cropland into shallow-rooted (spinach, beans, carrots, etc.), moderately deep-rooted (corn, cereal grains, etc.), and deep-rooted (alfalfa, pastures, shrubs, etc.) cover types. The Anderson classification system lumps all cropland and pastures into one land cover type. Since the fields in Wisconsin are primarily corn or wheat with some fields of pasture or deeper-rooted crops and very few fields of shallow-rooted crops, we estimated root zone depths for the Cropland and Pasture cover type (21) as a weighted average composed of ¾ moderately deep-rooted and ¼ deep-rooted crops. Thornthwaite – Mather's deep – rooted crop category was used for Rangelands (31 - 33), considering most ranges are covered primarily in shrubs.

Root zones for the Orchards (22) and Forest (41 - 43) cover types were taken directly from Thornthwaite and Mather.

Water (51 - 54) and Wetland (61 - 62) categories are considered to be fully saturated at all times such that there is no requisite holding capacity that needs to be satisfied before runoff and recharge occurs. Bare Exposed Rock (74) and Gravel Pits (75) are also considered to have no moisture withholding capacity; rainfall that doesn't runoff goes directly to recharge the groundwater system.

As for the other barren land cover types (72, 73, 76, 77, 23), we assumed a fixed evapotranspiration depth of ½ a foot for all texture types.

Appendix H
SCS Curve Numbers for all Soil / Land Cover Combinations (Condition II)
Estimates which Minimize Recharge

		Hydrologic Soil Group			
	Land Use Description	A	B	C	D
Urban or Built Up Land					
11	**Residential (1/3 acre lots)[1]**	**57**	**72**	**81**	**86**
12	**Commercial and Services[1]**	**89**	**92**	**94**	**95**
13	**Industrial[1]**	**81**	**88**	**91**	**93**
14	**Transportation / Communication[1]**	**91**	**94**	**95**	**96**
15	**Industrial / Commercial Complex[1]**	**85**	**90**	**92**	**94**
16	**Mixed Urban or Built Up[1]**	**81**	**88**	**91**	**93**
17	**Other Urban or Built Up[1]**	**49**	**69**	**79**	**84**
Agricultural Land					
21	**Cropland and Pasture[1]**	**72**	**81**	**88**	**91**
22	**Orchards, Groves, Vineyards[2]**	**41**	**55**	**69**	**71**
23	**Confined Feeding Operations[2]**	**72**	**82**	**87**	**89**
24	**Other Agricultural Land[2]**	**59**	**74**	**82**	**86**
Rangeland					
31	**Herbaceous Rangeland[1]**	**68**	**79**	**86**	**89**
32	**Shrub and Brush Rangeland[1]**	**68**	**79**	**86**	**89**
33	**Mixed Rangeland[1]**	**68**	**79**	**86**	**89**
Forest Land					
41	**Deciduous Forest Land[1]**	**45**	**66**	**77**	**83**
42	**Evergeen Forest Land[1]**	**45**	**66**	**77**	**83**
43	**Mixed Forest Land[1]**	**45**	**66**	**77**	**83**
Water					
51	**Streams and Canals**	**100**	**100**	**100**	**100**
52	**Lakes**	**100**	**100**	**100**	**100**
53	**Reservoirs**	**100**	**100**	**100**	**100**
54	**Bays and Estuaries**	**100**	**100**	**100**	**100**
Wetland					
61	**Forested Wetland**	**100**	**100**	**100**	**100**
62	**Nonforested Wetland**	**100**	**100**	**100**	**100**
Barren Land					
72	**Beaches**	**5**	**5**	**5**	**5**
73	**Sandy Areas Other than Beaches**	**5**	**5**	**5**	**5**
74	**Bare Exposed Rock**	**5**	**5**	**5**	**5**
75	**Strip Mines, Quarries, Gravel Pits**	**5**	**5**	**5**	**5**
76	**Transitional Areas[2]**	**77**	**86**	**91**	**94**
77	**Mixed Barren Land[2]**	**77**	**86**	**91**	**94**

[1] taken from Handbook of Hydrology, 1993.
[2] taken from U.S. SCS, 1964.

We used data from the literature to reassign curve numbers to all the possible soil and land cover combinations so as to minimize recharge. The following changes were made:

1. We assume that the majority of the Other Urban (17) lots are open spaces, parks, cemeteries, golf courses, etc. with grass cover on 50 - 75% of the area.
2. We used the 'cultivated land with no conservation treatment' curve numbers for our Cropland and Pasture (21) category.
3. We used the upper end curve number estimates from an orchard in California for the Orchard (22) cover type.
4. Curve numbers for a Packed Dirt Road are used for the Confined Feeding Operation (23).
5. The Rangeland (31-33) plots are assumed to be in poor condition. The Forest (41-43) plots are assumed to have thin cover. The curve numbers for these categories are taken directly from the Handbook of Hydrology (Maidment, 1993)

Soil Moisture Storage Coefficients which Minimize Recharge
(Adapted from Thornthwaite and Mather, 1957)

Urban or Built-Up Land Categories (Cover Types 11, 24) … 3/4 trees and 1/4 grass

Texture	Available Water (in/ft)	Root Zone (ft)	Water Holding Capacity (in)
sand	1.20	6.62	7.9
loamy sand	1.40	6.18	8.6
sandy loam	1.60	5.73	9.2
fine sandy loam	1.80	5.30	9.5
very fine sandy loam	2.00	5.27	10.5
loam	2.20	5.25	11.5
silt loam	2.40	5.23	12.6
silt	2.55	4.97	12.7
sandy clay loam	2.70	4.71	12.7
silty clay loam	2.85	4.44	12.7
clay loam	3.00	4.17	12.5
sandy clay	3.20	3.80	12.2
silty clay	3.40	3.42	11.6
clay	3.60	3.05	11.0

Urban or Built-Up Land Categories (Cover Types 16) …1/2 trees and 1/2 grass

Texture	Available Water (in/ft)	Root Zone (ft)	Water Holding Capacity (in)
sand	1.20	4.92	5.9
loamy sand	1.40	4.59	6.4
sandy loam	1.60	4.26	6.8
fine sandy loam	1.80	3.93	7.1
very fine sandy loam	2.00	3.88	7.8
loam	2.20	3.83	8.4
silt loam	2.40	3.80	9.1
silt	2.55	3.61	9.2
sandy clay loam	2.70	3.41	9.2
silty clay loam	2.85	3.22	9.2

clay loam	3.00	3.02	9.0
sandy clay	3.20	2.75	8.8
silty clay	3.40	2.47	8.4
clay	3.60	2.20	7.9

Urban or Built-Up Land Categories (Cover Types 12, 15, 17) …1/3 trees and 2/3 grass

Texture	Available Water (in/ft)	Root Zone (ft)	Water Holding Capacity (in)
sand	1.20	3.75	4.5
loamy sand	1.40	3.50	4.9
sandy loam	1.60	3.25	5.2
fine sandy loam	1.80	3.00	5.4
very fine sandy loam	2.00	2.93	5.9
loam	2.20	2.87	6.3
silt loam	2.40	2.83	6.8
silt	2.55	2.68	6.8
sandy clay loam	2.70	2.53	6.8
silty clay loam	2.85	2.38	6.8
clay loam	3.00	2.23	6.7
sandy clay	3.20	2.03	6.5
silty clay	3.40	1.82	6.2
clay	3.60	1.62	5.8

Urban or Built-Up Land Categories (Cover Types 13, 14) …1/4 trees and 3/4 grass

Texture	Available Water (in/ft)	Root Zone (ft)	Water Holding Capacity (in)
sand	1.20	3.21	3.8
loamy sand	1.40	2.99	4.2
sandy loam	1.60	2.78	4.4
fine sandy loam	1.80	2.57	4.6
very fine sandy loam	2.00	2.49	5.0
loam	2.20	2.42	5.3
silt loam	2.40	2.37	5.7
silt	2.55	2.24	5.7
sandy clay loam	2.70	2.12	5.7
silty clay loam	2.85	1.99	5.7
clay loam	3.00	1.86	5.6
sandy clay	3.20	1.69	5.4
silty clay	3.40	1.52	5.2
clay	3.60	1.35	4.9

Cropland and Pastures (Cover Type 21) … 1/2 moderate + 1/2 deep

Texture	Available Water (in/ft)	Root Zone (ft)	Water Holding Capacity (in)
sand	1.20	2.92	3.5
loamy sand	1.40	3.06	4.3
sandy loam	1.60	3.20	5.1
fine sandy loam	1.80	3.33	6.0
very fine sandy loam	2.00	3.47	6.9
loam	2.20	3.61	7.9
silt loam	2.40	3.75	9.0

silt	2.55	3.56	9.1
sandy clay loam	2.70	3.38	9.1
silty clay loam	2.85	3.19	9.1
clay loam	3.00	3.00	9.0
sandy clay	3.20	2.65	8.5
silty clay	3.40	2.30	7.8
clay	3.60	1.95	7.0

Orchards, Groves, Vineyards, Nurseries (Cover Type 22)

Texture	Available Water (in/ft)	Root Zone (ft)	Water Holding Capacity (in)
sand	1.20	5.00	6.0
loamy sand	1.40	5.18	7.3
sandy loam	1.60	5.36	8.6
fine sandy loam	1.80	5.55	10.0
very fine sandy loam	2.00	5.36	10.7
loam	2.20	5.18	11.4
silt loam	2.40	5.00	12.0
silt	2.55	4.58	11.7
sandy clay loam	2.70	4.16	11.2
silty clay loam	2.85	3.74	10.7
clay loam	3.00	3.33	10.0
sandy clay	3.20	2.96	9.5
silty clay	3.40	2.59	8.8
clay	3.60	2.22	8.0

Rangeland (Cover Types 31 - 33)

Texture	Available Water (in/ft)	Root Zone (ft)	Water Holding Capacity (in)
sand	1.20	3.33	4.0
loamy sand	1.40	3.33	4.7
sandy loam	1.60	3.33	5.3
fine sandy loam	1.80	3.33	6.0
very fine sandy loam	2.00	3.61	7.2
loam	2.20	3.89	8.6
silt loam	2.40	4.17	10.0
silt	2.55	3.96	10.1
sandy clay loam	2.70	3.75	10.1
silty clay loam	2.85	3.54	10.1
clay loam	3.00	3.33	10.0
sandy clay	3.20	2.96	9.5
silty clay	3.40	2.59	8.8
clay	3.60	2.22	8.0

Forest Land (Cover Types 41 - 43)

Texture	Available Water (in/ft)	Root Zone (ft)	Water Holding Capacity (in)
sand	1.20	8.33	10.0
loamy sand	1.40	7.77	10.9
sandy loam	1.60	7.21	11.5
fine sandy loam	1.80	6.66	12.0

very fine sandy loam	2.00	6.66	13.3
loam	2.20	6.66	14.7
silt loam	2.40	6.66	16.0
silt	2.55	6.33	16.1
sandy clay loam	2.70	6.00	16.2
silty clay loam	2.85	5.67	16.2
clay loam	3.00	5.33	16.0
sandy clay	3.20	4.85	15.5
silty clay	3.40	4.37	14.9
clay	3.60	3.90	14.0

Barren Lands, Confined Feeding Operations (Cover Types 23, 72, 73, 76, 77)

Texture	**Available Water (in/ft)**	**Root Zone (ft)**	**Water Holding Capacity (in)**
sand	1.20	1.00	1.2
loamy sand	1.40	1.00	1.4
sandy loam	1.60	1.00	1.6
fine sandy loam	1.80	1.00	1.8
very fine sandy loam	2.00	1.00	2.0
loam	2.20	1.00	2.2
silt loam	2.40	1.00	2.4
silt	2.55	1.00	2.6
sandy clay loam	2.70	1.00	2.7
silty clay loam	2.85	1.00	2.9
clay loam	3.00	1.00	3.0
sandy clay	3.20	1.00	3.2
silty clay	3.40	1.00	3.4
clay	3.60	1.00	3.6

The maximum soil moisture storage values were modified so as to minimize recharge. The following changes from the original values were made:

For the urban cover types:

1. ¾ of the Residential (11) and Other Agricultural Land (24) blocks is tree covered; the other ¼ is covered in grass
2. $^1/_3$ of Commercial and Services (12), Industrial and Commercial Complexes (15), and Other Urban (17) plots is tree covered; the other $^2/_3$ is covered in grass
3. ½ of Mixed Urban (16) plots is tree covered; the other ½ is grass
4. ¼ of the Industrial (13) and Transportation, Communication, and Utility (14) blocks is tree covered; the other ¾ is covered in grass

We estimated root zone depths for the Cropland and Pasture cover type (21) as a weighted average composed of ½ moderately deep-rooted and ½ deep-rooted crops.

We assumed a fixed evapotranspiration depth of a foot for the barren land cover types (72, 73, 76, 77, 23) for all texture types.